ABANT IZZET BAYSAL UNIVERSITY

THE GRADUATE SCHOOL OF NATURAL AND APPLIED SCIENCES

COMPARISON OF ISOTROPIC MICELLAR SOLUTION AND LYOTROPIC LIQUID CRYSTALLINE PROPERTIES OF SOME CHIRAL AND ACHIRAL PARTLY FLUORINATED SURFACTANTS WITH THEIR HYDROGENATED COUNTERPARTS

MASTER OF SCIENCE

SİNAN YURDAKUL

BOLU, JANUARY 2018

ABANT IZZET BAYSAL UNIVERSITY

THE GRADUATE SCHOOL OF NATURAL AND APPLIED SCIENCES

DEPARTMENT OF CHEMISTRY

COMPARISON OF ISOTROPIC MICELLAR SOLUTION AND LYOTROPIC LIQUID CRYSTALLINE PROPERTIES OF SOME CHIRAL AND ACHIRAL PARTLY FLUORINATED SURFACTANTS WITH THEIR HYDROGENATED COUNTERPARTS

MASTER OF SCIENCE

SİNAN YURDAKUL

BOLU, JANUARY 2018

APPROVAL OF THE THESIS

COMPARISON OF ISOTROPIC MICELLAR SOLUTION AND LYOTROPIC LIQUID CRYSTALLINE PROPERTIES OF SOME CHIRAL AND ACHIRAL FLUORINATED SURFACTANTS WITH THEIR HYDROGENATED COUNTERPARTS submitted by **SİNAN YURDAKUL** in partial fulfillment of the requirements for the degree of **Master of Science** in **Department of Chemistry, The Graduate School of Natural and Applied Sciences of ABANT IZZET BAYSAL UNIVERSITY in 26/01/2018** by

Examining Committee Members	**Signature**
Supervisor Assoc. Prof. Dr. Erol AKPINAR Abant Izzet Baysal University	.....
Member Assoc. Prof. Dr. Öznur DEMİR ORDU Abant Izzet Baysal University	.....
Member Assist. Prof. Dr. Özgür MASALCI Ege University	.....

Graduation date: ……./……./20.…

Assoc. Prof. Dr. Ömer ÖZYURT ……

Director of Graduate School of Natural and Applied Sciences

To my family

DECLARATION

I hereby declare that all information in this document has been obtained and presented in accordance with academic rules and ethical conduct. I also declare that, as required by these rules and conduct, I have fully cited and referenced all material and results that are not original to this work.

Sinan YURDAKUL

_____

ABSTRACT

COMPARISON OF ISOTROPIC MICELLAR SOLUTION AND LYOTROPIC LIQUID CRYSTALLINE PROPERTIES OF SOME CHIRAL AND ACHIRAL PARTLY FLUORINATED SURFACTANTS WITH THEIR HYDROGENATED COUNTERPARTS

MSC THESIS

SİNAN YURDAKUL

ABANT IZZET BAYSAL UNIVERSITY GRADUATE SCHOOL OF NATURAL AND APPLIED SCIENCES

DEPARTMENT OF CHEMISTRY

(SUPERVISOR: ASSOC. PROF. DR. EROL AKPINAR)

BOLU, JANUARY 2018

In this study, we mainly examined lyotropic intrinsic cholesteric phase properties of some amino acid based chiral surfactants with partly fluorinated and hydrogenated chains to investigate the effect of the twist structure of fluorocarbon chain on the helical twisting power of chiral surfactants. For this purpose, we synthesized some chiral and achiral surfactants and determined fluorinated/hydrogenated counterpart surfactants, taking into account 1 CF_2=1.5 CH_2 rule in terms of hydrophobicity, from their critical micelle concentrations via electrical conductivity measurements. Then, we prepared lyotropic mixtures exbiting discotic cholesteric phases by dissolution of chiral surfactants L-alaninehydrochloride undecylester (L-AUnDE), L-serinehydrochloride undecylester (L-SUnDE) and their partlyfluorinated counterparts (L-APFOE and L-SPFOE, respectively) into sodium chloride (NaCl)/water mixtures, separately. The pitch measurements were performed by laser diffraction method to evaluate the helical twisting powers of each fluorinated/hydrogenated chiral surfactants. The results indicated that the twist structure of fluorocarbon chain provides higher helical twisting power with respect to the hydrocarbon chain, which supports the intramicellar chirality model proposed in the literature.

KEYWORDS: Lyotropic discotic cholesteric phase, chirality, chiral induction mechanism, chiral fluorinated surfactant, chiral hydrogenated surfactant, pitch, helical twisting power, isotropic micellar solutions, critical micelle concentration, electrical conductivity, laser diffraction.

ÖZET

BAZI KİRAL VE AKİRAL KISMEN FLORLU SÜRFAKTANTLARIN İZOTROP MİSELLİ ÇÖZELTİ VE LİYOTROPİK SIVI KRİSTAL ÖZELLİKLERİNİN HİDROJENLİ EŞDEĞERLERİ İLE KARŞILAŞTIRILMASI

YÜKSEK LISANS TEZI

SİNAN YURDAKUL

ABANT İZZET BAYSAL ÜNİVERSİTESİ FEN BİLİMLERİ ENSTİTÜSÜ KIMYA ANABILIM DALI

(TEZ DANIŞMANI: DOÇ.DR. EROL AKPINAR)

BOLU, OCAK - 2018

Bu çalışmada esas olarak, kiral sürfaktantların heliksi döndürme (bükme) güçleri üzerine florokarbon zincirinin bükülmüş (twist) yapısının etkisini incelemek için kısmen florlu ve hidrojenli bazı amino asit bazlı kiral sürfaktantların liyotropik kendi öz kolesterik faz özellikleri araştırılmıştır. Bu amaçla bazı kiral ve akiral sürfaktanlar sentezlenmiş ve hidrofobisite açısından 1 CF_2=1.5 CH_2 kuralı gözönünde bulundurularak florlu/hidrojenli eşdeğer sürfaktantlar elektriksel iletkenlik ölçümleri ile kritik misel derişimlerinden belirlenmiştir. Daha sonra, kiral sürfaktantlar L-alaninhidroklorür undesilester (L-AUnDE), L-serinhidroklorür undesilester (L-SUnDE) ve florlu eşdeğerlerinin (sırasıyla L-APFOE ve L-SPFOE) ayrı ayrı sodium klorür (NaCl)/su karışımında çözünmesiyle diskotik kolesterik faz veren karışımlar hazırlanmıştır. Herbir florlu/hidrojenli kiral sürfaktantın heliksi döndürme güçlerini belirlemek için kendi öz liyotropik kolesterik fazların adım uzunluğu ölçümleri lazer kırınımı yöntemi ile yapılmıştır. Elde edilen sonuçlar, florokarbon zincirinin bükülmüş yapısının hidrokarbon zincirine göre daha büyük heliksi döndürme gücüne sebep olduğunu göstermiştir ve bu durum daha önce literatürde önerilen miseliçi kiralite modelini desteklemektedir.

ANAHTAR KELİMELER: Liyotropik diskotik kolesterik faz, kiralite, kiral indüklenme mekanizması, kiral florlu sürfaktant, kiral hidrojenli sürfaktant, adım uzunluğu, heliksi dündürme gücü, izotrop miselli çözeltiler, kritik misel derişimi, elektriksel iletkenlik, lazer kırınımı.

TABLE OF CONTENTS

Page

LIST OF FIGURES

Page

LIST OF TABLES

Page

LIST OF ABBREVIATIONS AND SYMBOLS

Surfactants : Surface Active Molecules or Amphiphiles

CMC : Critical Micelle Concentration

β : The Degree of Counterion Binding to Micelle

α : The Degree of Counterion Ionization

$\Delta H°_{mic}$: The standard entalphy of the micellization

$\Delta G°_{mic}$: The standard Gibbs free energy of the micellization

$\Delta S°_{mic}$: The standard entropy of the micellization

κ : Conductivity

S_2 : The Slope of Postmicellar Region

S_1 : The Slope of Premicellar Region

X : Mole Fraction

LLCs : Lyotropic Liquid Crystals

N : Nematic Phase

N_D : Discotic Nematic Phase

N_C : Calamitic Nematic Phase

N_B : Biaxial Nematic Phase

MCD Model : Mixtures of Cylindrical and Disc-like Micelles

IBM Model : Intrinsically Biaxial Micelles Model

Ch : Cholesteric Phase

ChD : Cholesteric Discotic Phase

ChC : Cholesteric Calamitic Phase

ChB : Cholesteric Biaxial Phase

P : Pitch

htp : Helical Twisting Power

POM : Polarizing Optical Microscope

ACKNOWLEDGEMENTS

The author wishes to express his deepest gratitude to his supervisor Assoc. Prof. Dr. Erol AKPINAR for their guidance, advice, criticism, encouragements and insight throughout the research.

The author would also like to thank Assoc. Prof. Dr. Muhammet YILDIRIM and Assist. Prof. Dr. Erhan BUDAK for their suggestions and comments.

The technical assistance of Mr. Serdar HİZARCI is gratefully acknowledged.

This study was supported by the Abant Izzet Baysal University Directorate of Research Projects Commission (BAP), Grant No: 2017.03.03.1154.

1. INTRODUCTION

Lyotropic cholesteric phases differ from other lyotropic ones because their structural units, so-called ‘micelle’, form macroscopic helical structure as a result of chirality of chiral molecules present in lyotropic mixtures. Over some decades, researchers proposed some chiral induction mechanisms to explain how chiral molecules transfer their chirality to the whole phase, however, although these mechanisms made some useful contributions to the understanding of the formation of cholesteric phases, there are still unclear points on the chiral induction mechanism of the cholesteric phases.

There are some studies reported in the literature, in general, to examine the correlation of the chirality transfer with molecular structures of the chiral guest molecules and/or location of the chiral molecules in the micelles. Of course, these studies provided important developments on understanding the chiral induction mechanism. However, it is too difficult to say that this mechanism has been understood well yet. From this respect, in this thesis, it is aimed to find some hints for better understanding the chiral induction mechanism and to clarify some controversies on it.

Some experimental studies in the literature showed that lyotropic liquid crystals are in close contact with other micellar system ‘isotropic micellar solutions’. It means that some information obtained from the isotropic micellar solutions may be applied to lyotropic liquid crystals. Thus, this thesis consists of two main parts. In the first part, isotropic micellar solution properties of some achiral and chiral surfactants were studied. Then, in the second part, the lyotropic cholesteric liquid crystalline properties of those surfactants were investigated and compared with those obtained from their isotropic micellar solutions. As it can be seen in the further parts of the thesis, the experimental results help to clarify some points on the chirality transfer and some controversies existing in the literature.

Some chiral and achiral surfactants, with fully hydrogenated alkyl chains or partly fluorinated ones, were synthesized in the frame of this thesis and their properties were studied by electrical conductivity, polarizing optical microscopy and laser diffraction.

1.1 Isotropic Micellar Solutions

1.1.1 Micellization of Surfactants

Surfactants (surface active molecules or amphiphiles) are widely used in industrial and technological applications such as cosmetics, detergents, pharmacy, etc. (Antonio and Salinas, 2005). They consist of two main parts in their molecular structures, one is hydrophilic head or polar part (water-loving part) and the other is hydrophobic or non-polar part (water-hating part), Figure 1.1. Depending on the head groups and hydrophobic chains, surfactants are, in general, classified as cationic, anionic, nonionic, zwitterionic (amphoteric) and gemini surfactants, Figure 1.2. In the case of anionic (cationic) surfactants, the hydrophilic head groups are negatively (positively) charged which are highly soluble in water. Because zwitterionics have both negatively and positively charged parts, their head groups are in contact with water. For non-ionic surfactants, although there exist no charged head groups, highly polar head groups make them water soluble. The surfactants are composed of long-chain hydrocarbon chains. Those groups may have different structures such as long straight chain alkyl groups, branched-chain alkyl groups, unsaturated alkenyl chains, alkylbenzenes, alkyl naphthalenes, fluoroalkyl groups, polydimethylsiloxanes and polyoxypropylene glycol derivatives (Myers, 2006).

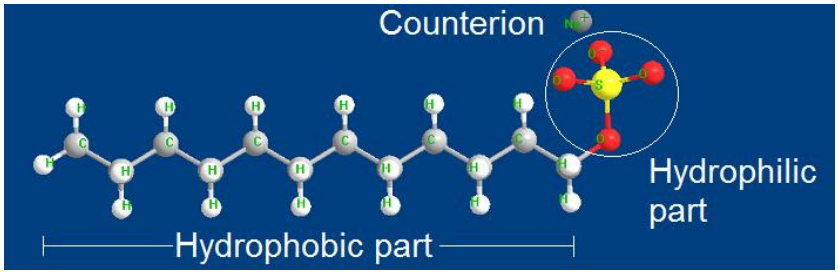

Figure 1.1 Molecular structure of a surfactant molecule.

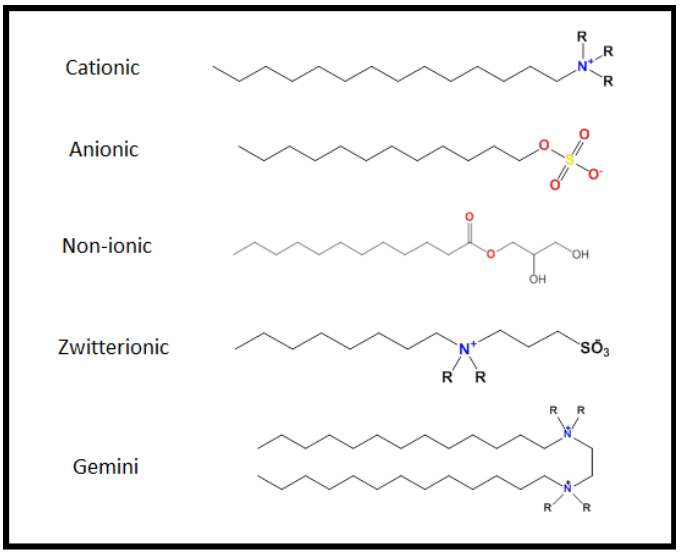

Figure 1.2 Some examples for surfactant types depending on the surfactant head group.

When surfactants are dissolved in a solvent (mostly water) at very low concentrations, they are first located at the air/solvent interface, Figure 1.3. If the surfactant concentration is increased to a specific value, then the surface of the solvent is saturated. Further addition of the surfactant gives rise to the transfer of excess amount of the surfactant into the solution to form a supermolecular structure, so-called 'micelle', Figure 1.4. This structure is formed by the aggregation of surfactant monomers at the 'critical micelle concentration (cmc)' (Shinoda, 1963). In other words, the cmc is a minimum surfactant concentration at and above which micelles form and below which surfactants remain as monomers in the solution, i.e. no micelles exist. In the structure of a normal micelle, if the solvent is water or a polar solvent, the head groups of the surfactants, which are in contact with the solvent, cover the surface of the micelles and protect the hydrophobic tails from the water molecules, Figure 1.4. However, if the solvent has apolar character, for instance decane, the reversed or inversed micelles are present in the solution, Figure 1.5.

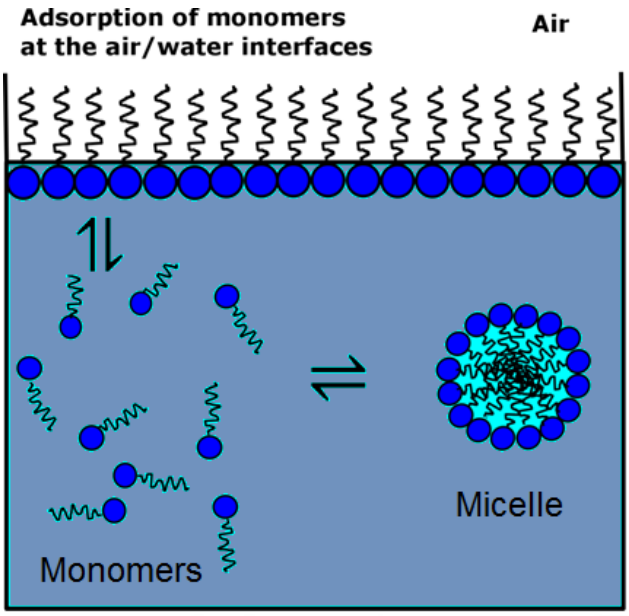

Figure 1.3 Representation of the three states in which surfactant molecules exist in water. Monomers adsorbed at the air/water interface, monomers in the bulk solution and in the micelles (Holmberg, 2002).

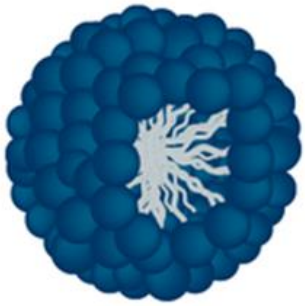

Figure 1.4 Structure of a micelle. While the hydrocarbon tails of the surfactants molecules are located in the micelle, the ionic/polar heads are located at the surfaces.

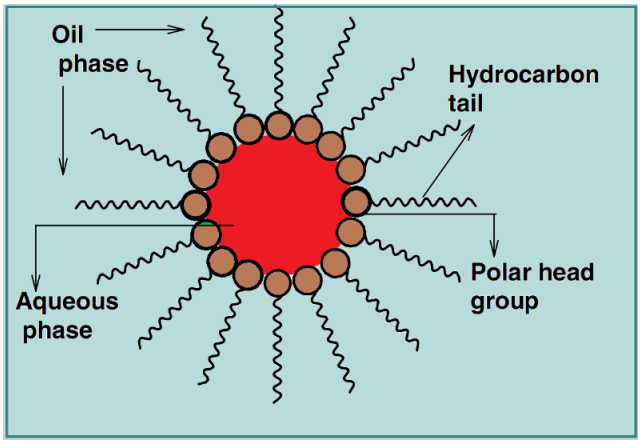

Figure 1.5 Formation of a reversed micelle in the case of apolar (oil) solvent (Malik et.al., 2012).

1.1.2 Micellization Parameters

Because surfactants are been widely using in industrial applications, especially for cleaning processes, researchers have been working on their micellization properties for a long time. Micellization of the surfactants are controlled by some micellization parameters. They are mainly (a) critical micelle concentration, (b) degree of counterion binding/ionization (β/α) and (c) micellization thermodynamic functions (enthalpy, $\Delta_{mic}H$, Gibbs free energy, $\Delta_{mic}G$, and entropy, $\Delta_{mic}S$).

Among the micellization parameters, the most important one is the critical micelle concentration (cmc). It is widely determined by electrical conductivity measurements, Figure 1.6 (Akpinar et.al., 2016a). In addition, surface tensiometry, turbidity, fluorescence spectrometry, osmotic pressure, self-diffusion and solubilization are also used for determining the critical micelle concentration (Dominguez et al., 1997; Garcia-Mateos et al., 1990; Chattopadhyay and Erwin London, 1984; Lin et al., 1999; Salem et al., 2016). In the case of electrical conductivity, not only the critical micelle concentration but also the degree of counterion binding (ionization) to (from) the micelle are evaluated. Then, by using these two parameters, the micellization thermodynamic functions can be calculated. These functions are important because they give us hints under which conditions micellization is more favored or not. For instance, by changing the temperature, the more the negative Gibbs energy of the micellization means that the surfactant molecules prefer to form the micelles, i.e. micellization is more favored. In addition, from the micellization thermodynamic functions, we may determine whether the micellization is entropy-driven or enthalpy-driven (Chen et.al, 1998).

Thermodynamic functions of micellization are based on the temperature dependence of the cmc and degree of counterion binding to the micelle (β). The latter is related to the degree of ionization of counterions (α) by $\alpha=1-\beta$. Cmc and α or β are, in general, calculated from electrical conductivity method (Tarus et al., 2003; Jiang, et al., 2005). A plot of conductivity (κ) of an ionic surfactant and its total concentration in aqueous solution (C_{tot}) gives two linear curves in the premicellar and postmicellar regions, Figure 1.6.

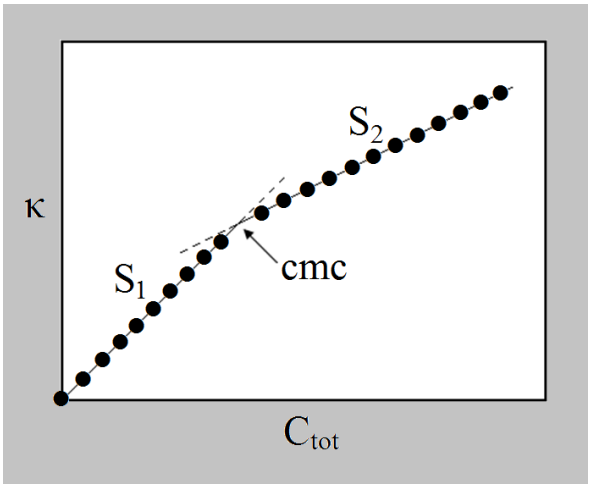

Figure 1.6 A plot of conductivity (κ) versus total surfactant concentration. The ratio of the slope of postmicellar region (S_2) to the slope of premicellar one (S_1) corresponds to the degree of counterion ionization. The break point observed on the plot arises from the condensation of some part of free counterions of the ionic surfactants to the micelle.

The ratio of slopes of postmicellar region to premicellar region on the κ-C_{tot} graph is eqaul to α (Myers, 2006).

$$\alpha = \frac{S_2}{S_1} \qquad (1.1)$$

The α or β takes the values between 0 and 1. The micellization thermodynamic parameters for ionic surfactants, the standard Gibbs free energy of micellization (ΔG^o_{mic}), the standard enthalpy of micellization (ΔH^o_{mic}) and the standard entropy change (ΔS^o_{mic}), can be evaluated from the values of cmc and β via following equations (Müller 1993)

$$\Delta G^o_{mic} = (1+\beta)RTlnX_{cmc} \qquad (1.2)$$

$$\Delta H^o_{mic} = -(1+\beta)RT^2\left(\frac{\partial lnX_{cmc}}{\partial T}\right) \qquad (1.3)$$

$$\Delta S^o_{mic} = \frac{(\Delta H^o_{mic} - \Delta G^o_{mic})}{T} \qquad (1.4)$$

where X_{cmc} is expressed as the mole fraction of the surfactant at the critical micelle concentration. For nonionic surfactants,

1.1.3 Factors Affecting the Micellization

Some factors such as temperature, pH, presence of electrolyte in the solution, interactions between the surfactant head groups and the counterions, solvent, pressure, surfactant properties (alkyl chain length, head group area and hydrophobic or alkyl chain volume) control the micellization of the surfactants (Sinnko, 2006; Mohajeri and Noudeh, 2012; Akpinar et.al., 2016). Thus, optimum conditions taking into account these factors have to be chosen to obtain the most stable micellar systems for desired goals. In the frame of this thesis, temperature, surfactant alkyl chain length and presence of electrolyte are important factors and, for this reason, their effects are given below in detail.

1.1.3.1 Temperature

The effect of the temperature on the cmc of ionic surfactants in aqueous solutions varies depending on the surfactant types and the temperature range studied (Gonzalez-Perez and Sanchez-Dominguez, 2013). Several studies were reported in the literature to examine its effect and different temperature dependences of the cmc were observed. Indeed, the effect of temperature on the cmc of ionic surfactants arises from the change in hydrophobic and head group interactions with temperature (Mohajeri and Noudeh, 2012). In general, U-shaped temperature dependence of the cmc are very common (Stead and Taylor, 1969; Kresheck, 1975; Müller, 1993; Kang et al., 2001; Noudeh et. al., 2007). It means that first the cmc value decreases as the temperature is increased and then it increases by further increase in the temperature. The U-shaped dependence is explained in the literature by the following mechanism (Kumar et al., 2000): the increase in temperature gives rise to lowering the hydration of hydrophilic groups by free water molecules in aqueous media and the micellization gets more favored, i.e. the critical micelle concentration decreases. Then, the disruption of the structured water molecules, which surround the hydrophobic groups of surfactant molecules, occurs by further increase in temperature and the micellization turns into unfavored, i.e. the critical micelle concentration increases. In addition, temperature dependence of the cmc for ionic surfactants obeying to high order polynomial functions, such as 4^{th}, 5^{th} and 6^{th} order, etc., was reported in the literature (Kang et. al., 2001).

1.1.3.2 Surfactant Alkyl Chain Length

The hydrophobic effect, which is related to the interaction of surfactant alkyl chains with water molecules, is an important phenomena in micelle formation (Tanford, 1980). In other words, it is a driving force for the aggregation of surfactant molecules to form micelles in aqueous solutions (Maibaum et.al., 2004). As expected, the hydrophobic character of the surfactant enhances as a result of an increase in surfactant alkyl chain length, which leads to a more favorable location of surfactants in the micelles than those in water (Tadros, 2014). This situation causes a decrease in the critical micelle concentrations of both ionic and nonionic surfactants (Lin et.al., 1974; Chen et.al., 1998; Rosen et.al., 2001; Bouchal et.al., 2016; Sharma et.al., 2016).

1.2 Lyotropic Liquid Crystals

Lyotropic liquid crystals (LLCs) are also micellar systems because their building units are micelles. Different LLCs structures can be obtained by changing the concentration of the constituents of lyotropic mixtures and/or temperature (Dunmur, 2002; Neto and Salinas, 2005). Lamellar, hexagonal, cubic, nematic and cholesteric (or chiral nematic) phases are well-known LLCs structures (Dunmur, 2002; Burducea, 2004; Neto and Salinas, 2005; Bilinov, 2011). Because the LLCs are in close contact with biology, their phases are important for biotechnological applications (Neto and Salinas, 2005).

In each LLCs structures, surfactant molecules aggregate in the micelles differently. In the lamellar phases, surfactants produce infinitely large bilayers, where the head groups of the surfactants are in contact with water while hydrophobic tails are located within the bilayers in one dimension. In the hexagonal phases, there exist infinitely long cylindrical micelles and they arrange in two-dimensional hexagonal array, i.e. there is a two-dimensional repeating order in the hexagonal phases. Spherical micelles form cubic phases in three-dimensions and, because of this three-dimensional repeating order, these phases are also known as viscous isotropic phases.

Nematic and cholesteric phases exhibit very similar properties and they are assumed as counterparts. For instance, micelles have finite sizes and they organize along a certain direction in both phases, so-called phase director (Lawson and Flautt, 1967; Rosevear, 1968; Acımış and Reeves, 1980). However, the main difference between those phases is that micelles form helical macrostructure around helix axis in the cholesteric phases but not in the nematic ones. Because cholesteric phases are subjected to this thesis, further information about nematic and cholesteric phases are given in the next part.

1.2.1 Lyotropic Nematic Phases

The LLC nematic phases were found for the first time through the end of 1960s (Lawson and Flautt, 1967; Rosevear, 1968) and they have been studied by several research groups in the literature. There exist a long-range orientational order with a short-range translational order in the nematic phases (Forrest and Reeves, 1980, 1981; hendrikx et.al., 1983; Boden and Holmes, 1984; Fisch et.al., 1986). In these phases, the local director of the anisometric micelles exhibits preferred alignment along a certain direction, which is known as phase director or optical axis of the phase, $\vec{n}$, with respect to magnetic field direction (Lawson and Flautt, 1967; Rosevear, 1968; Acımış and Reeves, 1980; Akpinar et.al., 2012a, 2012b). In addition to the magnetic field, surface effect also plays a role on the micelle alignment when the LLC nematic sample is transferred into a capillary as a result of interactions between the micelles and surface of the capillaries (Dan et.al., 2011; Kim et.al., 2014). In general, by surface effect or magnetic field, two types of alignment are described: if we sketch a molecule with a brick-like object, whose local director is long-molecular axis, the molecules may align with their local directors perpendicular or parallel to the capillary surfaces. The former and latter alignments are known as planar and homeotropic alignment, respectively (Kleman and Lavrentovich, 2006; Senyuk et.al., 2011; Serra, 2016), Figure 1.7. These alignments are common for thermotropic nematic liquid crystals because their building blocks are molecules, not micelles. In the case of nematic LLC, similar alignments are observed, except that because local directors of the micelles may be perpendicular and parallel to the flattest micelle surfaces, the micellar

organizations in both homeotropic and planar alignments are given in Figure 1.8 (Akpinar et. al., 2014, 2015, 2016b).

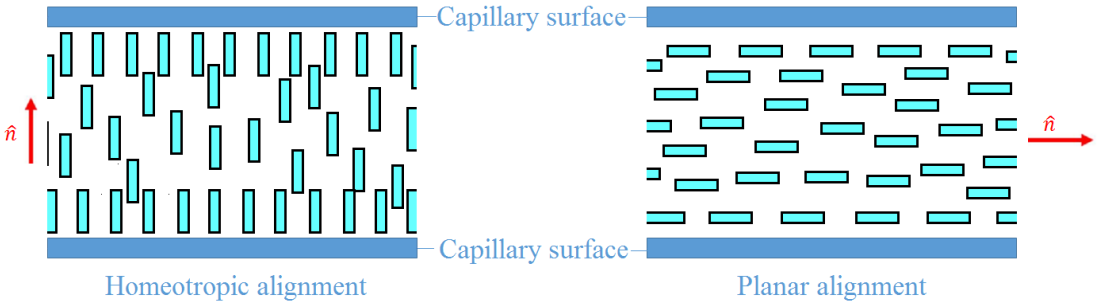

Figure 1.7 Homeotropic and planar alignments of molecules in flat capillaries for a thermotropic nematic liquid crystal sample. Molecules may be sketched as brick-like objects. Because long-molecular axes are, at the same time, local directors of those molecules, local directors are parallel and perpendicular to the phase director, $\vec{n}$, in the homeotropic and planar alignments, respectively. These representations are sketched when well-aligned nematic samples are obtained. Otherwise, the local directors of the micelles are a little bit tilted with respect to the phase director.

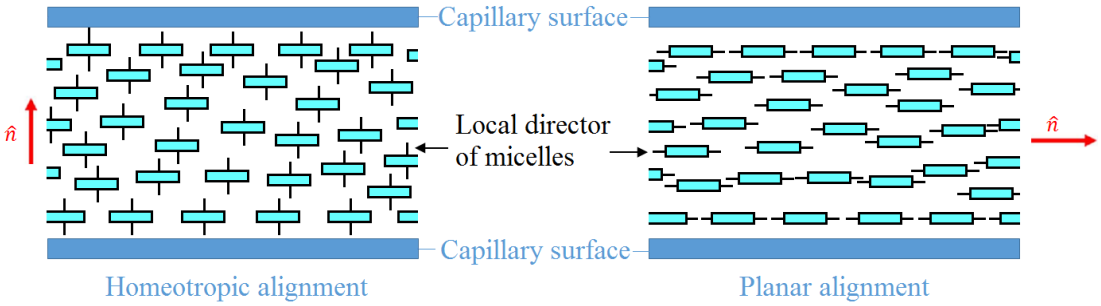

Figure 1.8 Homeotropic and planar alignments of micelles in nematic LLCs. These alignments are sketched when well-aligned nematic samples are obtained. Otherwise, the local directors of the micelles are a little bit tilted with respect to the phase director.

In the literature, three types of lyotropic nematic phases were defined as discotic (N_D), calamitic (N_C) and biaxial (N_B) nematic phases (Neto et al. 1985a, 1985b; Galerne et al. 1987;). While the N_D and N_C phases are uniaxial (one optical axis), the N_B phase is biaxial (two optical axes). Furthermore, it was proved by some studies that the N_B phase is an intermediate phase located between other two uniaxial phases in the phase diagrams (Yu and Saupe, 1980; Bartolino et. al., 1982; Galerne

and Marcerou, 1983; Neto et al. 1985a; Ho et.al., 1991; Filho et.al., 2003; Akpinar et. al., 2012a, 2012b) and uniaxial-to-biaxial phase transitions are of second order as well-described by the mean-field theory (Freiser, 1970; Alben, 1973; Galerne and Marcerou, 1985).

Although lyotropic nematic phases have been studied during last 50 years, some discussions on the micelle shapes in three nematic phases have been still continuing. Indeed, these discussions started between the scientists after the discovery of first lyotropic mixture presenting biaxial nematic phase in 1980 (Yu and Saupe, 1980). Two important models, 'mixtures of cylindrical and disc-like micelles (MCD) model (Stroobants and Lekkerkerker, 1984)' and 'intrinsically biaxial micelles (IBM) model (Neto et.al., 1985a; Galerne et. al., 1987)', were proposed in the literature to explain the formation mechanism of lyotropic nematic phases. The former states that discotic (calamitic) nematic phases consist of disc-like or oblate (cylindrical-like or prolate) micelles and coexistence of the discotic and calamitic nematic phases gives rise to the formation of biaxial nematic phase, Figure 1.9 (Stroobants and Lekkerkerker, 1984). However, up to now, this theoretical prediction has not been supported by experimental results.

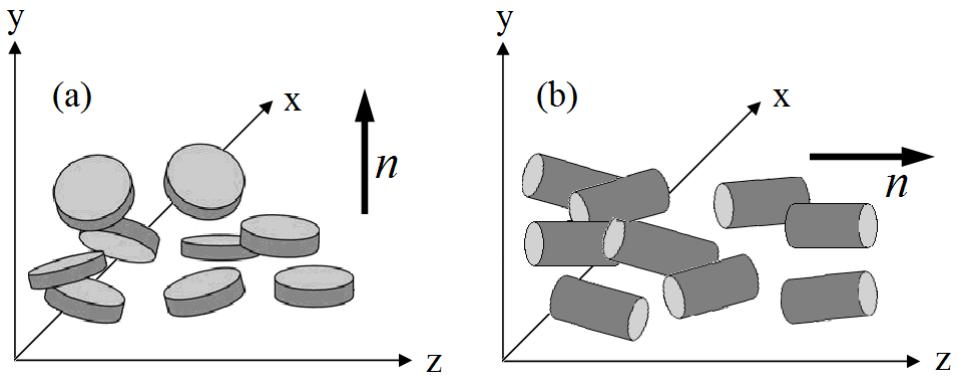

Figure 1.9 (a) Disc-like and (b) cylindrical-like micelles of lyotropic discotic nematic and clamaitic nematic phases, respectively. *n* (phase director) represents the preferred alignment of the individual micelles with their local directors with respect to the magnetic field direction which is along the axis z.

The latter model, IBM, is more reliable model than MCD type models and it was proposed by Neto (Neto et al., 1985a) and Galerne (Galerne et al., 1987). This

model rejects the MCD types models for the formation of not only N_B phases but also N_D and N_C phases. The IBM model assumes two parameters to explain the formation mechanism of lyotropic nematic phases. These parameters are (a) micelle symmetry and (b) orientational fluctuations. In the IBM model, the micelles have orthorhombic symmetry with typical dimensions A', B' and C' and the axes of the coordinate system, fixed in the micelles, as α, β and γ, Figure 1.10a, in the N_D, N_B and N_C phases and different orientational fluctuations are responsible for the occurrences of those phases. Then, the orthorhombic micelles exhibit different orientational fluctuations around/along the symmetry axes for the formation of N_D, N_B or N_C phases. The orientational fluctuations along the symmetry axis γ, which is perpendicular to the largest micelle surface, lead to the formation of the N_D phases, Figure 1.10b. In the N_D phases, the micelle size A' is approximately equal to B' (A'~ B'). Going from the N_D phase to N_B phase by changing temperature, the micelle size along the symmetry axis α elongates (A') and the small amplitude orientational fluctuations along all three axes (1, 2 and 3) give rise to the formation of the N_B phase, Figure 1.10c. By further changing the temperature to obtain N_C phase, the elongation of the micelle size A' along α enhances which favors the orientational fluctuations around the long micellar axis (paralel to the axis z), Figure 1.10d.

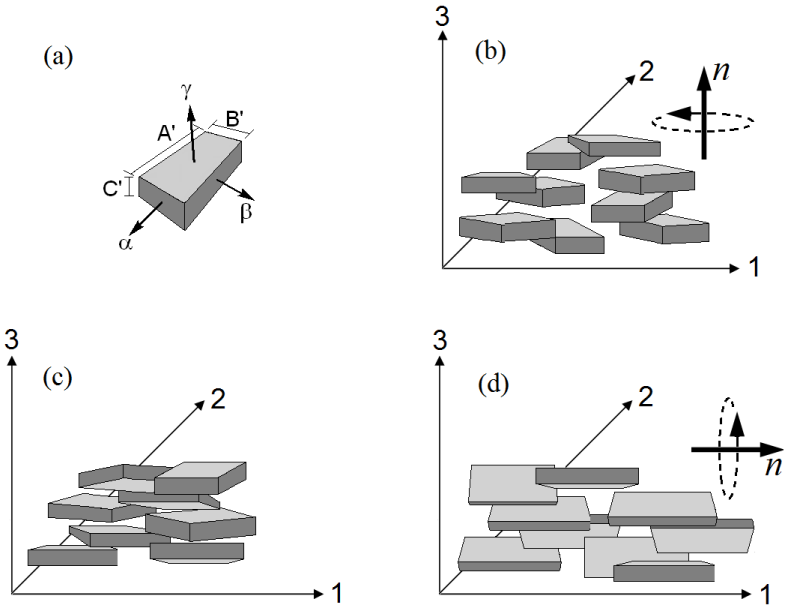

Figure 1.10 (a) Sketch of the orthorhombic micelle in the framework of the IBM model. The surfactant bilayer is represented by C'. (b) N_D, (c) N_B and (d) N_C (Akpinar et.al., 2012a)

1.2.2 Lyotropic Cholesteric Phases

Three different lyotropic cholesteric phases are defined similar to the nematic phases in terms of micelle shapes or symmetry, being discotic cholesteric (Ch_D), biaxial cholesteric (Ch_B) and calamitic cholesteric (Ch_C) phases. There is a long-range orientational order and a short-range translational order like the nematic counterparts. From the sample preparation point of view, they are obtained by either directly using L-enantiomers whose DL-racemic mixtures give nematic phases (Akpinar et al., 2001; Radley and Cattey, 1992), or doping a chiral guest agent into a nematic phase (Lee and Labes, 1984; Reis et al., 2013). Cholesteric phases obtained by the former and latter ways are called 'intrinsic' and 'induced' ones. In the lyotropic cholesteric phases, the micelles are chiralized which causes the formation of 'helical' structure. In this structure, those chiralized micelles are arranged around 'helix axis', Figure 1.11. The helix axis is also optical director of the phases. Cholesteric phases are characterized by two important quantities. They are pitch (*P*) and helical twisting power (*htp*). P and htp are mathematically related by

$$P^{-1} = (\pm)\, htp.x_i \qquad (1.5)$$

where P^{-1} is the reciprocal of the pitch (twist) and x_i is the mole fraction of the L-enantiomer or chiral guest molecule in the lyotropic mixture. The local director of the micelles varies by a constant angle coming from one layer to the next that leads to a helical structure. A 2π rotation of the local director is necessary to regain its original direction. The pitch is given by the linear distance traveled by this 2π rotation of the local director (Ferrarini et.al., 1999; Kuball and Türk, 1999). In Figure 1.11, the rotation of the local director of the micelle corresponds to P/2.

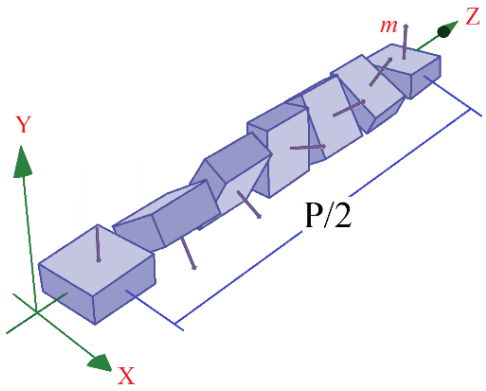

Figure 1.11 Orientation of chiral micelles with their local directors (m) around helix axis which is along z-axis. *m* is the local director of the micelles.

Some models were proposed in the literature to explain the chiral induction mechanism of lyotropic cholesteric phases. These models tried to clarify how chiral molecules conduct their chiralities to the whole phase. In general, two important models are in demand among scientists for the chiral induction mechanism (Radley and Saupe, 1978; Partyka and Hiltrop, 1996; Pape and Hiltrop, 1997). Both models take into account the spatial arrangement of chiralized micelles and intermicellar interactions for the transfer of the chirality of the chiral molecules to form the helical structure. In the first model, which is known as 'a chiral dispersion interaction model', a direct pairwise interaction between one dopant present in a micelle and another dopant in a neighboring micelle gives rise to the occurrence of a chiral dispersion interaction. The basis of the formation of this dispersion interaction depends on Goosen's theory (Goossens, 1970). The second model, so-called a chiral sterical interaction model, assumes the distortion of the non-chiral micelle into the chiralized micelle due to the chirality of the chiral dopant added into a lyotropic mixture presenting a nematic phase. According to this model, the presence of a chiral dopant in the lyotropic nematic mixture leads to the distortion of the achiral micelles of the nematic phase. Then, thermal motions and the collisions of the distorted or chiralized micelles result in the transfer of chirality to the whole phase sterically from one micelle to its neighbours (Partyka and Hiltrop, 1996; Pape and Hiltrop, 1997). Consequently, in the first model, a macroscopic twist arises from the intermicellar interactions, however, in the second model, it arises as a result of the intramicellar twist (Partyka and Hiltrop, 1996). Then, the chiral information is transferred from one micelle to the

adjacent micelle along the helix axis, if the intermicellar interactions are sensitive. The macroscopic twist gives rise to the formation of the fingerprint texture of the chiral nematic phases and it can be easily characterized by a polarizing light microscope, Figure 1.12. Notice that the chiral induction models were proposed assuming the micelles have disc-like shape and cylindrical-like shape in Ch_D and Ch_C phases, respectively. As we mentioned before, taking into account the MCD and the IBM models, there still exist some controversies on micelle shapes in cholesteric phases as well as in nematic phases. However, from the goals of this thesis, we studied just the Ch_D phases and we are not deal with micelle shapes.

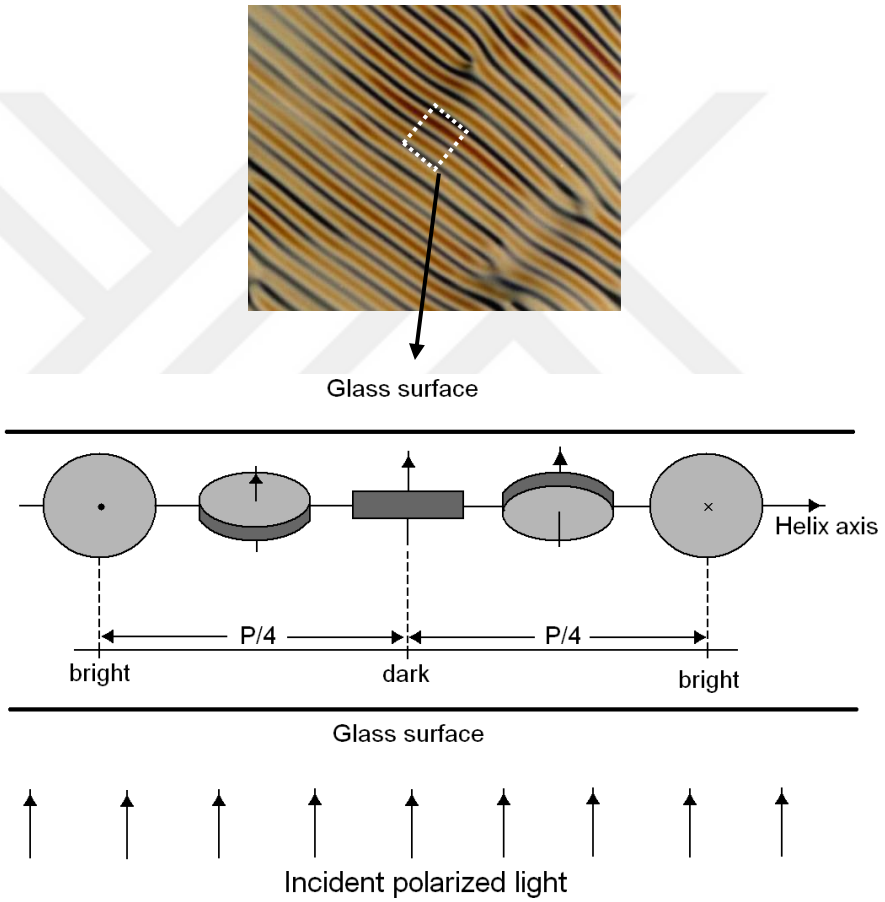

Figure 1.12 Top: The stripes of the well-aligned fingerprint texture (spaghetti-like) of the lyotropic discotic cholesteric phase. Bottom: The arrangement of the micelles along the helix axis and the interaction of the incident polarized light with the micelles. The helix axis is parallel to the glass surface (Akpinar, 2010). In this figure, micelles are assumed to be disc-like in shape. Alternatively, according to the IBM model, micelles may be shown having an orthorhombic symmetry (Figures 1.10 and 1.11).

1.3 Characterization of Lyotropic Nematic and Cholesteric Phases

Lyotropic nematic phases are characterized by their 'schlieren' textures observed under polarizing optical microscope (POM). Figure 1.13 shows some completely non-aligned nematic textures of N_D, N_B and N_C phases. It is too difficult to differentiate the non-aligned lyotropic nematic samples from one another by POM. To do so, the nematic samples are put in a strongly enough magnetic field to obtain uniformly well-aligned textures, Figure 1.14, and their symmetric invariants of tensor order parameters σ_2 and σ_3 are evaluated from the birefringences measurements of the nematic phases by laser conoscopy (Galerne and Marcerou, 1983; Akpinar et.al., 2012a). In the case of the uniaxial nematic phases (N_D and N_C), the invariant σ_3 is related to other one σ_2 by $\sigma_3 = \pm \sigma_2^{3/2}$. When σ_3 is plotted against σ_2 for a lyotropic mixture presenting just N_D (N_C) phase, the positive (negative) dependence of σ_3 with σ_2 is obtained, Figure 1.15a (Figure 1.15b). If a lyotropic mixture exhibits three nematic phases as a function of temperature, σ_3 changes with σ_2 as given in Figure 1.15c. In other words, the measurements of these invariants show that the biaxial phase is an intermediate phase between other two uniaxial ones.

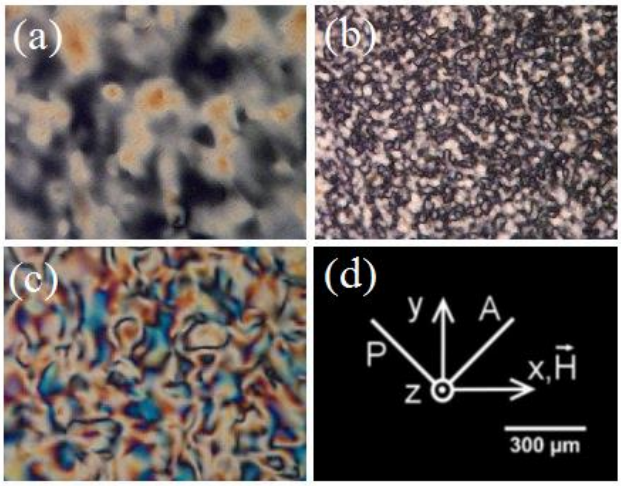

Figure 1.13 The textures of lyotropic (a) N_D, (b) N_B and (c) N_C phases observed under POM. In (a), the dark regions corresponds to partly homeotropically aligned domains. (d) A: analyzer; P: polarizer; x, y and z are laboratory frame axes; H is the magnetic field direction.

Figure 1.14 Uniformly well-aligned POM textures of (a) N_D, (b) N_B and (c) N_C phases.

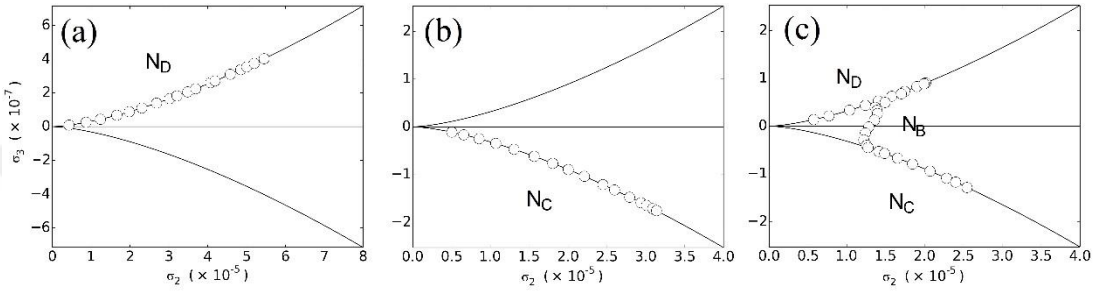

Figure 1.15 σ_3 versus σ_2 plots of lyotropic samples presenting (a) just N_D, (b) just N_C and (c) three nematic phases as a function of temperature. Solid lines in the positive and negative regions of the graphs are theoretically predicted for the uniaxial nematic phases, i.e. N_D and N_C phases, and the experimentally measured data are in good agreement with the theory (Akpinar et.al., 2016b).

Similar to the lyotropic nematic phases, cholesteric ones can also be characterized by their textures under polarizing optical microscope. In general, two types of textures are known as 'fingerprint', Figure 1.16, and 'spaghetti-like', Figure 1.12. Indeed, if the magnetic field is applied to the former one, the well-aligned spaghetti-like texture may be obtained. The textures given not only in Figure 1.12 but also in Figure 1.16 are characteristic for uniaxial Ch_D phases but not for Ch_B and Ch_C phases. Because, in the case of Ch_B phases, the micelles have two-optical axes and the incident light passing through the Ch_B sample is not parallel to the director in the dark regions (see Figure 1.12) observed for the textures of Ch_D phases. The cholesteric stripes cannot be seen in the Ch_C phases because the magnetic field or surface effect give rise to unwinding the helical structure where local director of the micelles are parallel to the helix axis. In Figure 1.17, the textures of the lyotropic sample potassium

laurate (KL)/nonanol/water/brucine are given as examples for three lyotropic cholesteric phases (Reis et.al., 2013).

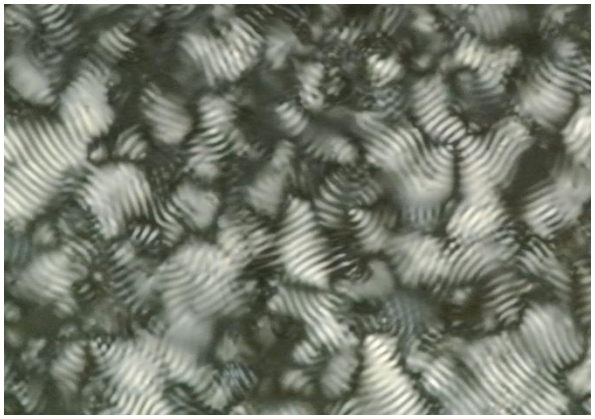

Figure 1.16 Fingerprint texture of a lyotropic discotic cholesteric phase under polarizing optical microscope in the absence of magnetic field.

Figure 1.17 Magnetically well-aligned lyotropic cholesteric textures of (a) Ch_D, (b) Ch_B and (c) Ch_C phases. External magnetic field causes the Ch_C phase unwounded, i.e. helical structure is dissappeared and its texture is similar to N_C phase. The distance between three parallel lines in (a) and (b) is equal to the pitch length, P. In (a) and (b), a green filter (λ=546 nm) was used for the calculation of biaxial order parameter (Reis et.al., 2013).

Biaxial order parameter (ξ) is also used to describe the Ch_B phases. As it is expected the ξ is zero for uniaxial Ch_D phase and it cannot be evaluated for uniaxial Ch_C phase because of the disappearance of the helical structure. For the calculation of the ξ, a green filter is put between the incident light and lyotropic cholesteric sample (Figure 1.17a and 1.17b). Then, the textures are analyzed by a special computer software from the light intensity between two chosen points on the textures, including both dark and bright (stripes) regions. For instance, the evaluated biaxial order parameters for the textures of Figure 1.17a and 1.17b are shown in Figure 1.18b.

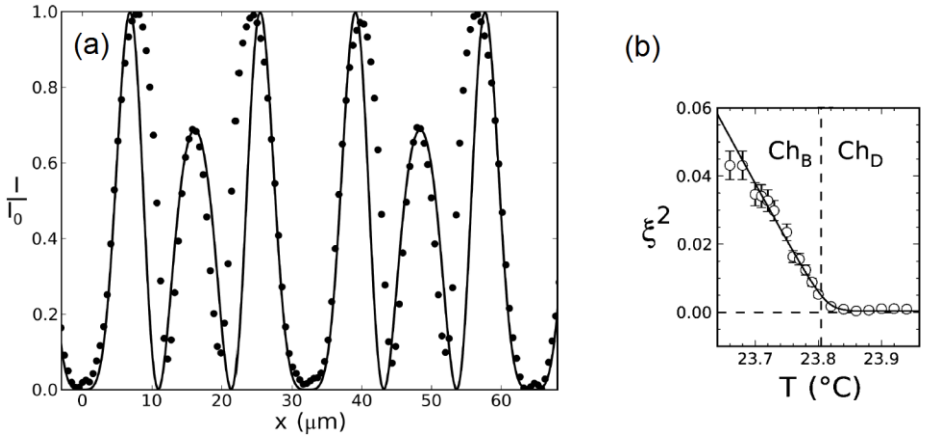

Figure 1.18 For the textures of Ch_D and Ch_B in Figure 1.17, (a) the change in the intensity between two-points on the textures and (b) calculated biaxial order parameters as a function of temperature (de Sant'Ana and Neto, 1992; Reis et.al., 2013).

1.4 Magnetic properties of Lyotropic Nematic and Cholesteric Phases

The director alignment of lyotropic nematic and cholesteric phases is related to the diamagnetic susceptibility anisotropy, $\Delta\chi=\chi_{//}-\chi_{\perp}$, of alkyl chains of the surfactant molecules present in lyotropic liquid crystalline mixtures (Boden et.al., 1981). The diamagnetic susceptibility anisotropy can be greater or smaller than zero (Saupe, 1977; Forrest and Reeves, 1981). In the case of $\Delta\chi>0$ ($\Delta\chi<0$), the director of a uniaxial nematic phase aligns parallel (perpendicular) to the magnetic field direction. For surfactants whose alkyl tail consists of hydrocarbon chains, $\Delta\chi$, is greater (smaller) than zero in the N_C (N_D) phases (Neto and Salinas, 2005). The opposite behavior of diamagnetic susceptibility anisotropies was also reported for surfactants with fluorocarbon tails instead of the hydrocarbon tails (Boden et.al., 1979). In addition to micelle shapes, both uniaxial nematic and uniaxial cholesteric phases are classified with the sign of their $\Delta\chi$s. For instance, if those phases have positive (negative) $\Delta\chi$, they are abbreviated as N_D^+, N_C^+, Ch_D^+ and Ch_C^+ (N_D^-, N_C^-, Ch_D^- and Ch_C^-).

Biaxial nematic (cholesteric) phases are identified with positive and negative $\Delta\chi$, N_{B+} and N_{B-} (Ch_B^+ and Ch_B^-) by taking into account the diamagnetic susceptibilities along three two-fold symmetry axes, being χ_{33}, χ_{22} and χ_{11}, For the biaxial phases, the diamagnetic susceptibility anisotropy is defined as:

$$\Delta\chi = \chi_{33} - \frac{\chi_{11} + \chi_{22}}{2} \tag{1.6}$$

When $\Delta\chi>0$ ($\Delta\chi<0$), the largest (smallest) diamagnetic susceptibility is larger (less) than the average of the diamagnetic susceptibilities of other axes and the biaxial phase aligns parallel (perpendicular) to the magnetic field direction (Filho et al. 2003; Akpinar et al., 2014).

1.5 Fluorinated and Hydrogenated Surfactants in Micellar Systems

Surfactants whose alkyl chains are fully hydrogenated, Figure 1.19a, partly fluorinated, Figure 1.19b, or fully fluorinated (perfluorinated), Figure 1.19c, exhibit different properties. The existence of $-CF_2-$ groups in the surfactant hydrophobic chains leads to a dramatic change in micellar properties with respect to the hydrogenated counterpart surfactants. For instance, the cmc values of perfluorinated surfactants are much lower than those of hydrogenated ones (Asakawa et.al., 2006). Furthermore, perfluorinated surfactants have higher surface activity than hydrogenated counterparts, resulting in the reduction of the surface tension of water to ~15-20 mN/m by the former and ~30-40 mN/m by the latter ones (Krafft, 2001).

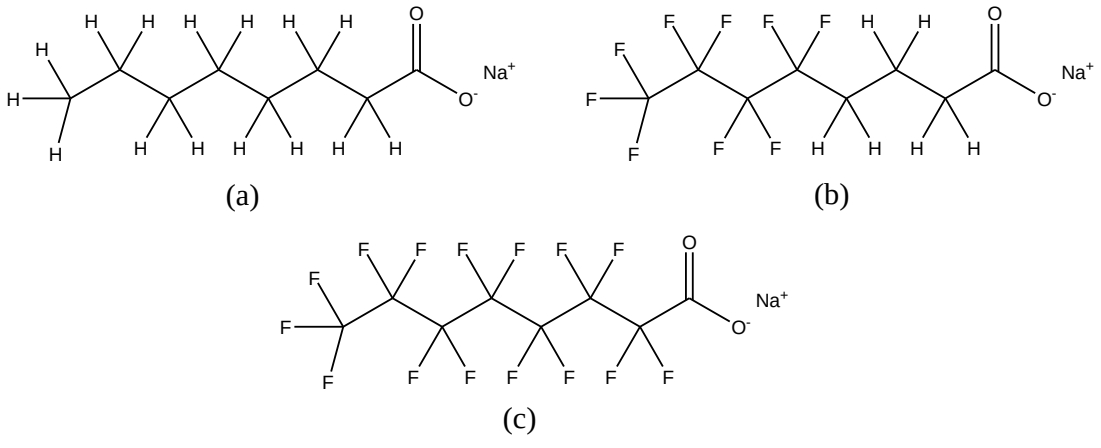

Figure 1.19 (a) Fully hydrogenated surfactant sodium octanoate, (b) partly fluorinated sodium 2H,2H,3H,3H,4H,4H-perfluorooctanoate and (c) fully fluorinated sodium perfluorooctanoate.

Because the hydrophobic effect plays a key role on the micellization and fluorinated surfactants have lower cmc than hydrogenated ones, fluorinated surfactants are more hydrophobic than hydrogenated surfactants (Sakai et.al., 2014). The hydrophobicity of a $–CF_2–$ group in perfluoroalkyl chain, in general, is found to be approximately 1.5 times larger than that of $–CH_2–$ group in hydrocarbon chain (Shinoda et.al., 1972; Shinoda and Nomura, 1980; Ravey et.al., 1988). For instance, at 303 K, while the cmc value of sodium perfluorooctanoate, 0.0302 mol/kg, (Figure 1.19c) is very similar to that of sodium dodecanoate, 0.0261 mol/kg, however, it is very different than that of sodium octanoate 0.3733 mol/kg (Figure 1.19a) (Blanco et.al., 2005). Similar results were also reported for some other fluorinated and their hydrogenated surfactants (Kissa, 1994; Carmelita et.al., 2011). As it is expected, the difference in the hydrophobicities of fluorinated and hydrogenated surfactants arises from the low polarizability of the fluorine atoms (Kissa, 1994). The relatively lower cmc of fluorinated surfactants is also attributed to the strong hydrophobic interactions and low van der Waals interactions between fluorocarbon chains of the fluorinated surfactants with respect to the hydrogenated surfactants (Krafft, 2001). In other words, these two interactions make the micellization of the fluorinated surfactants more favored than that of the hydrogenated ones.

From the micellization properties point of view, the $CF_2 \approx 1.5CH_2$ rule is not valid for partly fluorinated surfactants, for example the surfactant given in Figure 1.19, (Sadtler et.al., 1998; Krafft, 2001; Sakai et.al., 2014; Polidori et.al., 2016). So, partly fluorinated surfactants cannot be assumed as the counterparts of the hydrogenated surfactants by taking into account $CF_2 \approx 1.5CH_2$, i.e. sodium 2H,2H,3H,3H,4H,4H-perfluorooctanoate is not a counterpart of sodium dodecanoate.

In addition to the hydrogenated surfactants, fluorinated surfactants are used in other micellar systems, lyotropic liquid crystals. Some lyotropic nematic, cholesteric and lamellar phase properties of fluorinated surfactants, such as cesium perfluorooctanoate (Dawin et.al., 2010), L-alanine partly fluorinated ester (Acimis and Karaman, 2006), lithium perfluorooctanoate (Long et.al., 2012), were reported in the literature. However, the investigation of lyotropic liquid crystalline properties of the fluorinated surfactants have been remained limited with respect to the hydrogenated surfactants.

The steric effect of fluorine atom has to be taken into account not only for isotropic micellar solution properties but also lyotropic liquid crystalline properties. Because the fluorine atom has larger volume than hydrogen atom, the fluoroalkyl chains are less flexible (more rigid) and stiff well in the micelles with respect to the hydrocarbon chains (Krafft, 2001). In this rigid structure of the fluoroalkyl chains, the steric hindrance is minimized by the formation of a helical conformation in the alkyl chains of fluorinated surfactants (Krafft, 2001; Rigby and Bunn, 1949; Furukawa et.al., 1952). It means that fluorinated chains form a helical twist along the chain (Rosoff, 2001).

2. AIM AND SCOPE OF THE STUDY

Cholesteric phases are one of the most common structures of lyotropic liquid crystals. They differ from their nematic counterparts since they show a helical structure with finite pitch. Although their thermotropic counterparts have been used in electro-optical devices such as liquid crystal displays, optical imaging, thermometers etc. (Coates, 2015), however, lyotropics have potential applications in biotechnology (Neto and Salinas, 2005). For instance, some studies in the literature stated that lyotropic cholesteric phases were used for delivering drugs such as Cromolyn (Cox et.al., 1971; Hartshorne and Woodard, 1973; Stephenson and Diseroad, 2000). Some models were proposed to understand the chiral induction mechanism (Radley and Saupe, 1978; Partyka and Hiltrop, 1996; Pape and Hiltrop, 1997), however, it was not completely understood yet.

From the lyotropic mixture preparation point of view, two types of cholesteric families are identified. If a chiral guest molecule (e.g. brucine) is added to a lyotropic host mixture of an achiral surfactant, which exhibits a nematic phase, the "induced or extrinsic" cholesteric phase is obtained (Lee and Labes, 1984; Reis et al., 2013). In the case of "intrinsic" cholesteric phase, an enantiomeric surfactant such as potassium N-dodecanoyl-L-alaninate may be used to form the cholesteric lyotropic mixture (Akpinar et al., 2001; Radley and Cattey, 1992). These two cholesteric families (intrinsic and extrinsic) have been widely studied in the literature to understand the chiral induction mechanism. Comparing both families, the enantiomeric surfactants in the intrinsic cholesteric phases, in general, transfer their chiralities to the whole structure with shorter (higher) helical pitch length (helical twisting power) with respect to the chiral guest molecules in the induced cholesteric phases (Akpinar et.al., 2013).

It is known that the racemic DL-forms of the enantiomeric surfactants originates nematic phases (Akpinar et.al., 2014a). So, keeping the compositions of the lyotropic mixtures D- or L-enantiomeric surfactants and their DL-racemic forms the same, the differences observed between DL-racemic nematic phase and D/L-cholesteric phase should come from the chirality of the enantiomers. Though, the information obtained from the intrinsic cholesteric phases are very interesting and, in some aspects, complementary to those from the induced ones. The reason is that while the number of molecules of constituents in the lyotropic mixture of intrinsic cholesteric phases is same as that of racemic nematic one, the addition of chiral dopant into the

mixture changes not only the number of the molecules but also the packing of the surfactants in the micelles, as a result of the dopant localization in the micelles or at the micelle surfaces.

For several years, researchers have been trying to understand the chiral induction mechanism by means of studying the effects of some factors that affect the transfer of the chirality of the chiral molecule to the phase (Gottarelli and Spada, 1985; Gottarelli vd., 1983a, 1983b; Spada et.al., 1988; Ferrarini and Nordio, 1992, 1998; Ferrarini et.al., 1992, 1994, 1995, 1996a, 1996b; Berardi et.al., 1998; Pieraccini et.al., 2008; Akpınar et.al., 2013, 2014b). Of course, because the structural units of lyotropic liquid crystals are micelles, these factors play important roles on the chirality via eventual changes in the micellar structures. For instance, when an electrolyte concentration is increased in the mixture, the helical pitch length increases, (Dawin et.al., 2010). It is known that the addition of electrolytes in isotropic dilute micellar solutions (Israelachvili, 1991; Lin et.al., 1994; Sein and Engberts, 1995; Aswal and Goyal, 2000; Umlong et.al., 2006; Hooshyar and Sadeghi, 2015) and also in lyotropic liquid crystals (Dawin et.al., 2009) causes micellar growth. Indeed, the addition of an electrolyte into a lyotropic mixture presenting cholesteric phase decreases the repulsions between the surfactant head groups at the micelle surfaces and hinders the solubilization of chiral guest molecule in the micelles, which leads to lowering the helical twist (Dawin et.al., 2010).

The micellar growth by the addition of the electrolytes arises from the interactions between the ionic species, ions of the electrolytes and the polar or ionic head groups of the surfactants at the micelle surfaces. However, according to our recent studies on lyotropic nematic phases, the modifications in the interior of the micelles also provide the micellar growth (Akpinar et.al., 2016a, 2017). If the surfactant alkyl-chain length is increased, keeping the same surfactant head group, for instance, potassium undecanoate and potassium dodecanoate, the maximum birefringences of the nematic phases are approximately doubled for the surfactant with the longer alkyl chain length by the addition of just one $–CH_2$ group. The bigger the birefringences mean the higher the micellar shape anisotropy that may imply in micellar growth. Consequently, two factors, i.e. addition of the electrolyte in the lyotropic mixture and the surfactant alkyl chain length, have to be taken into account when studying lyotropic systems.

In the literature we find studies discussing the chiral induction mechanism in the presence of chiral molecule in the lyotropic mixtures (Dörfler, 2002). Among them, in 2006, Acimis and Karaman (Acimis and Karaman, 2006) investigated the helical twisting power of some cholesteric phases of L-enantiomeric esters with fully hydrogenated aliphatic alkyl chain by comparing them with their partly fluorinated counterparts. They chose L-alaninehydrochloride dodecylester (L-ADDE) and L-serinehydrochloride dodecylester (L-SDDE) and their fluorinated counterparts L-alaninehydrochloride 1H,1H,2H,2H-perflourooctylester (L-APFOE) and L-serinehydrochloride 1H,1H,2H,2H-perflourooctylester (L-SPFOE). They studied the cholesteric phases to understand the effect of $-CF_2$ groups on the chirality assuming that L-ADDE (L-SDDE) is a counterpart of L-APFOE (L-SPFOE). Still according to the literature, the condition for a hydrogenated surfactant to be a counterpart of a fluorinated one is that both surfactants have to exhibit approximately the same critical micelle concentrations (cmc), obtained from their isotropic diluted binary surfactant/water solutions (Kissa, 1994; Blanco et.al., 2005; Carmelita et.al., 2011). Due to the energy contribution of each CH_2 or CF_2 group in the surfactant alkyl chain to the micellization (indeed, to the micellization Gibbs energy), one CF_2 group corresponds to almost 1.5 CH_2 for the surfactants with the same head groups (Shinoda et.al., 1972; Shinoda and Nomura, 1980; Ravey et.al., 1988). Thus, for instance, it is expected that the cmc of sodium dodecanoate (0.0261 mmol/kg) is similar to that of sodium perfluorooctanoate (0.0302 mmol/kg) (Blanco et.al., 2005). However, the cmcs of partly fluorinated surfactants are different than those of fully hydrogenated ones (Sadtler et.al., 1998; Krafft, 2001; Sakai et.al., 2014; Polidori et.al., 2016). So, partly fluorinated L-APFOE (L-SPFOE) could not be the counterpart of fully hydrogenated L-ADDE (L-SDDE). Acimis and Karaman (Acimis and Karaman, 2006) already showed that those molecules are not counterparts one to another because the partly fluorinated L-APFOE and L-SPFOE surfactants have approximately two times higher cmc values than L-ADDE and L-SDDE (Olutas and Acimis, 2012). In other words, wrong surfactant molecules were chosen for the comparison as was aimed in that study related to the lyotropic cholesteric phases (Acimis and Karaman, 2006). So, the results obtained from lyotropic cholesteric phases have serious problems and the Ref. (Acimis and Karaman, 2006) includes some crucial doubts on understanding the chiral induction mechanism as discussed in that reference.

In this study, we aimed to investigate the cholesteric phase behavior of partly fluorinated surfactants by comparing them with their exact hydrogenated counterparts. To do so, we synthesized some novel hydrogenated and partly fluorinated surfactants in addition to the ones given in the Ref. (Acimis and Karaman, 2006). All surfactants were studied via electrical conductivity measurements on their diluted isotropic binary solutions to determine their cmcs and lyotropic liquid crystalline properties from both polarizing optical microscopy for textural analysis and laser diffraction for sensitive pitch measurements.

3. EXPERIMENTAL

All chemicals (sodium dodecylsulfate, undecanoic acid, dodecanoic acid, DL-alanine, L-alanine, DL-serine, L-serine, 1-undecanol, 1-dodecanol, 1H,1H,2H,2H-perfluorooctanol, chlorosulfonic acid, sodium carbonate, sodium chloride, sodium sulfate, potassium hydroxide, sulfuric acid, chromium VI oxide, carbon tetrachloride, ethanol, butanol, acetone, ethyl acetate and diethylether) were commercially purchased from Sigma, Merck, Aldrich and Alfa-Aesar in high purities (99%), except that 1H,1H,2H,2H-perfluorooctanol was of 97%. Ultrapure water was provided by Millipore Direct-Q3 UV (18.2 MΩ.cm of resistivity at 25ºC) for the preparation of isotropic micellar solutions and lyotropic liquid crystal samples.

Some basic laboratory equipments such as rotatory evaporator (Heidolph Hei-Vap), electronic balance (Radwag, five digits), vortex (IKA 4 basic), centrifuge (Hettich Zentrifugen EBA 20), magnetic stirrer (Heidolph MR Hei-End.) were used for all experimental measurements and surfactant syntheses. To keep the surfactants dry, they were kept in a vacuum oven (Nüve EV 018) connected to a vacuum pump (Vacuubrand 2.5).

A HeNe laser (Newport, 633 nm, 12.0 mW, 500:1 Polarization, USA), a Nikon Eclipse E200POL (Japan) microscope, Mettler-Toledo (S470 SevenExcellence) electrical conductivity meter were used in the laser diffraction, microscopic (polarizing optical microscope) and conductivity measurements, respectively. Flat capillaries of 0.2 mmx5.0 mm and 0.3 mmx5.0 mm (in thickness x length) were purchased from Vitrocom for POM measurements. A Lakeshore 335 temperature controller with an accuracy of 0.001ºC provided sensitive temperature control in laser diffraction measurements.

3.1 Synthesis of Surfactants

Totally 18 chiral and achiral surfactants were synthesized in the scope of the thesis. These surfactants are given in Table 3.1 one with their short abbreviations. Their synthesis procedures are given in the further parts.

Table 3.1 Synthesized chiral and achiral surfactants. C/A: Chiral surfactant/Achiral surfactant.

Surfactant	**Abbreviation**	**C/A**
Potassium undecanoate	KC11	A
Potassium dodecanoate	KC12	A
Potassium 2H,2H-perfluorooctanoate	KPFO	A
Sodium undecylsulfate	NaC11S	A
Sodium dodecylsulfate	NaC12S	A
Sodium 1H,1H,2H,2H-perfluorooctylsulfate	NaPFOS	A
DL-alaninehydrochloride undecylester	DL-AUnDE	A
L-alaninehydrochloride undecylester	L-AUnDE	C
DL-alaninehydrochloride dodecylester	DL-ADDE	A
L-alaninehydrochloride dodecylester	L-ADDE	C
DL-alaninehydrochloride 1H,1H,2H,2H-perfluorooctylester	DL-APFOE	A
L-alaninehydrochloride 1H,1H,2H,2H-perfluorooctylester	L-APFOE	C
DL-serinehydrochloride undecylester	DL-SUnDE	A
L-serinehydrochloride undecylester	L-SUnDE	C
DL-serinehydrochloride dodecylester	DL-SDDE	A
L-serinehydrochloride dodecylester	L-SDDE	C
DL-serinehydrochloride 1H,1H,2H,2H-perfluorooctylester	DL-SPFOE	A
L-serinehydrochloride 1H,1H,2H,2H-perfluorooctylester	L-SPFOE	C

3.1.1 Synthesis of KC11 and KC12

To the solution of 0.58 mole of undecanoic acid in 150 mL of ethanol in a beaker, 0.58 mole of potassium hydroxide (KOH) solution in 100 mL ethanol was added step by step under strong stirring with a magnetic stirrer at room temperature of ~25°C. During the neutralization reaction of the undecanoic acid, the solution pH was controlled by pH-meter by keeping it in the range of 10.40-10.80 with 10% ethanolic KOH solution about 2 hours (Berejnov, et. al., 2000). KC11 was completely precipitated as white crystals at room temperature. The white precipitate KC11 was filtered off from ethanol and washed with ether to remove impurities. Then, the white product was dissolved into hot toluene for removing non-neutralized undecanoic acid from KC11, which could rarely remain in the solution without neutralizing. This is very important key point for the preparation of isotropic micellar solutions and lyotropic liquid crystalline samples for obtaining the reproducible and reliable results. Hot toluene solution was filtered off from the KC11 under vacuum and then washed with diethyl ether several times. The KC11 was recrystallized from ethanol at least two times, filtered off, washed with diethyl ether and dried in a vacuum oven during a few days (yield 80-85%). The characterization of KC11 was performed by FT-IR spectroscopy. As was shown in the literature (Berejnov, et al., 2000), the disappearance of carbonyl absorption peak (1700 cm^{-1}) of carboxylic acid and appearance of carboxylate ($-COO^-$ at 1550 cm^{-1}) peak in the IR spectrum of the final product KC11 showed that all non-neutralized undecanoic acid was completely removed from KC11. The KC12 surfactant was synthesized and purified by the same manner, except that dodecanoic acid was used as an initial carboxylic acid instead of undecanoic acid. For an example, FT-IR spectrum of KC12 was given in Figure 3.1.

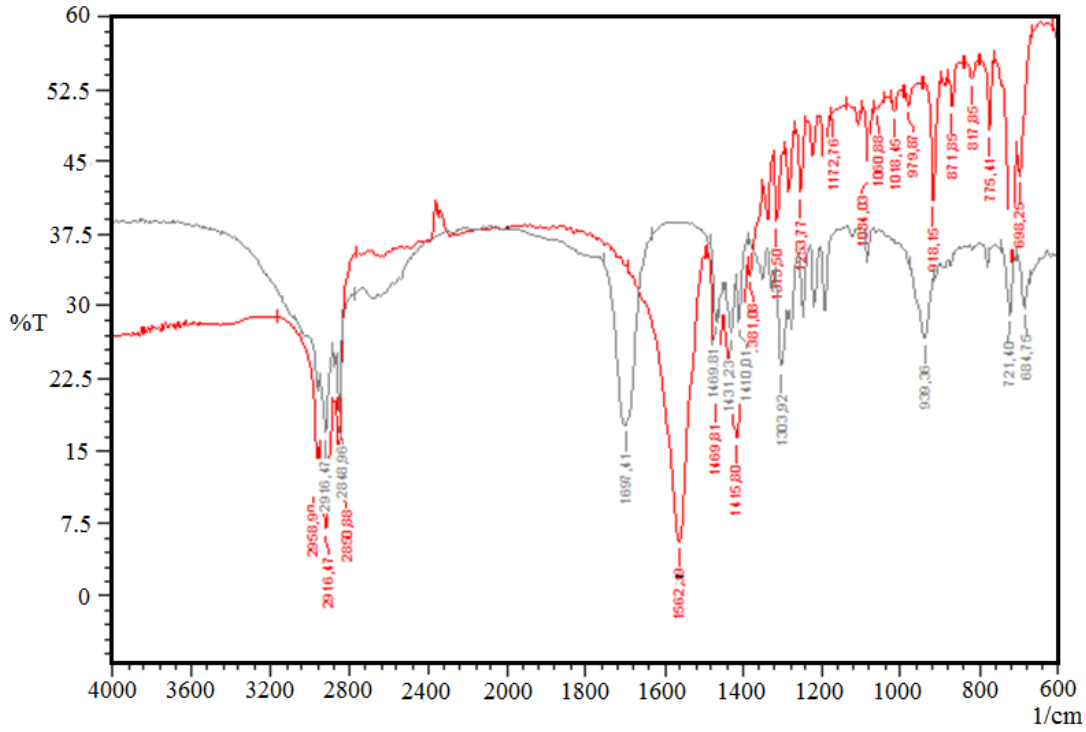

Figure 3.1 Infrared spectra of potassium dodecanoate (KC12, red) and dodecanoic acid (grey).

3.1.2 Synthesis of KPFO

Synthesis of KPFO consisted of two steps. In the first step, 1H,1H,2H,2H-perfluorooctanol was oxidized to 2H,2H-perluorooctanoic acid (2H,2H-PFOA). In the second step, the latter was neutralized with KOH to obtain the final product KPFO.

2H,2H-perfluorooctanoic acid was obtained from the 1H,1H,2H,2H-perfluorooctanol by using freshly prepared Jones's reagent (Achilefu et. al., 1995; Sanchez-Dominguez et. al., 2008). 75 mL H_2SO_4 was carefully added to a solution of chromium (VI) oxide (1.25 mole in 350 mL water). In a round-bottom flask, 0.165 mole solution was prepared in 300 mL acetone and 100 mL ether and, the Jones's reagent was added dropwise to this solution until a persistent red-brown solution was obtained. After addition of the Jones's reagent and obtaining the red-brown solution, the last solution was extracted with 10x100 mL ether. Then, the ether extracts were combined and washed with water 3x200 mL water. Na_2SO_4 was added into the ether phase as a drying agent to remove trace amount of water. The drying agent was filtered

off and the solvent ether was evaporated by a rotatory evaporator. The final product 2H,2H-perfluorooctanoic acid was recrystallized from CCl_4 two times and it was well dried in a vacuum oven. The FTIR spectrum of 2H,2H-PFOA was very similar given in the literature (Achilefu et.al., 1995), Figure 3.2, i.e. 2H,2H-PFOA exhibited peaks at 3072 (3080) cm^{-1}, 1724 (1720) cm^{-1} and 1249-1186 (1230-1190) cm^{-1} for −OH, −C=O and $-CF_2$, respectively. The numbers in the parentheses are literature values. In the second step, 2H,2H-PFOA was neutralized with KOH similar to the KC11 or KC12 to obtain KFPO. The FTIR spectrum of KPFO is given in Figure 3.3.

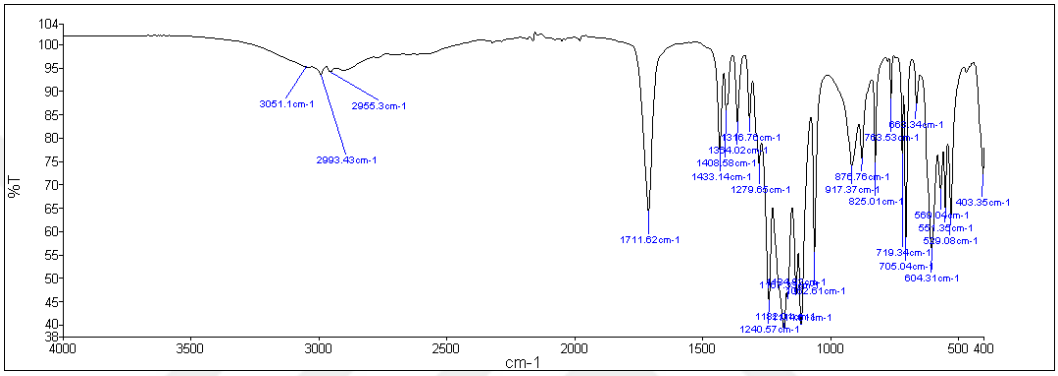

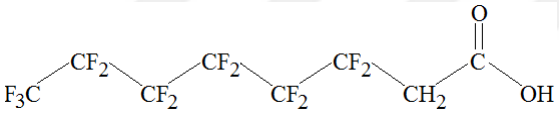

Figure 3.2 FT-IR spectrum of 2H,2H-PFOA.

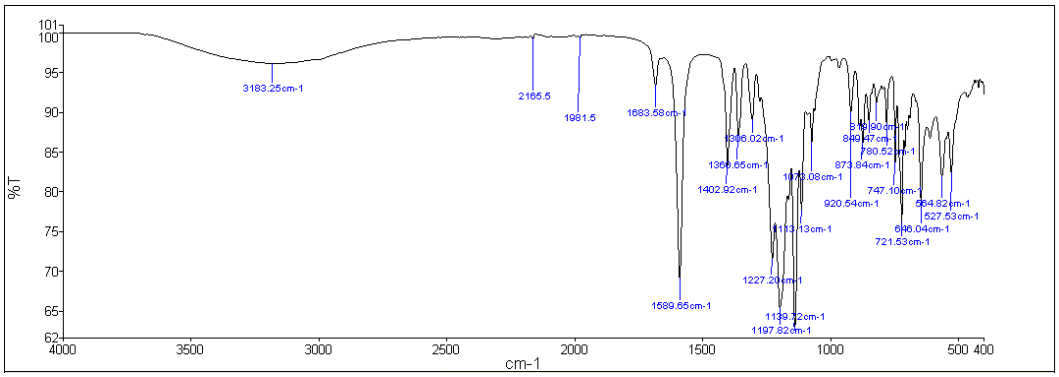

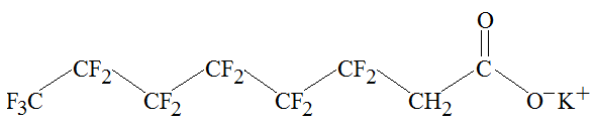

Figure 3.3 FT-IR spectrum of KPFO.

3.1.3 Synthesis of NaC11S and NaPFOS

Synthesis procedure of surfactant NaC11S is well-known in the literature (Dreger et al., 1944). The reaction procedure of the NaC11S was completed by two steps, Figure 3.4 In the first step, long chain alcohol, undecanol, is reacted with 1-chlorosulfonic acid to give mid-product undecylhydrogensulfate. In the second step, the addition of Na_2CO_3 into the reaction mixture gives the formation of the product NaC11S. The synthesis procedure of NaC11S is given below.

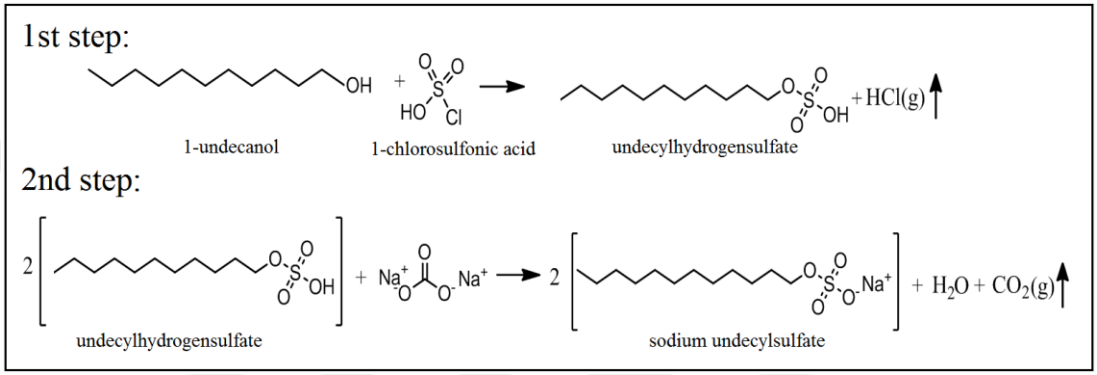

Figure 3.4 Reaction mechanism of NaC11S.

0.085 mole of 1-undecanol was dissolved in 33 mL of CCl_4 in a beaker and the reaction temperature was kept ~5°C with an ice bath. To the solution of 1-dodecanol, 6.7 mL of $ClSO_3H$ was added dropwise and the sulfonation reaction was completed in 5 min. Then, the reaction mixture was stirred at 5°C for an hour until all HCl gas evolution ceased. It means that the reaction between 1-undecanol and chlorosulfonic acid to give undecylhydrogensulfate was completed (step 1). By keeping the reaction mixture at ~5 °C, 57.2 mL of 1-Butanol was added into the reaction mixture and mixed well for the formation of homogenous mixture. Then, the solution of sodium carbonate 0.102 in 30 mL of distilled water was carefully added into the last solution at 5°C to control the CO_2(g) evolution produced during the neutralization of undecylhydrogensulfate to give product sodium undecylsulfate. After all CO_2 (g) has evolved, the reaction was stopped (step 2). The solution was transferred into a flask and concentrated by rotatory evaporator to remove the solvents (CCl_4, butanol and water) from the product. To the concentrated solution, ethyl acetate was added and then cooled in the deep freeze. The white product sodium undecylsulfate (NaC11S)

was filtered off under vacuum, washed with diethyl ether and then recrystallized from ethanol/ethyl acetate mixture two times. The FT-IR spectrum of the synthesized NaC11S was given in Figure 3.5.

NaPFOS was also synthesized by the same manner, except that 1H,1H,2H,2H-perfluorooctanol was used instead of 1-undecanol and characterized by FT-IR, Figure 3.6.

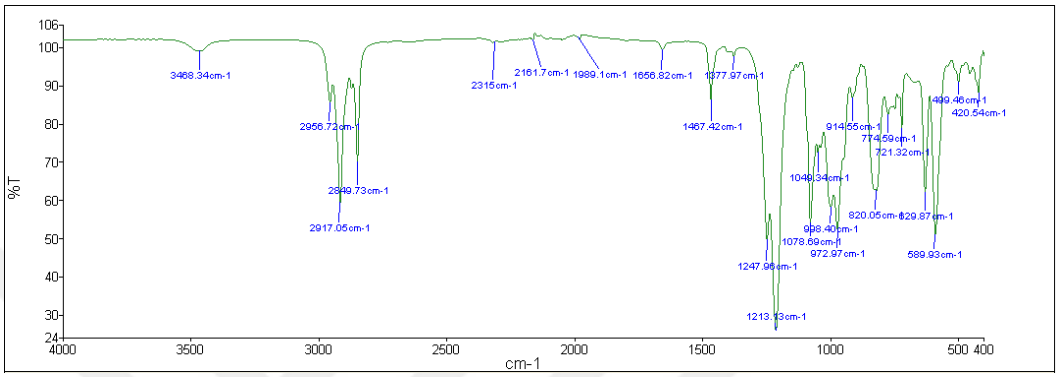

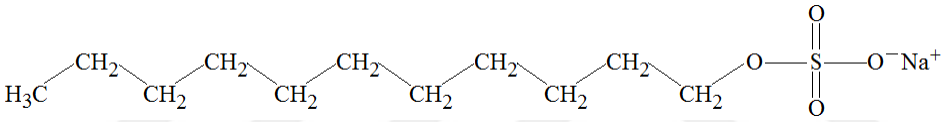

Figure 3.5 FT-IR spectrum of NaC11S.

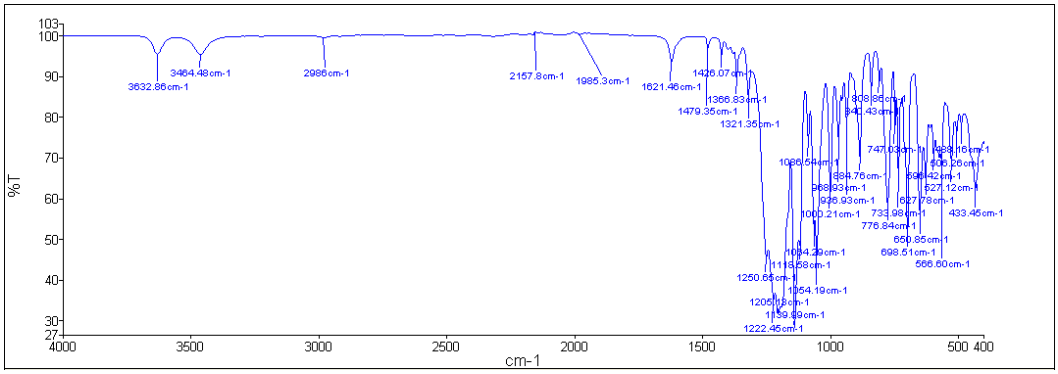

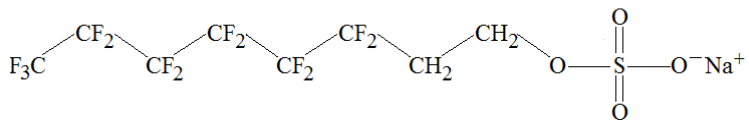

Figure 3.6 FT-IR spectrum of NaPFOS.

3.1.4 Synthesis of Alanine and Serine Hydrogenated Ester Surfactants

All hydrogenated alanine and serine ester surfactants were synthesized according the the well-known procedure reported in the literature (Acimis and Reeves, 1980; Acimis and Akpinar, 2003). The synthesis of DL-AUnDE is given below as an example and other hydrogenated ester surfactants were obtained by the same procedure.

1 mole of 1-undecanol was placed in a 3-necked round bottom flask and the temperature was controlled by putting the 3-necked flask in a glycerine bath. Before adding the DL-alanine, HCl(g) produced from the reaction of NaCl(s) with H_2SO_4(aq) was passed through 1-undecanol at a temperature range of 75-77°C during 15 min. Then, by stirring 1-undecanol and passing the HCl(g), DL-alanine was added in small parts in ~7 hours. Within this time, all DL-alanine reacted with 1-undecanol and a yellowish solution was obtained. Passage of HCl(g) was stopped and the reaction solution was kept overnight at 75-77°C. Next day, the HCl(g) was passed through the reaction solution during ~6 hours and then the gas passing was stopped and the temperature was decreased to the room temperature. The reaction flask was connected to water pump to provide a vacuum of 17-18 mmHg and excess amount of HCl(g) was removed from the solution. Diethylether was added into the solution until the product DL-AUnDE was precipitated in the flask and kept overnight in the deep-freeze. The white product DL-AUnDE was separated from excess amount of 1-undecanol by filtering under vacuum and washed with ether several times. The solid product was dried and recrystallized from ethylacetate at least two times. The final purified product DL-AUnDE was well dried in a vacuum oven and characterized by FT-IR, Figure 3.7, which is in a good agreement with the literature (Sivaramakrishna and Swamy, 2015). Other chiral and achiral alanine (L-AUnDE, DL-ADDE, L-ADDE) and serine (DL-SUnDE, L-SUnDE, DL-SDDE, L-SDDE) hydrogenated surfactants were synthesized by the same procedure, using the appropriate starting alcohols, and characterized by FT-IR, Figure 3.8-3.14.

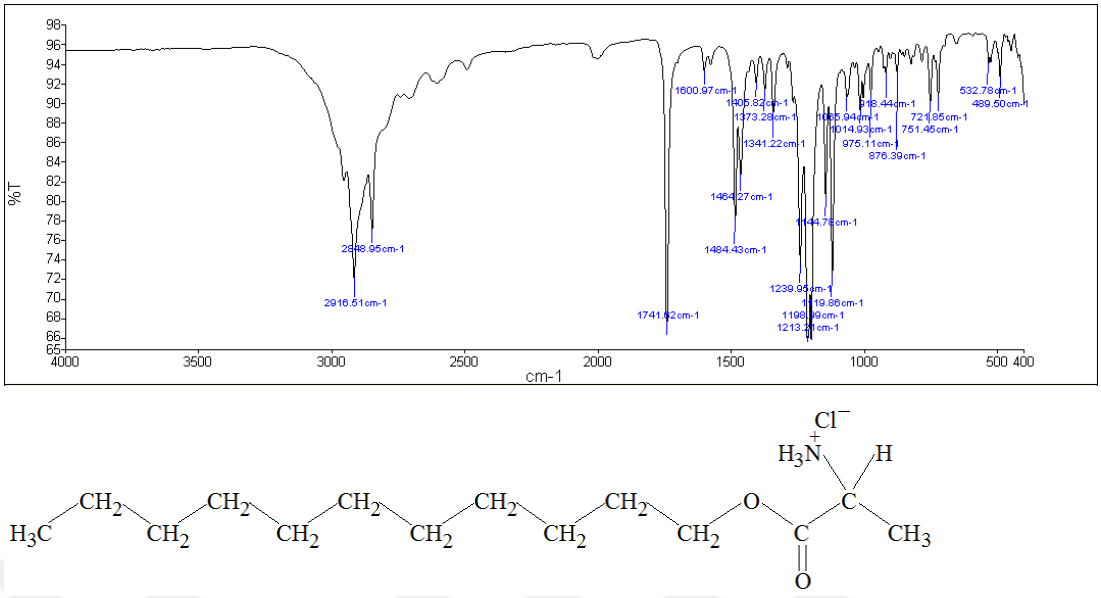

Figure 3.7 FT-IR spectrum of DL-AUnDE.

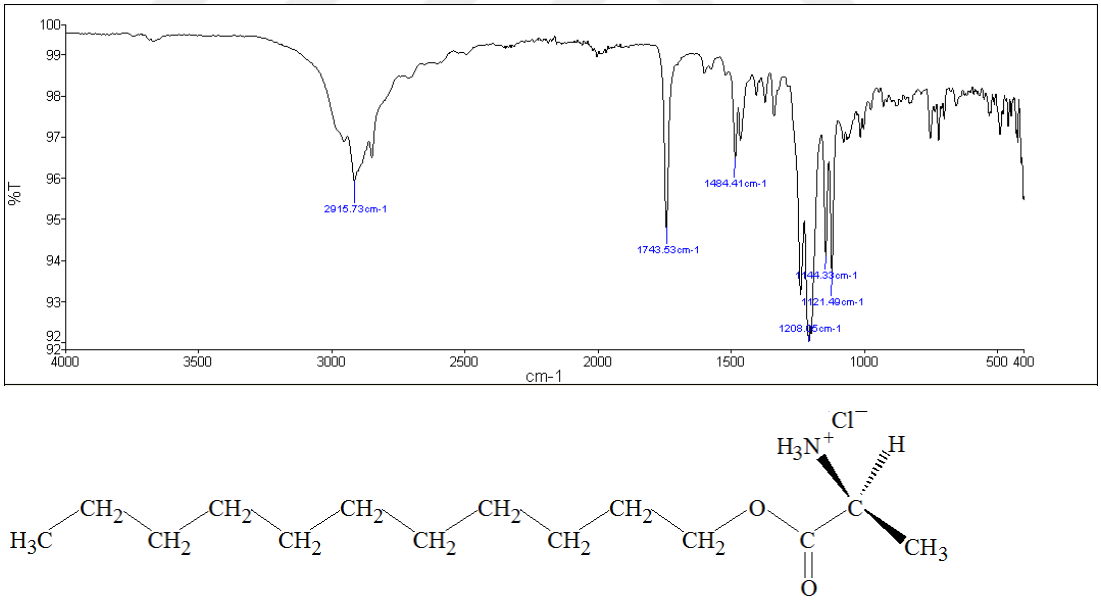

Figure 3.8 FT-IR spectrum of L-AUnDE

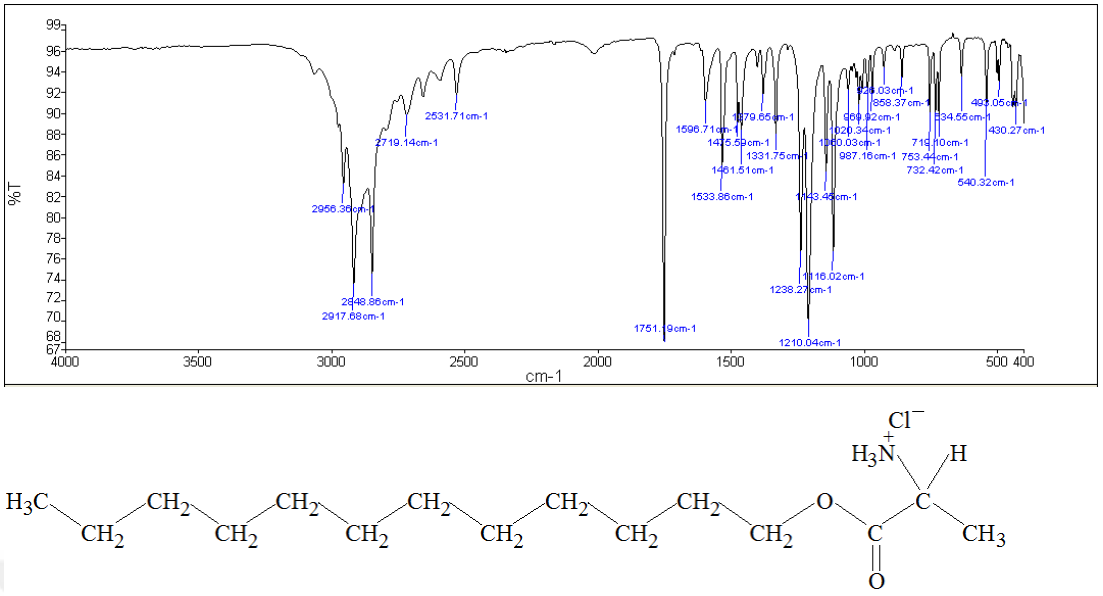

Figure 3.9 FT-IR spectrum of DL-ADDE

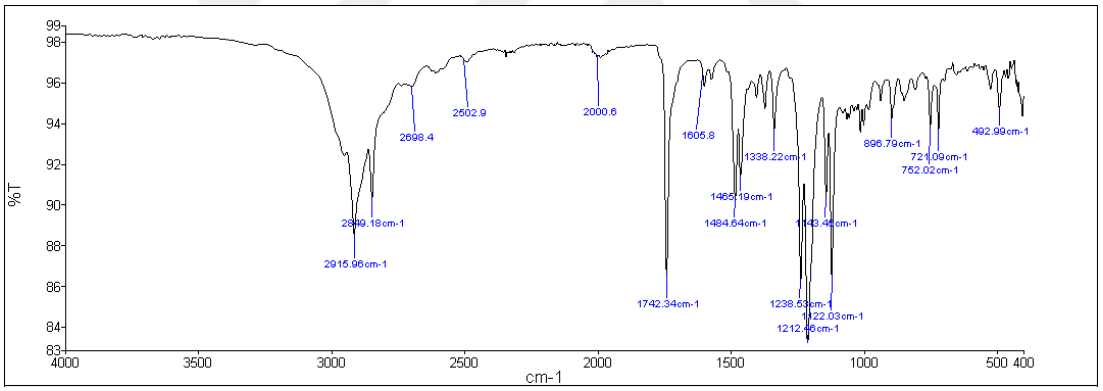

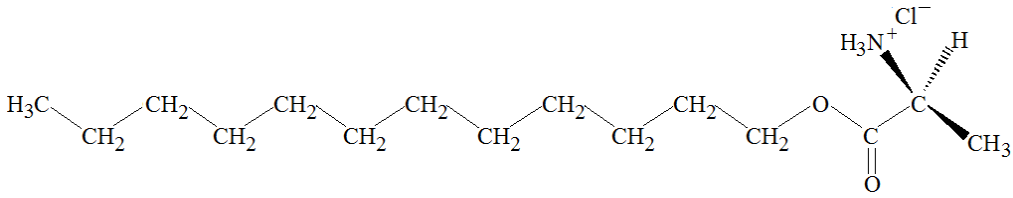

Figure 3.10 FT-IR spectrum of L-ADDE

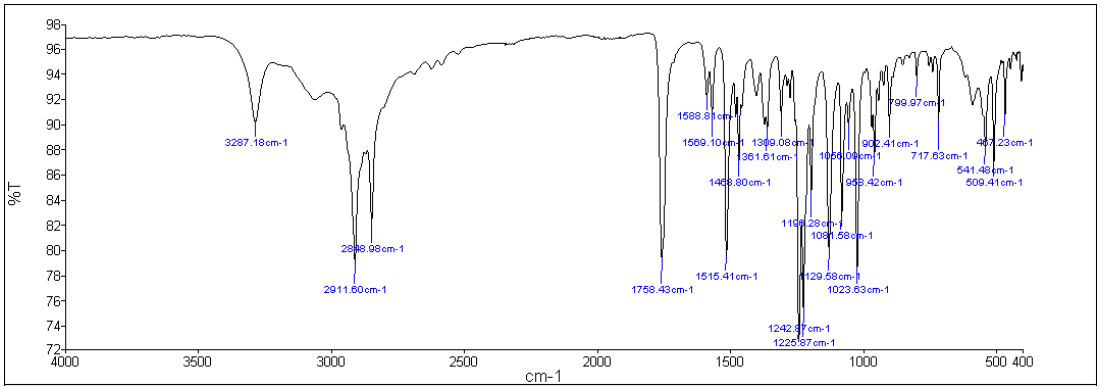

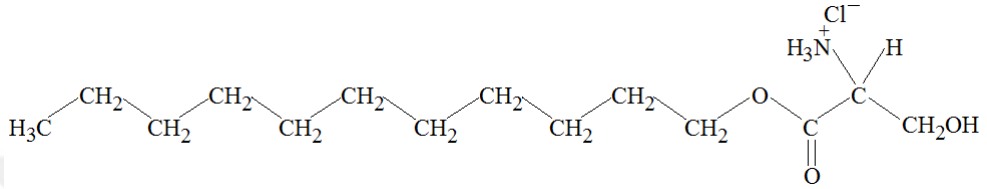

Figure 3.11 FT-IR spectrum of DL-SUnDE

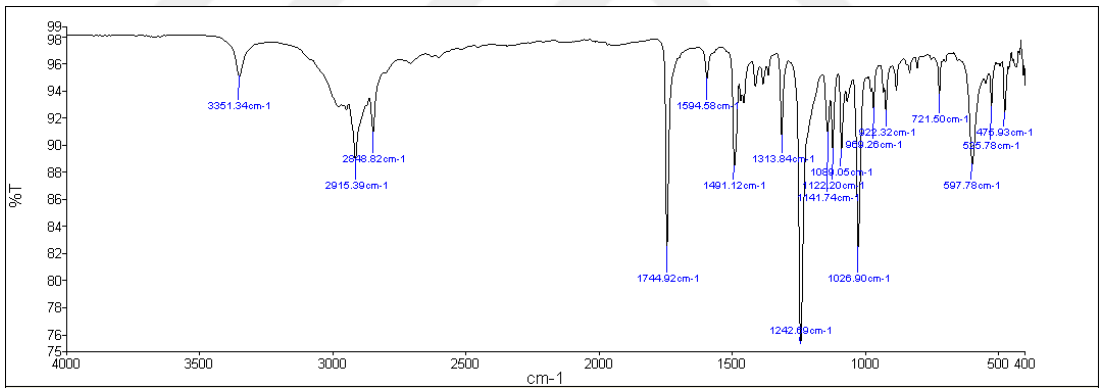

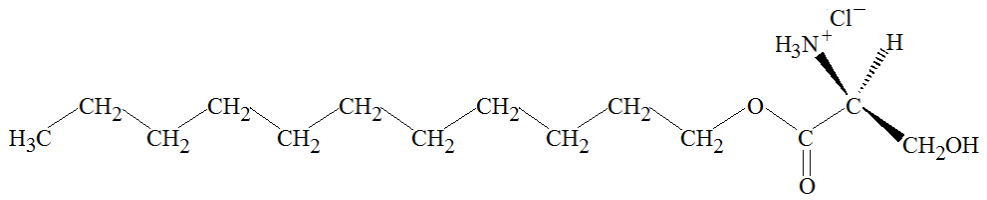

Figure 3.12 FT-IR spectrum of L-SUnDE

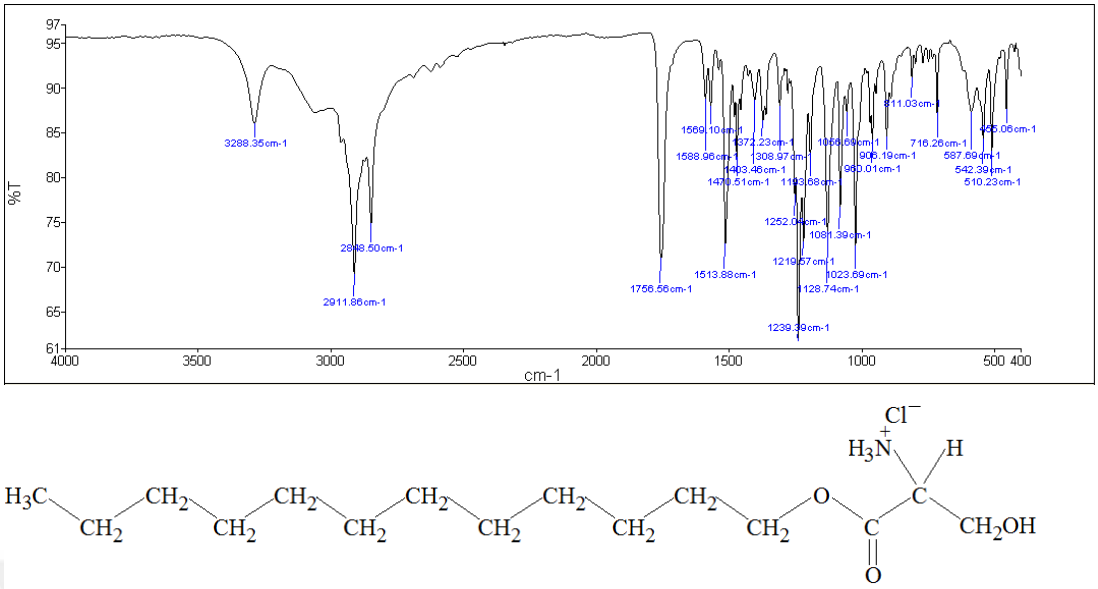

Figure 3.13 FT-IR spectrum of DL-SDDE

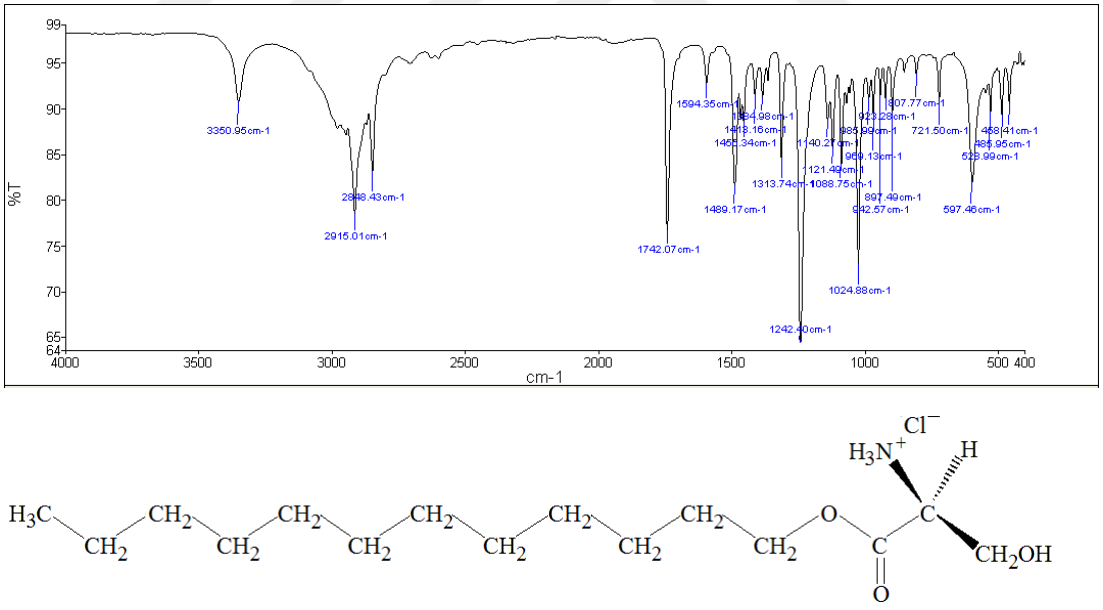

Figure 3.14 FT-IR spectrum of L-SDDE

3.1.5 Synthesis of Alanine and Serine Fluorinated Ester Surfactants

The synthesis procedure of hydrogenated ester surfactants was also applied for synthesizing the partly fluorinated ester surfactants with some modifications (Acimis and Karaman, 2006). To the 3-necked reaction flask, a condenser was put in vertical direction to prevent sublimation of 1H,1H,2H,2H-perfluorooctanol during HCl(g) passing through the reaction solution. After the products were obtained as white products, partly fluorinated alanine esters (DL-APFOE and L-APFOE) were recrystallized from ethyl acetate, whereas serine ones (DL-SPFOE and L-SPFOE) were purified by recrystallization from diethyl ether/ethanol (4/1) two times. The FT-IR spectra of both partly fluorinated alanine and serine octylesters are given in Figures 3.15-3.18.

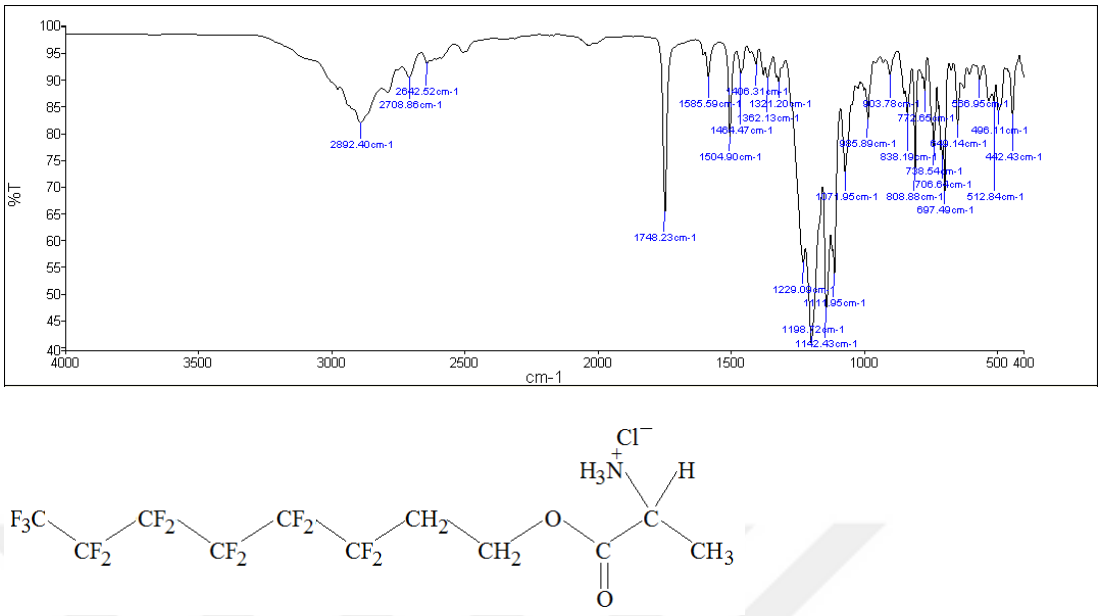

Figure 3.15 FT-IR spectrum of DL-APFOE

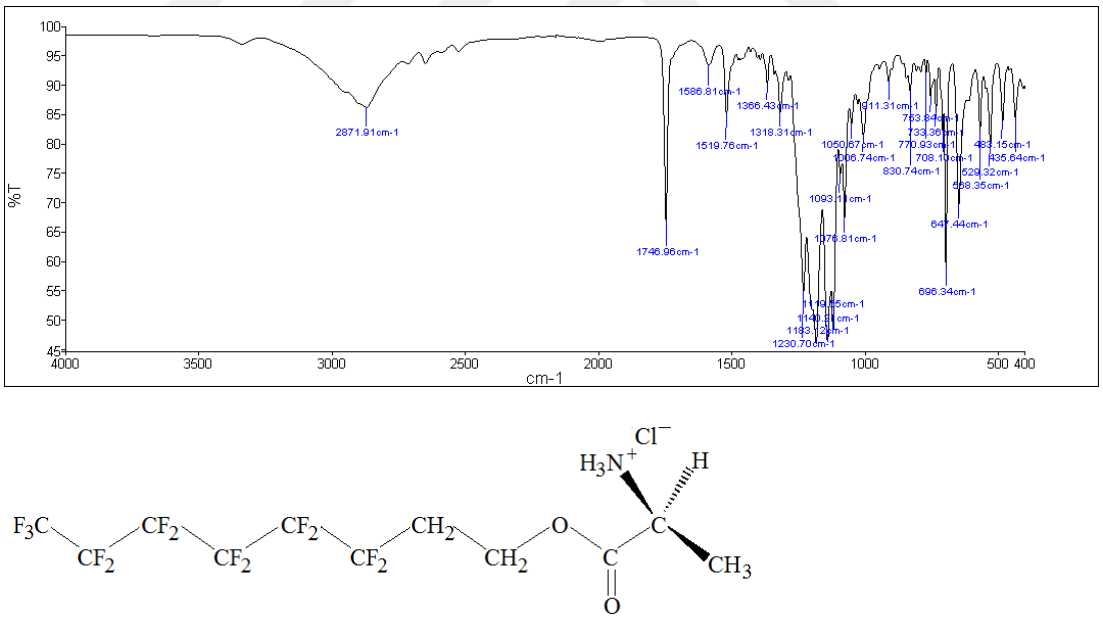

Figure 3.16 FT-IR spectrum of L-APFOE

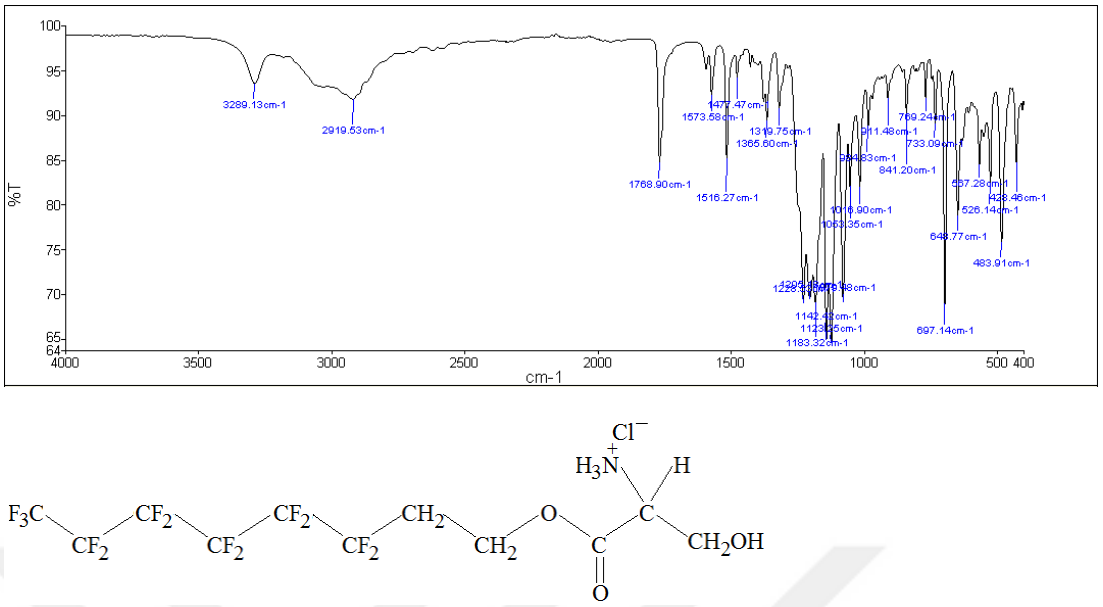

Figure 3.17 FT-IR spectrum of DL-SPFOE.

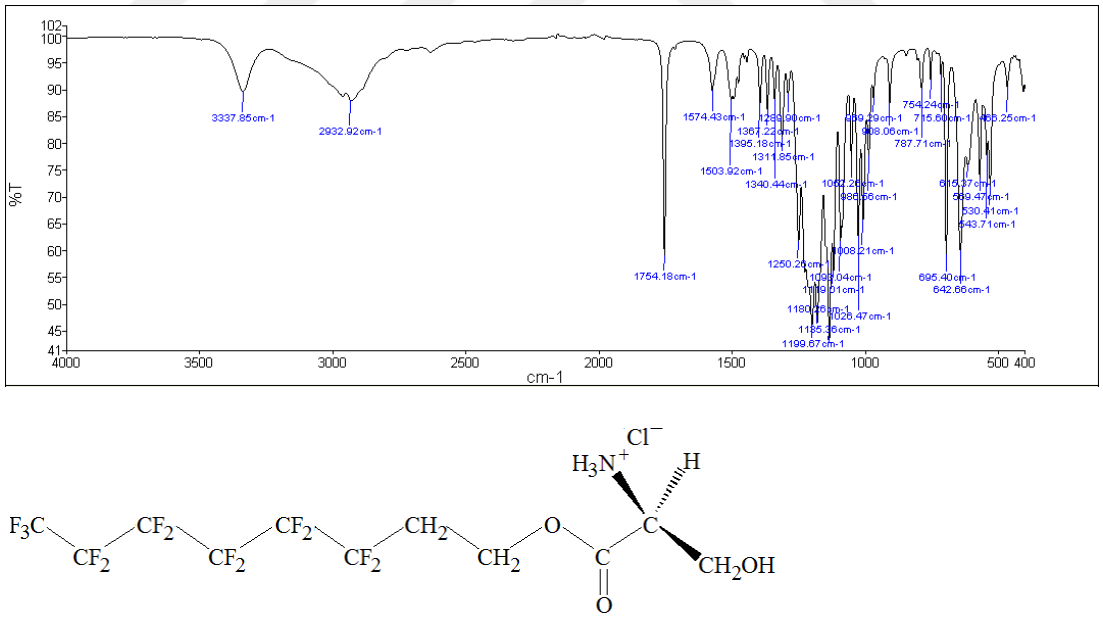

Figure 3.18 FT-IR spectrum of L-SPFOE.

3.2 Electrical Conductivity Measurements

Electrical conductivity measurements were performed in a closed dip-type conductivity cell, which was placed in an aluminum sample holder, at constant temperature. The temperature stabilization of ±0.1ºC was provided by water circulation. The conductivity cell constant was determined as 1.03 cm^{-1} from standard diluted KCl solutions. The conductivities of isotropic micellar solutions of each surfactant were measured as a function of total surfactant concentration by the successive addition of standard surfactant solutions into 8 g of pure water present in the conductivity cell. For each surfactant/water binary solutions, the conductivities were measured at 30-50 different total surfactant concentrations, until reaching the value of 2-2.5xcmc. For each surfactant/water binary system, the electrical conductivity measurements were repeated, at least three times.

3.3 Lyotropic Liquid Crystalline Sample Preparation

Lyotropic liquid crystalline samples were prepared by weighing the constituents in appropriate amounts into the well-closed test tubes. They homogenized well by applying vortex and centrifuging occasionally. Notice that sample preparation (careful weighing on a balance and homogenization) is a very important key point to obtain reproducible and reliable results.

3.4 Polarizing Optical Microscopy (POM)

Textural analyses of lyotropic samples were performed under the polarizing optical microscope. First, lyotropic samples were transferred into the flat microscope capillaries of 0.2 or 0.3 mm of thickness. Then, the capillaries were placed in a precise temperature control unit (a Linkam T95-PE temperature controller with a temperature stability of, at least, 0.01ºC and LTS120E heating/freezing stage) with water circulation (Polyscience SD07R with an accuracy of ±0.04ºC). By this way, a homogenous heat distribution in the temperature control unit was provided.

3.5 Pitch Measurements by Laser Diffraction

The pitch of the lyotropic cholesteric phases can be precisely measured by laser diffraction technique (Lasic et.al., 1983; Tracey and Radley, 1985; Radley and Lilly, 1993; Radley et.al., 1996). Mainly, the laser diffraction experimental set-up consists of the parts shown in Figure 3.19.

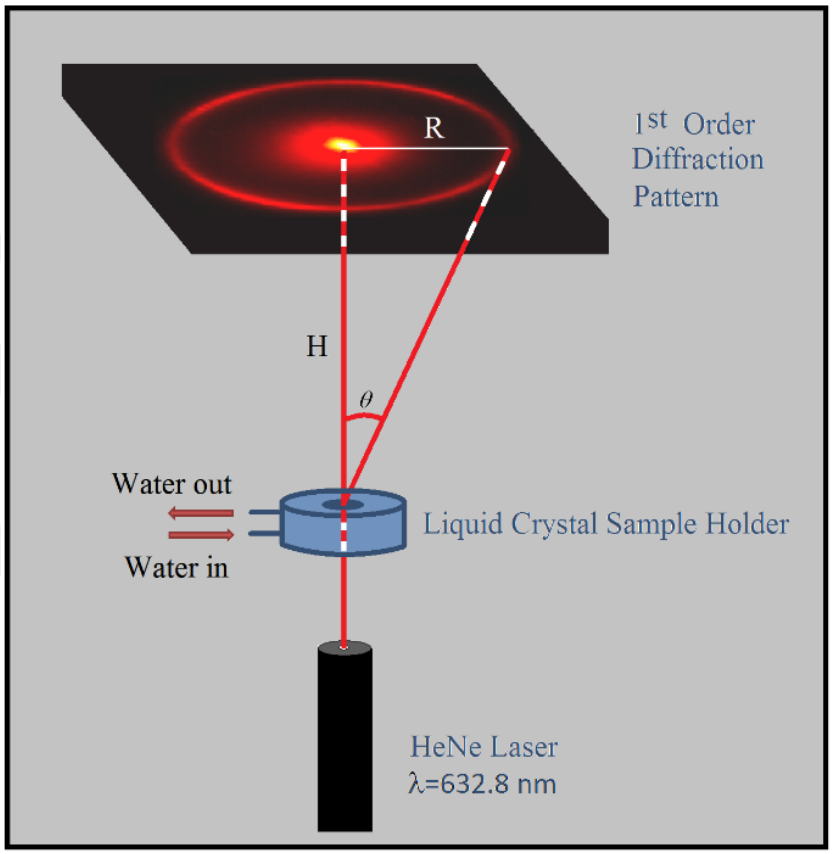

Figure 3.19 A laser diffraction set-up mainly consists of three parts: (a) laser light source, (b) sample holder in which liquid crystal sample is placed and (c) screen on which the laser diffraction pattern is seen. Heat distribution is provided by a water circulation (water in and water out) around the sample holder with a refrigerating-circulating bath (Polyscience, SD07R with an accuracy of ±0.04ºC).

For laser diffraction measurements, the lyotropic samples were sandwiched between two circular optical glasses (Hellma, 22.5 mm diameter and 1.5 mm thickness), which were separated by 2.5 mm O-ring (Hellma, 2.5 mm thickness). So, 2.5 mm thick samples were obtained. The pitch of the cholesteric phase can be calculated from the radius, R, of the circular pattern observed on the screen. Indeed, we need the diffraction angle, θ, and it is evaluated from the determination of both R

and H (height between the screen and the liquid crystal sample). R and H can be easily determined by a sensitive ruler and the diffraction angle is evaluated from $\tan\theta$=R/H. Then the pitch (P) or twist (P^{-1}) is calculated from the following equation (Bragg's equation) (Tohyama, 1974; Radley and Tracey, 1985; Mizuno et.al., 1998)

$$P^{-1} = \frac{\sin\theta}{2\lambda} \tag{3.1}$$

where λ is the wavelength of the incident laser.

4. RESULTS AND DISCUSSIONS

4.1 Determination of Hydrogenated Counterparts of Partly Fluorinated Surfactants

Some studies in the literature stated that surfactants whose alkyl chains are fully hydrogenated have almost similar critical micelle concentrations with respect to fully fluorinated ones, where alkyl chains of the hydrogenated surfactants are 1.5 times longer than those of the fluorinated surfactants (Shinoda et.al., 1972; Shinoda and Nomura, 1980; Ravey et.al., 1988; Blanco et.al., 2005). These type of surfactants, with the same surfactant head groups, are accepted as being counterparts with one another and they exhibit similar hydrophobicity.

Surfactants are classified as kosmotrope and chaotrope depending on their water-matching affinities, i.e. Collins's concept (Collins, 1996, 2004; Collins et.al., 2007). This classification is related to the surfactant head groups (Vlachy et al., 2009; Marcus, 2009) but not to the surfactant alkyl chains (Vlachy et.al., 2008). In the frame of this study, the amino acid based surfactants were chosen and there is no information whether they are kosmotropes or chaotropes in the literature. Furthermore, to the best of our knowledge, there is no systematic investigation in the literature to show whether the different functional head groups of the surfactants (e.g. carboxylate, sulfate, ester, amide, etc.) affect the partly fluorinated surfactants to be the counterparts of the hydrogenated ones from being kosmotrope or chaotrope point of view. To clarify this point, we synthesized two novel surfactants potassium 2H,2H-perfluorooctanoate (KPFO) and sodium 1H,1H,2H,2H-perfluorooctylsulfate (NaPFOS). The former (latter) has carboxylate (sulfate) head group, which is known as kosmotrope (chaotrope) (Vlachy et.al., 2009). Their critical micelle concentrations were determined from the electrical conductivity measurements as shown in Figure 4.1.1. The break point observed on the specific conductivity versus total surfactant concentration corresponds to the critical micelle concentration. We also applied the electrical conductivity measurements to potassium undecanoate, KC11, and potassium dodecanoate, KC12 (sodium undecylsulfate, NaC11S, and sodium dodecylsulfate, NaC12S). By this way, we may decide which one, KC11 or KC12 (NaC11S or NaC12S), is a counterpart of KPFO (NaPFOS). The critical micelle concentrations of those surfactants at 35°C are given in Table 4.1.1. This temperature was chosen because some precipitates were observed for NaPFOS solutions below 35°C.

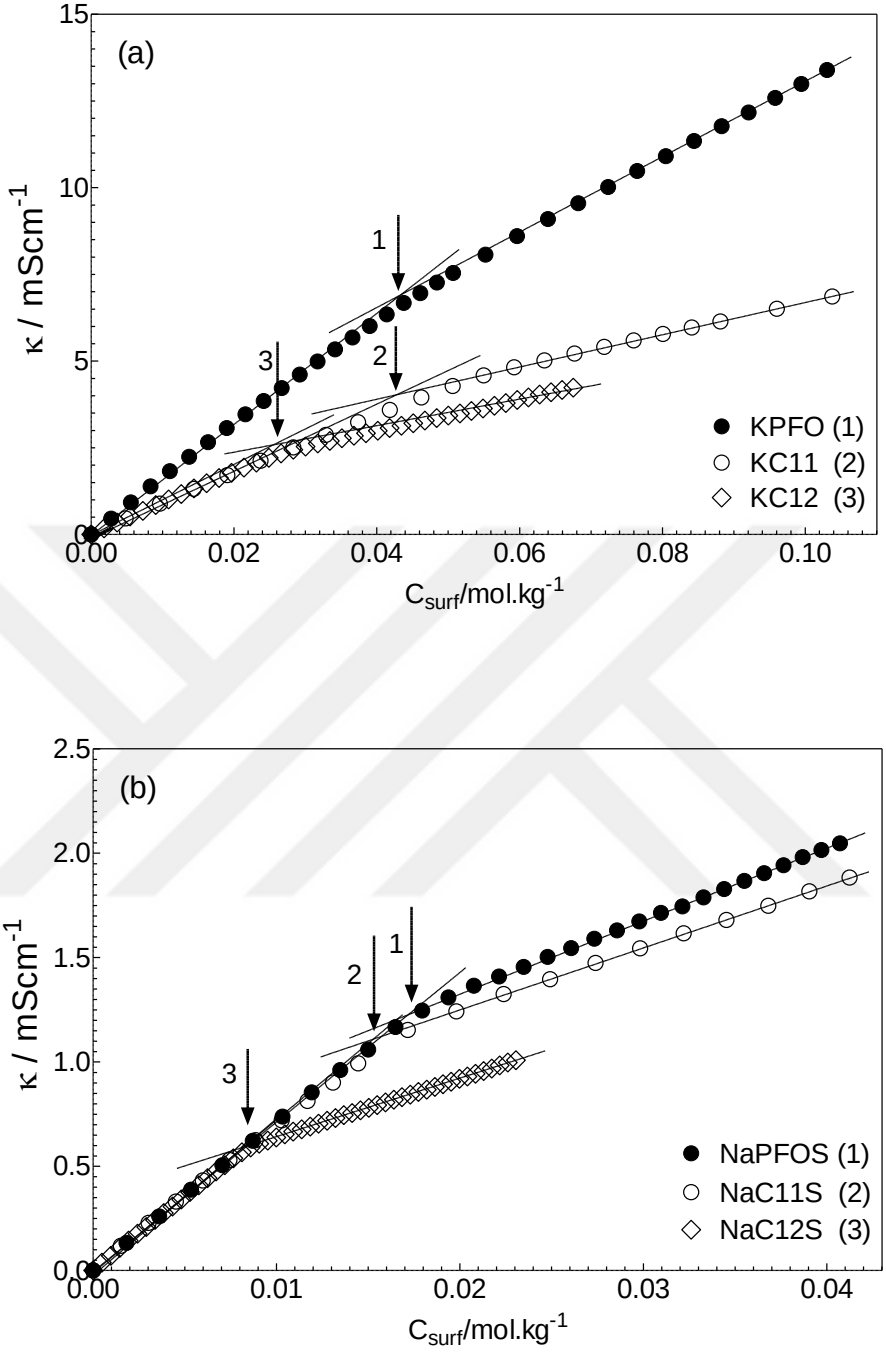

Figure 4.1.1 Specific conductivity (κ) versus total surfactant concentration (C_{surf}) for (a) KPFO, KC11 and KC12 and (b) NaPFOS, NaC11 and NaC12S at 35°C.

Table 4.1.1 The critical micelle concentrations and degree of counterion bindings of KPFO, KC11, KC12, NaPFOS, NaC11S and NaC12S at 35°C.

Surfactant	T/°C	cmc/mmol.kg^{-1}	β
KPFO	35.0	43.11±1.51	0.2790±0.0034
KC11	35.0	42.78±0.31	0.4108±0.0071
KC12	35.0	26.11±0.16 (27.2[a])	0.5029±0.0071
NaPFOS	35.0	17.24±0.22	0.5031±0.0015
NaC11S	35.0	15.22±0.12 (16.0)[b]	0.5337±0.0021
NaC12S	35.0	8.41±0.06 (8.6[c])	0.6013±0.0028

[a] At 25°C, from (Kale and Zana, 1977).
[b] At 21°C, from (Rosen, 2004).
[c] At 35°C, from (Das and Ismail, 2008).

As seen from the critical micelle concentrations given in Table 4.1.1, the partly fluorinated surfactants KPFO and NaPFOS have, within the experimental error, similar cmcs when compared with KC11 and NaC11S but not with KC12 and NaC12S, respectively. It means that, taking into account the rule 1 CF_2 = 1.5 CH_2 and their molecular structures (Figure 4.1.2), the counterpart surfactants of KPFO and NaPFOS have to be assumed as KC11 and NaC11S, respectively. In addition, we may say that 1 CF_2 = 1.5 CH_2 rule is not dependent on the kosmotrope or chaotrope character of the surfactants.

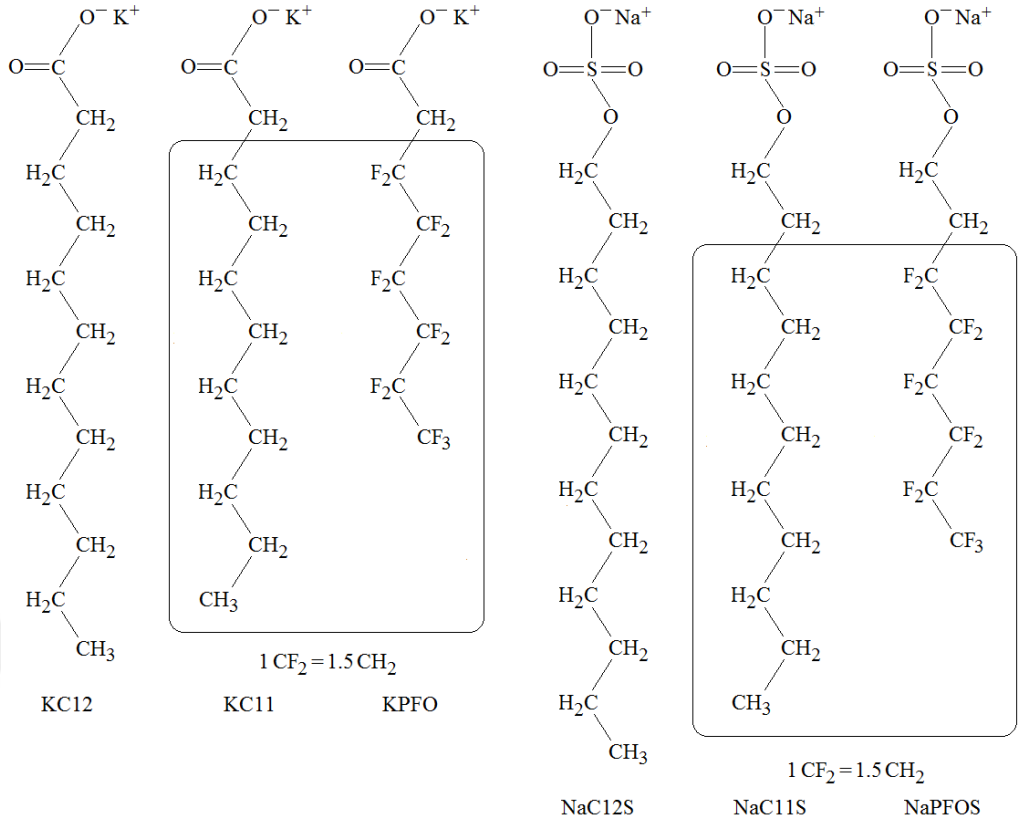

Figure 4.1.2 Comparison of molecular structures of the potassium alkanoates and sodium alkylsulfates studied in terms of being counterparts one another.

The electrical conductivity measurements were performed on the alanine and serine based partly fluorinated and fully hydrogenated ester surfactants, Figure 4.1.3 and 4.1.4, and their critical micelle concentrations are given in Table 4.1.2. While some of them were synthesized for the first time in this study, others were studied in both this study and the Refs. (Acimis and Reeves, 1980; Acimis and Karaman, 2006; Sivaramakrishna and Swamy, 2015). The cmc values of fluorinated surfactants DL/L-APFOE and DL/L-SPFOE and hydrogenated ones with 12 carbon atoms in their alkyl chains (DL/L-ADDE and DL/L-SDDE) determined in the frame of this study are, within the experimental error, very similar to those in the Ref. (Acimis and Olutas, 2012). The data given not only in this study but also in the Ref. (Acimis and Olutas, 2012) shows that the cmc values of both DL/L-APFOE and DL/L-SPFOE are about two times higher than those of DL/L-ADDE and DL/L-SDDE, respectively. In other words, DL/L-APFOE (DL/L-SPFOE) surfactants are not counterparts of DL/L-ADDE (DL/L-SDDE). Alternatively, we synthesized and determined the critical micelle concentrations of the DL/L-alaninehydrochloride undecylesters (DL/L-AUnDE) and DL/L-serinehydrochloride undecylesters (DL/L-AUnDE) at 25°C, Table 4.1.2.

According to the results, the cmc values of DL/L-AUnDE and DL/L/SUnDE are very similar to those of DL/L-APFOE and DL/L-SPFOE, respectively, i.e. they are assumed to be their counterparts. In other words, the rule 1 CF_2 = 1.5 CH_2 is valid even if partly fluorinated surfactants are compared with their hydrogenated ones, Figure 4.1.5.

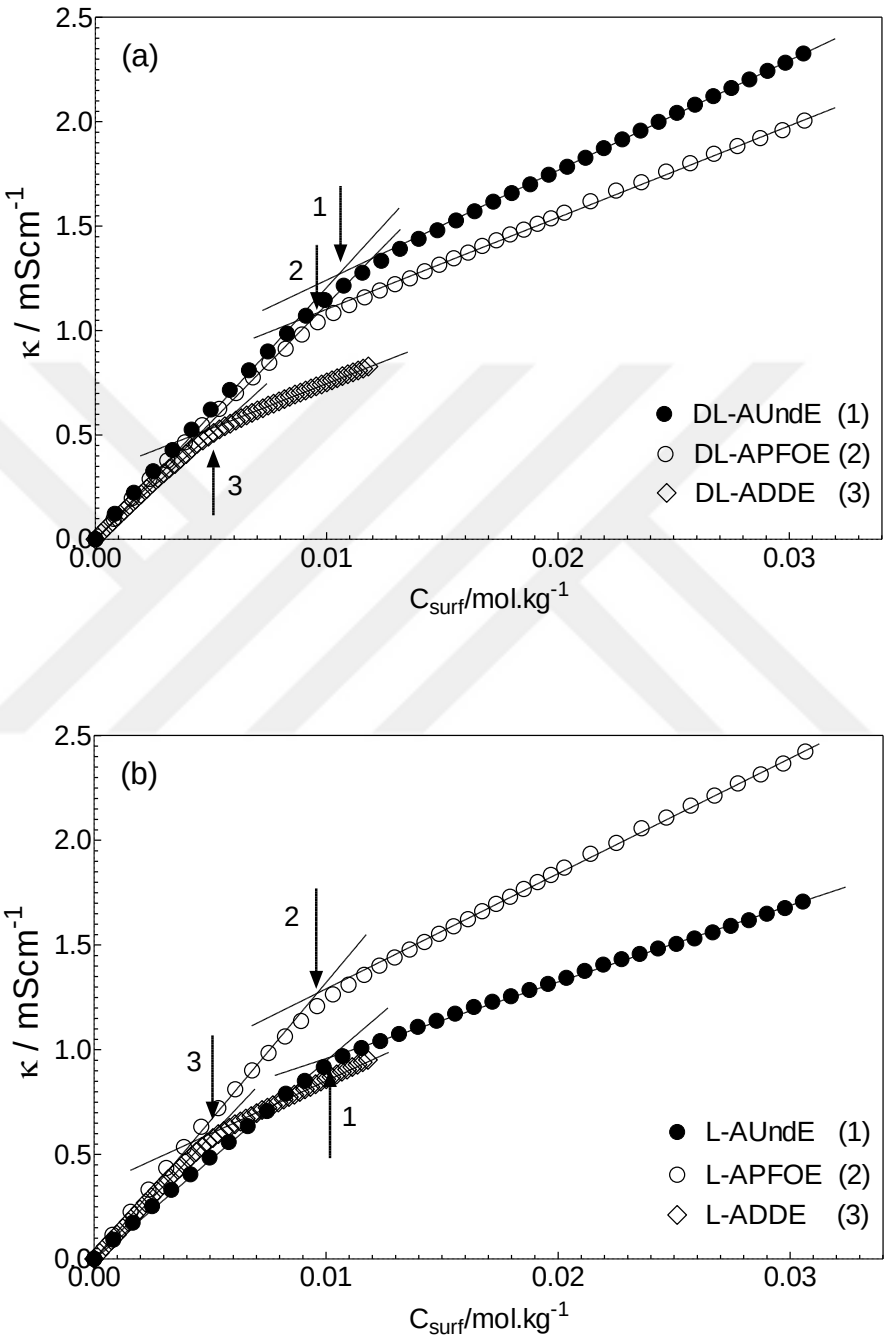

Figure 4.1.3 Specific conductivity versus total surfactant concentration graphs of (a) DL- and (b) L-alaninehydrochloride hydrogenated and partly fluorinated alkylesters at 25°C. The arrows show the break point observed on each curves, i.e. the critical micelle concentrations.

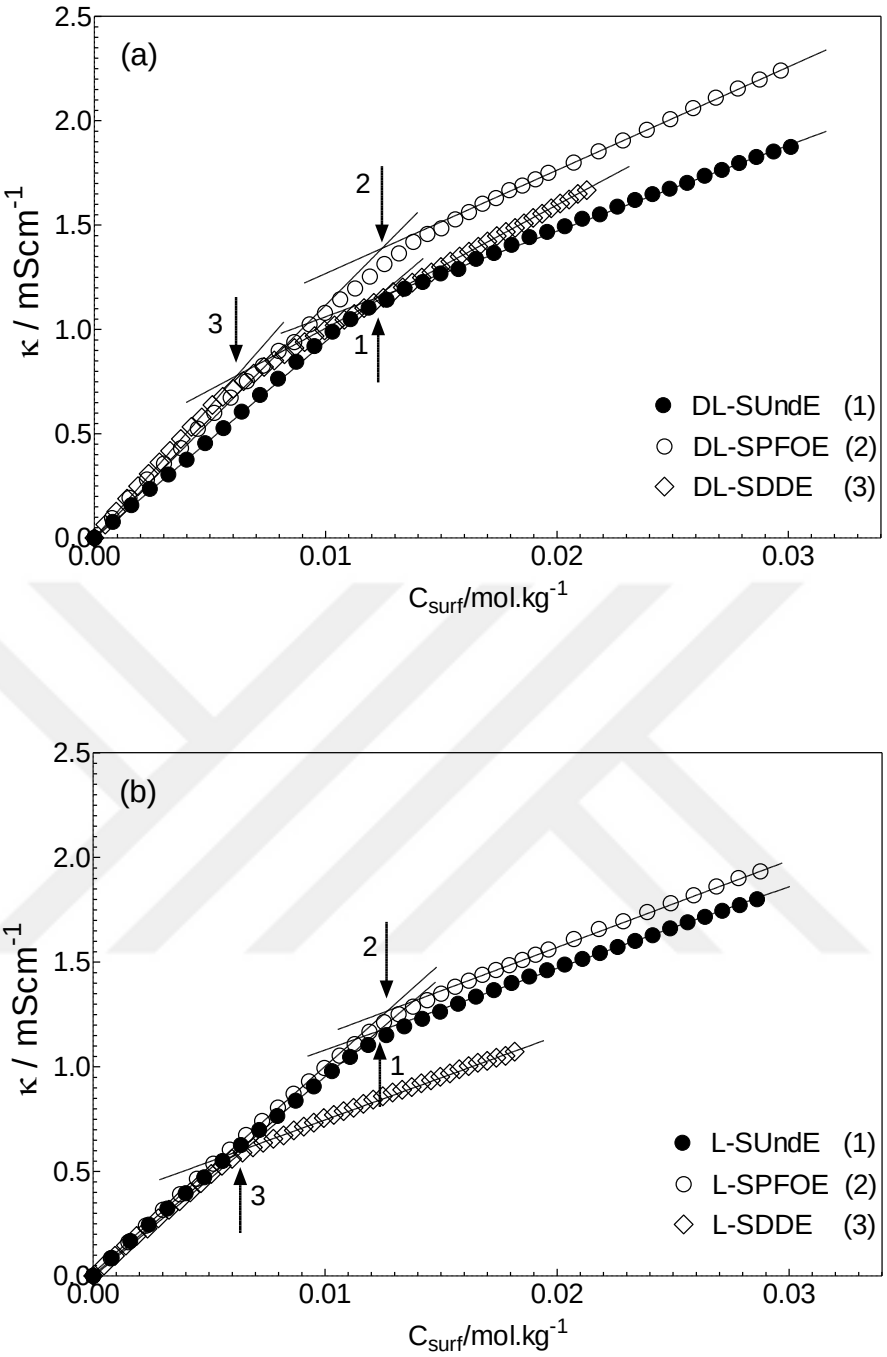

Figure 4.1.4 Specific conductivity versus total surfactant concentration graphs of (a) DL- and (b) L-serinehydrochloride hydrogenated and partly fluorinated alkylesters at 25°C. The arrows show the break point observed on each curves, i.e. the critical micelle concentrations.

Table 4.1.2 Critical micelle concentrations of studied amino acid based ester surfactants determined in this study (cmc) and in the Ref. (Acimis and Olutas, 2012) (cmc*).

Surfactant	T/°C	cmc/mmol.kg^{-1}	cmc*/mmol.kg^{-1}
DL-AUnDE	25.0	10.56±0.02	-----
DL-APFOE	25.0	9.66±0.21	9.32±0.04
DL-ADDE	25.0	5.02±0.02	5.24±0.04
L-AUnDE	25.0	10.19±0.14 (10.89)[a]	-----
L-APFOE	25.0	9.51±0.03	9.38±0.03
L-ADDE	25.0	5.02±0.07 (5.04)[a]	5.21±0.01
DL-SUnDE	25.0	12.16±0.13	-----
DL-SPFOE	25.0	12.34±0.17	11.67±0.09
DL-SDDE	25.0	6.00±0.13	6.20±0.05
L-SUnDE	25.0	12.37±0.10	-----
L-SPFOE	25.0	12.64±0.04	11.72±0.12
L-SDDE	25.0	6.43±0.13	6.29±0.02

[a] At 25.0°C, from (Sivaramakrishna and Swamy, 2015). Cmc values were given in the unit of mM.

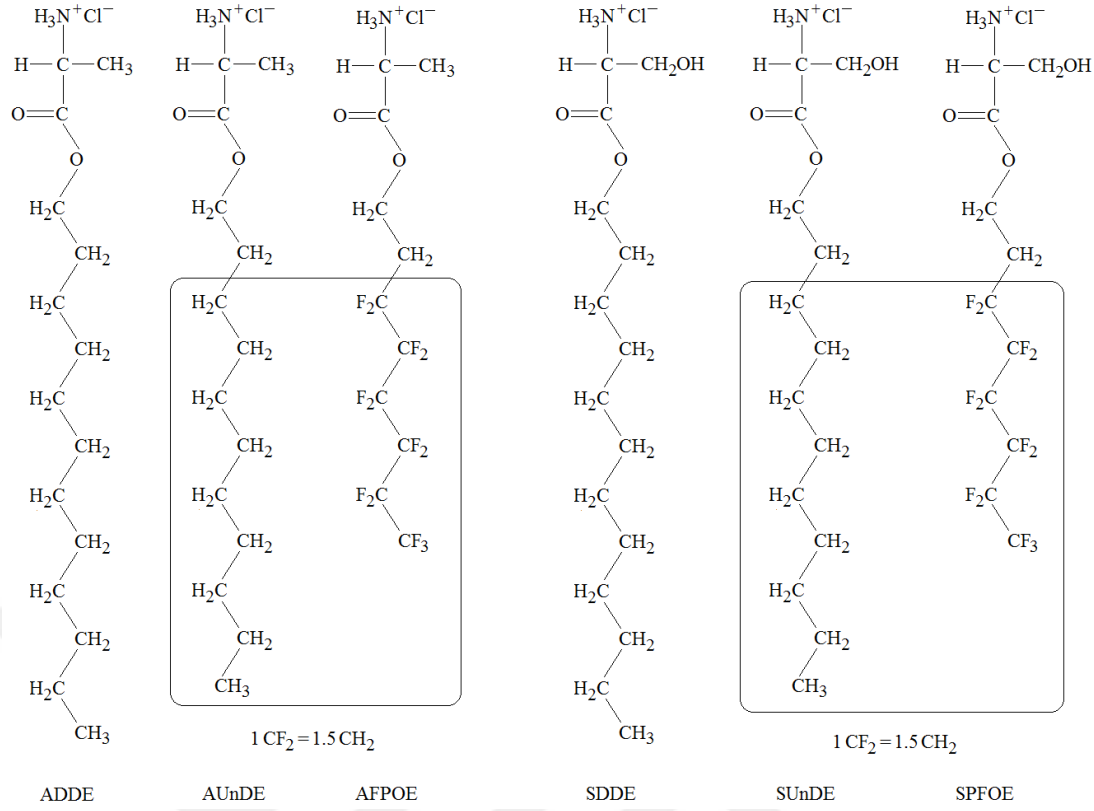

Figure 4.1.5 Comparison of molecular structures of the partly fluorinated and hydrogenated alanine and serine surfactants by omitting the enantiomerism, i.e. D-, L- or DL-forms of the surfactant head groups. Notice that the D- or L-enantiomerism is omitted in the structure of the head groups because DL- and L-forms exhibited similar results from the comparison of partly fluorinated and hydrogenated surfactants point of view (Table 4.1.2).

4.2 Lyotropic Intrinsic Cholesteric Phase Properties of Alanine and Serine Esters

It is clear from electrical conductivity measurements that partly fluorinated APFOE and SPFOE are counterparts of AUnDE and SUnDE, but not of ADDE and SDDE, respectively. At first sight, one CH_2 group difference between ADDE and AUnDE and between SDDE and SUnDE might not be thought as important to discuss their lyotropic cholesteric properties by comparing them with their partly fluorinated surfactants as did in the Ref. (Acimis and Karaman, 2006). However, according to our recent study related to the birefringences and small-angle x-ray scattering (saxs) measurements of the lyotropic nematic phases (Akpinar et.al., 2017), additional CH_2 group in the surfactant alkyl chains changes the micelle shape anisotropy and the phase structure efficiently. For instance, in that study, KC11/rubidium sulfate (Rb_2SO_4)/decanol (DeOH)/water mixture presented an isotropic phase at a specific mixture composition. If the surfactant KC11 was replaced by KC12 (KC13, potassium tridecanoate), the latter mixture exhibited three nematic phases, discotic nematic, N_D, calamitic nematic, N_C, and biaxial nematic, N_B, (just the N_D phase). In addition, the birefringences of the N_D phase in the KC13 mixture were approximately doubled with respect to those in the K12 mixture. Because the higher the birefringences means the higher micellar shape anisotropy and bigger micelles, which was supported by saxs measurements (micelle volumes in the discotic nematic phase of KC12 and KC13 were calculated as about 32 nm^3 and 74 nm^3, respectively), additional CH_2 group causes the micellar growth. As expected, the same number of chiral molecules existing in a lyotropic mixture may produce greater twist in the smaller micelles with respect to the bigger micelles in the induced cholesteric phases. In other words, the pitch decreases as the micelle size decreases, for the same chiral dopant added (Covello et. al., 1983). So, for the comparison of lyotropic liquid crystalline properties of the partly fluorinated surfactants with those of hydrogenated ones, the exact counterparts have to be chosen. However, in the case of intrinsic cholesteric phase, when the micelles grow, larger number of chiral surfactants are packed in the micelles, which may lead to shorter pitch.

Another crucial doubt of the Ref. (Acimis and Karaman, 2006) is that while the authors prepared the mixtures of hydrogenated surfactants including the strong electrolyte NaCl, the mixtures of fluorinated counterparts were composed of

surfactant/water, i.e. no electrolyte was added into the latter mixtures. It is known that the presence of electrolyte in a lyotropic mixture of induced cholesteric phase increases the pitch as the salt concentration increases (Dawin et. al., 2010). It means that, in this case, the chiral molecule cannot effectively transfer its chirality to the micelle and, of course, to the whole structure. Indeed, this is a result of the role of the strong electrolyte in the mixture, where the interactions between the surfactant head groups and the ions of the electrolytes at the micelle surfaces are present. When an electrolyte is added to a lyotropic mixture it causes the micellar growth, similar to the effect of the surfactant alkyl-chain length, as discussed before. Thus, the same amount of chiral molecule will not chiralize the bigger micelles as they would do in the case of smaller ones. Consequently, it is not correct to compare two different systems, one including electrolyte and other not, as did in the Ref. (Acimis and Karaman, 2006). In addition, we did not apply magnetic field for the sample alignment because, as reported for lyotropic discotic nematic phases in the literature, the hydrogenated (fluorinated) straight alkyl chains of the surfactants have negative (positive) diamagnetic susceptibility, $\Delta\chi<0$ (Chen et.al. 1977; Boden et.al., 1981; Hendrikx et.al., 1983; Antonio and Salinas, 2005) ($\Delta\chi>0$) (Boden et.al, 1979; Photinos and Saupe, 1986; Boden et.al., 1990; Cull et.al, 1994; Antonio and Salinas, 2005). It means that if a magnetic field is applied to both lyotropic mixtures of hydrogenated and fluorinated surfactants, which show nematic or cholesteric phases, they exhibit opposite responses to the magnetic field. While the helix axes of lyotropic mixtures of hydrogenated surfactants orient parallel to the magnetic field in the Ch_D phase (Covello et.al., 1983; Lasic et.al., 1983; Radley and Tracey, 1985) and unwind in the Ch_C phase (Forrest et.al., 1981; Lee and Labes, 1982; Alcantara et.al., 1984), those of fluorinated surfactants exhibit opposite behavior (Antonio and Salinas, 2005). We observed this situation, i.e. decreasing the twist as a result of the unwinding the helical structure, even if we did not apply magnetic field to the lyotropic discotic cholesteric phase of the L-APFOE and L-SPFOE. When we measured the pitch length of those phases as a function of time at constant temperature (Figure 4.2.1), we observed that the pitch increased and then diffraction pattern observed on the screen disappeared for longer times. This effect is due to the unwinding of the helical structure by the surfaces of the sample holder and, as it is expected, the application of magnetic field to the lyotropic cholesteric phase of the fluorinated surfactants causes the faster unwinding the helical structure. Within the same time interval, we could not observe any significant change

in the pitch lengths for the cholesteric phases of the hydrogenated esters, L-AUnDE and L-SUnDE. So, for the comparison of cholesteric phase properties of fluorinated surfactants with their hydrogenated counterparts, the application of the magnetic field to the cholesteric phases of L-APFOE and L-SPFOE is another serious error of the Ref. (Acimis and Karaman, 2006) from the experimental design point of view.

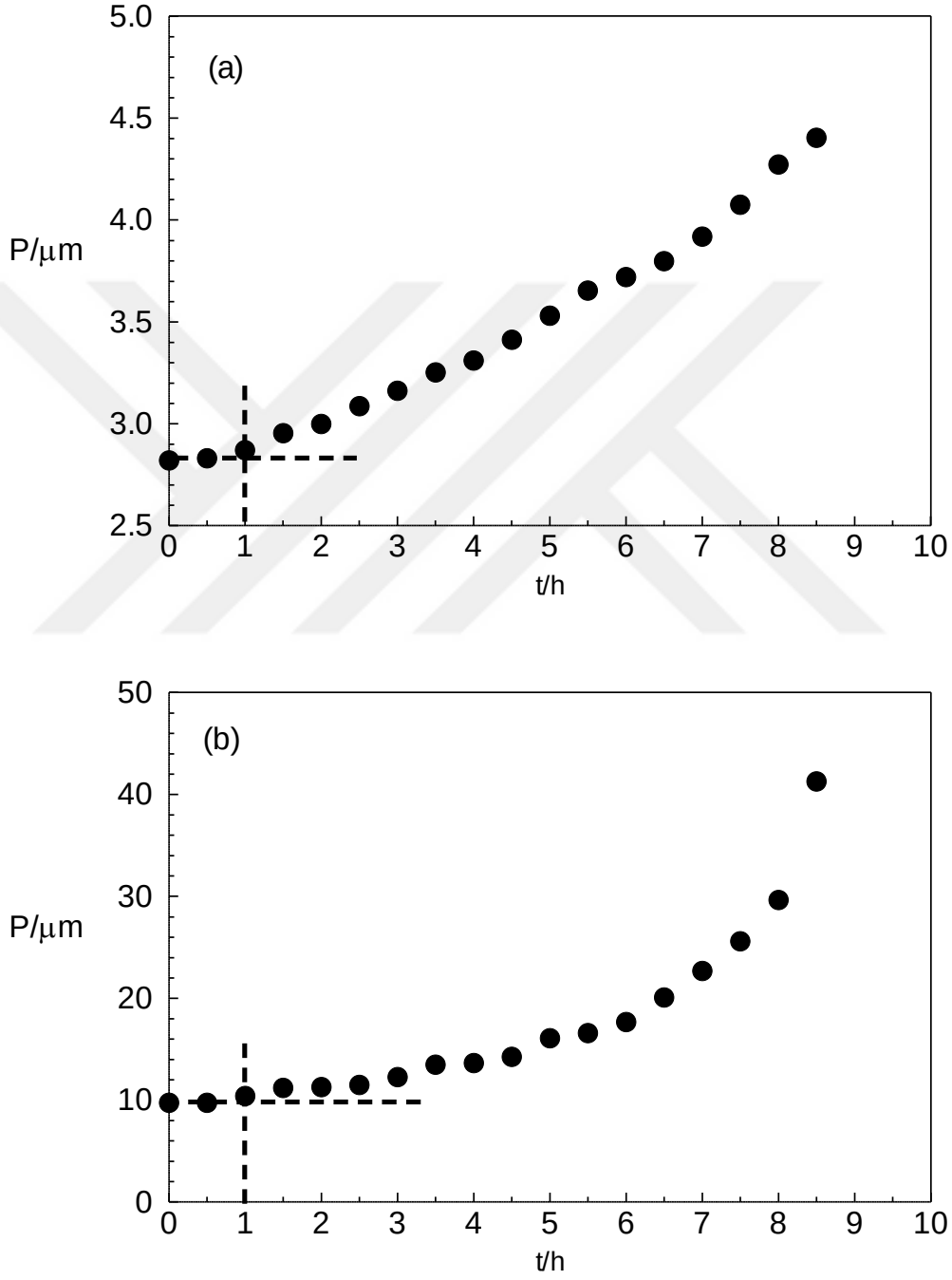

Figure 4.2.1 Pitch measurements of (a) L-APFOE at 30.0°C and (b) L-SPFOE at 22.0°C with time (in hour) in the absence of magnetic field. $\%X_{L\text{-}APFOE}$=0.788 given in Table 4.2.2 and $\%X_{L\text{-}SPFOE}$=0.617 given in Table 4.2.4.

In the case of lyotropic intrinsic cholesteric phases, it should be expected that the micellar growth by the addition of strong electrolyte exhibits opposite situation with respect to the lyotropic induced ones. In the latter phases, the ions of strong electrolytes screen the repulsions between the surfactant head groups at the micelle surfaces and this may cause not only the micellar growth as a result of denser packing of achiral surfactant molecules in the micelles (like potassium laurate) but also the transfer of some parts of the chiral dopant from the micelles to the intermicellar region (Dawin et.al., 2010). Thus, the pitch (twist or helical twisting power of chiral dopant) of induced cholesteric phases increases (decreases) with the increase in the electrolyte concentration. When an electrolyte is added into the lyotropic mixtures of intrinsic cholesteric phases, the micelles grow by packing of larger amount of 'chiral' surfactants in the micelles, leading to a shorter pitch. Thus, the micelles of lyotropic intrinsic cholesteric phases are more efficiently organized in the chiral structure when compared with those of lyotropic induced cholesterics.

For the comparison of lyotropic cholesteric liquid crystalline properties of partly fluorinated surfactants with their hydrogenated ones, we prepared some lyotropic mixtures. It was not possible to obtain the mixtures of partly fluorinated and hydrogenated surfactants in exactly same concentrations because of phase separations, gel-like phase formation instead of cholesteric phases. Thus, we prepared the lyotropic mixtures by keeping fixed the ratio of L-enantiomeric surfactant/electrolyte in mole percent for partly fluorinated and hydrogenated surfactants with different amount of water. By this way, it was provided that the effect of electrolyte, NaCl, is similar in the mixtures of both partly fluorinated and hydrogenated surfactants. The different water content in the mixtures does not include any risk for the comparison of lyotropic cholesteric phase behaviors of partly fluorinated surfactants with those of their hydrogenated counterparts. As it is well-known, the Coulombic interactions between ions of electrolytes and ionic head groups of surfactants are strong in not only short ranges but also long ranges, even if some amount of electrolyte ions stays in the intermicellar (water) region. The lyotropic mixture compositions of partly fluorinated and hydrogenated chiral alanine and serine esters are given in Tables 4.2.1-4.2.4.

Table 4.2.1 Compositions of L-AUnde/NaCl/water lyotropic mixtures in mole fractions (X) as percent (X%). R is the ratio of $X_{L\text{-enantiomer}}$ to X_{NaCl}. Errors in the pitch values were within ±3%.

$X_{L\text{-AUnDE}}$	X_{NaCl}	X_{water}	R	P/µm	$P^{-1}/\mu m^{-1}$
6.141	1.689	92.170	3.64	19.84	0.0504
6.175	1.688	92.136	3.66	20.53	0.0487
6.210	1.688	92.102	3.68	21.01	0.0476
6.244	1.687	92.069	3.70	22.08	0.0453
6.279	1.687	92.035	3.72	22.62	0.0442
6.313	1.686	92.001	3.74	23.81	0.0420
6.347	1.685	91.967	3.77	25.77	0.0388

Table 4.2.2 Compositions of L-APFOE/NaCl/water lyotropic mixtures in mole fractions (X) as percent (X%). R is the ratio of $X_{L\text{-enantiomer}}$ to X_{NaCl}. Errors in the pitch values were within ±3%.

$X_{L\text{-APFOE}}$	X_{NaCl}	X_{water}	R	P/µm	$P^{-1}/\mu m^{-1}$
0.761	0.209	99.030	3.64	2.34	0.4274
0.766	0.209	99.025	3.66	2.42	0.4139
0.770	0.209	99.021	3.68	2.48	0.4025
0.775	0.209	99.016	3.70	2.60	0.3845
0.779	0.209	99.012	3.72	2.67	0.3740
0.784	0.209	99.007	3.75	2.72	0.3678
0.788	0.209	99.003	3.77	2.82	0.3541

Table 4.2.3 Compositions of L-SUnDE/NaCl/water lyotropic mixtures in mole fractions (X) as percent (X%). R is the ratio of $X_{L\text{-enantiomer}}$ to X_{NaCl}. Errors in the pitch values were within ±4%.

$X_{L\text{-SUnDE}}$	X_{NaCl}	X_{water}	R	P/µm	$P^{-1}/\mu m^{-1}$
4.708	1.840	93.452	2.56	27.03	0.0370
4.756	1.839	93.405	2.59	27.45	0.0364
4.804	1.838	93.358	2.61	29.37	0.0340
4.852	1.837	93.311	2.64	30.46	0.0328
4.900	1.836	93.264	2.67	31.31	0.0319
4.947	1.836	93.217	2.70	34.25	0.0292
4.995	1.835	93.170	2.72	36.36	0.0275

Table 4.2.4 Compositions of L-SPFOE/NaCl/water lyotropic mixtures in mole fractions (X) as percent (X%). R is the ratio of $X_{L\text{-enantiomer}}$ to X_{NaCl}. Errors in the pitch values were within ±4%.

$X_{L\text{-SPFOE}}$	X_{NaCl}	X_{water}	R	P/µm	$P^{-1}/\mu m^{-1}$
0.580	0.226	99.194	2.56	8.11	0.1233
0.586	0.226	99.188	2.59	8.44	0.1185
0.592	0.227	99.181	2.61	8.48	0.1180
0.598	0.227	99.175	2.64	8.88	0.1126
0.604	0.227	99.169	2.67	9.04	0.1106
0.611	0.226	99.163	2.70	9.42	0.1062
0.617	0.226	99.157	2.72	9.74	0.1027

Helical twisting powers (htp's) of chiral ester surfactants were determined from the pitch measurements via laser diffraction. The pitch (P) and twist (P^{-1}) values obtained for each lyotropic system are given in the Tables 4.2.1-4.2.4. The htps were evaluated from the slope of the curve of P^{-1} vs $X_{L\text{-enantiomer}}$, Figures 4.2.2-4.2.5, and were given in Table 4.2.5.

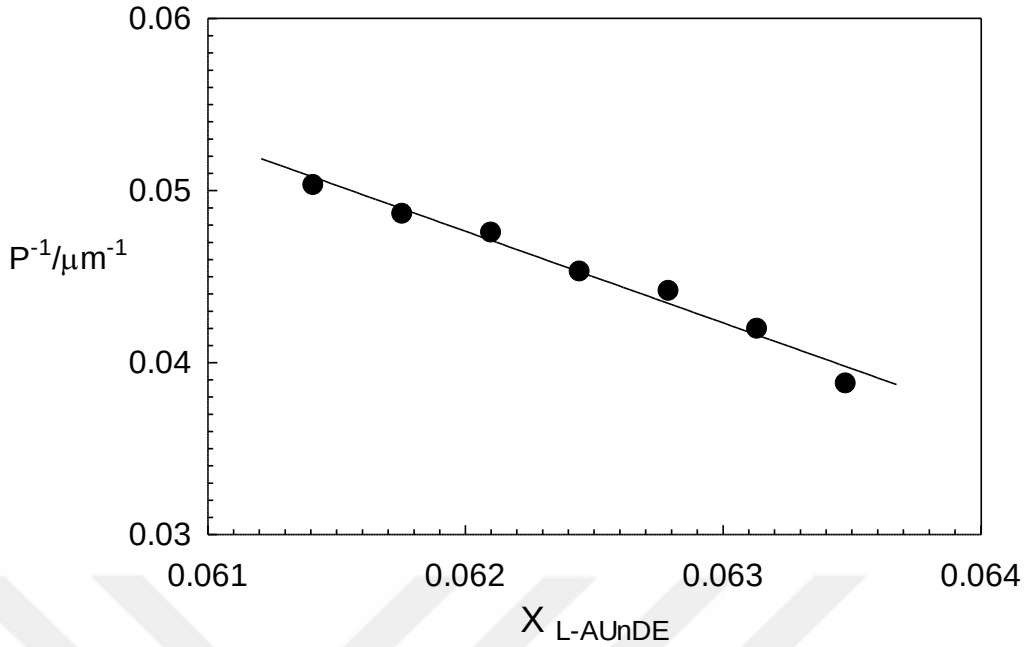

Figure 4.2.2 Twist versus mole fraction of L-enantiomeric surfactant graph for L-AUnDE/NaCl/water at 30.0°C. R: 0.9885, where R is regression.

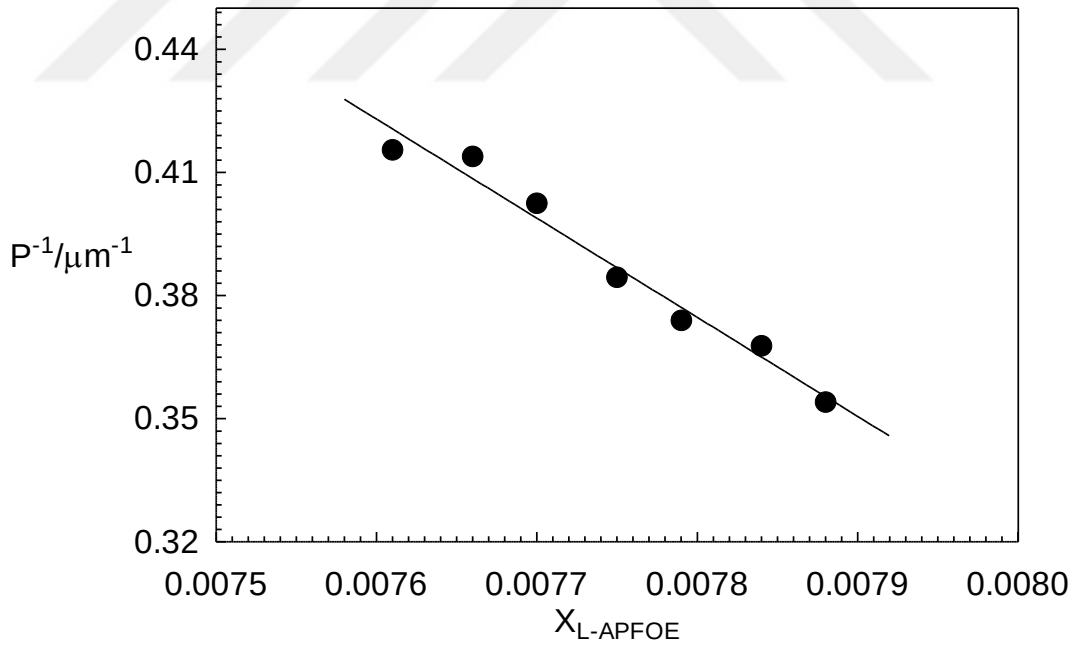

Figure 4.2.3 Twist versus mole fraction of L-enantiomeric surfactant graph for L-APFOE/NaCl/water at 30.0°C. R: 0.9945.

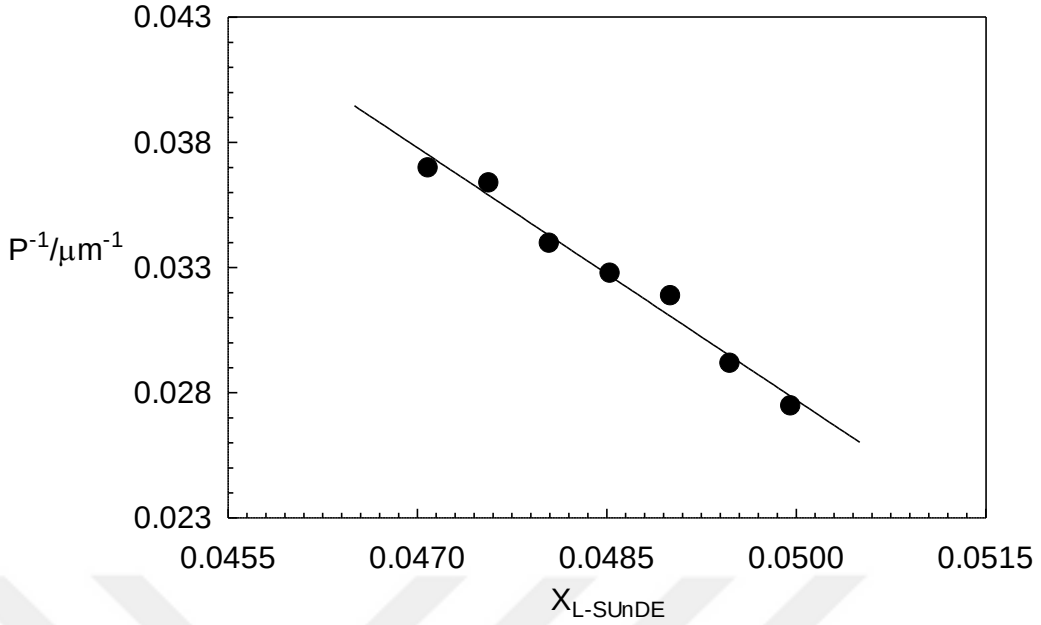

Figure 4.2.4 Twist versus mole fraction of L-enantiomeric surfactant graph for L-SUnDE/NaCl/water at 22.0°C. R: 0.9896.

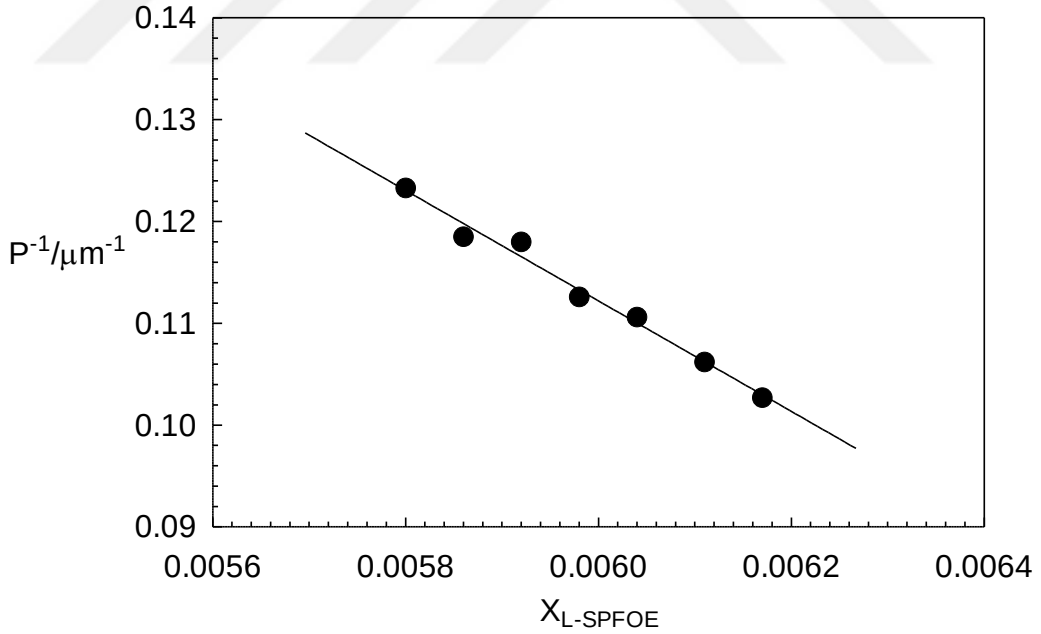

Figure 4.2.5 Twist versus mole fraction of L-enantiomeric surfactant graph for L-SPFOE/NaCl/water at 22.0°C. R: 0.9926.

Table 4.2.5 Helical twisting powers of alanine and ester surfactants evaluated in this study (htp) and taken from the literature for the comparison (htp[a]).

Lyotropic mixture	**htp/µm^{-1}**	**htp[a]/µm^{-1}**
L-ADDE/NaCl/water	-----	−4.0±0.1
L-APFOE/water	-----	−157.8±6.7
L-AUnDE/NaCl/water	−5.36±0.15	-----
L-APFOE/NaCl/water	−270.2±5.3	-----
L-SDDE/NaCl/water	-----	−2.4±0.1
L-SPFOE/water	-----	−13.7±0.7
L-SUnDE/NaCl/water	−3.4±0.12	-----
L-SPFOE/NaCl/water	−54.3±2.1	-----

[a] From Ref. (Acimis and Karaman, 2006), at 22°C.

In ref. (Acimis and Karaman, 2006) the pitch measurements were carried out at 22°C. However, in our case, the addition of electrolyte to the mixtures of L-APFOE/water changed the phase-diagram topology by shifting the lamellar-to-cholesteric phase transitions towards higher temperatures. Then, on condition of obtaining homogeneous and stable mixture, i.e. there is no phase separation with time (at least, keeping the mixture at room temperature during night after mixture preparation), we decreased the lamellar-to-cholesteric phase transitions to the lowest temperature possible by increasing the water content of the L-APFOE/NaCl/water mixture. Thus, the pitch measurements of L-APFOE/NaCl/water and L-AUnDE/NaCl/water were performed at 30.0°C. The main goal of this study is to compare the lyotropic cholesteric phase properties of partly fluorinated surfactants with their hydrogenated counterparts, choosing at any constant temperature, 22.0°C or 30.0°C, serves to this goal. So, temperature is not a key point in the framework of this study. For L-SPFOE/NaCl/water and L-SUnDE/NaCl/water mixtures, cholesteric phases were obtained for different mixture compositions at 22.0°C and we had a chance to compare the htps of these mixtures with the mixtures given in the Ref. (Acimis and Karaman, 2006).

As a result of large electron affinity of fluorine atoms, they are partially negatively charged (Roesler et.al., 2007). As it is expected, these negatively charged fluorine atoms prefer to keep away from one another to reduce the electrostatic energy between them. Because of this, they tend to produce a twist along fluorocarbon chain in a double helix structure around the carbon atoms core, which causes them to have a rigid structure (Bunn et.al., 1954; Lee, 2000; Mavrikis, 2003; Roesler et.al., 2007; Ebnesajjad, 2015; Mistri et.al., 2015; Liu and Grainger, 2017). For instance, the molecular structures of polytetrafluoroethylene and polyethylene given in the literature (Bunn et.al., 1954; Liu and Grainger, 2017) is a good example to show the main difference between a fluorinated chain and a hydrogenated chain, Figure 4.2.6.

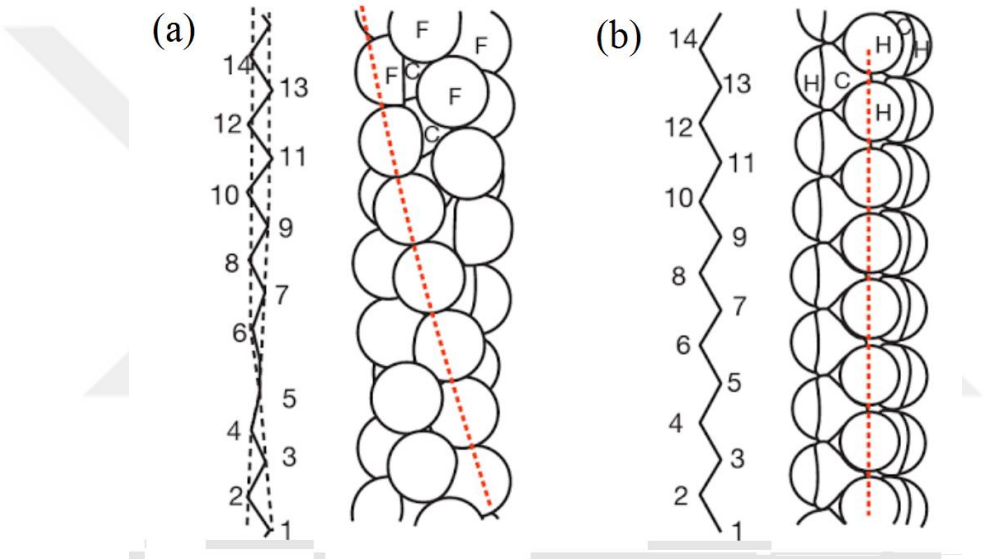

Figure 4.2.6 Zigzag chain and side space-filling views of (a) polytetrafluoroethylene, PTFE, and (b) polyethylene, PE. While there exists twisted zigzag chain for PTFE, PE has a molecular zigzag chain. This figure is adopted from a figure given in Ref. (Liu and Grainger, 2017).

If we take into account the structures of the fluorocarbon and hydrocarbon chains given in the Figure 4.2.6, the comparison of the htps of the fluorinated surfactants with their hydrogenated ones is more understandable. The ‘extra twist’ arising from the fluorocarbon chains of L-APFOE and L-SPFOE leads to their lyotropic cholesteric phases exhibit higher htps with respect to the L-AUnDE and L-SUnDE, respectively. In the Ref. (Acimis and Karaman, 2006), the result was explained by a ‘pivot’ effect of fluorocarbon chains of L-enantiomeric esters from the rigid structure of the fluorinated chain point of view, however, the higher htps of the

L-APFOE and and L-SPFOE may be attributed to the formation of the twist structure of fluorocarbon chain, as it has been recently reported on the comparison of PTFE and PE structures (Liu and Grainger, 2017).

Some models were proposed to explain the chiral induction mechanism. Two important models on lyotropic cholesteric phases were stated by Radley and Saupe, which are (a) chiral sterical interaction model and (b) chiral dispersion interaction model (Radley and Saupe, 1978). These models were mainly based on the intermicellar interactions. However, an alternative model, proposed by Hiltrop et.al., so-called 'intramicellar chirality model', states that the macroscopic twist of lyotropic cholesteric phase arises from 'intramicellar twist' as a result of the existing chiral guest molecule in the lyotropic mixture (Partyka and Hiltrop,1996; Figgemeier and Hiltrop, 1999). From this respect, all results of L-enantiomeric surfactants obtained in this study have strong evidences to support the intramicellar chirality model because we investigated the modifications in the micelle core by comparing the fluorocarbon chain with the hydrogenated counterparts, i.e. with the same hydrophobicity.

5. CONCLUSIONS

In this study, we mainly examined the isotropic micellar solutions and lyotropic cholesteric liquid crystalline phase behaviours of some partly fluorinated and fully hydrogenated DL-racemic and L-enantiomeric amino acid based surfactants. Furthermore, we synthesized some other non-amino acid based achiral surfactants. In the first part of the study, we showed that $1CF_2 \approx 1.5\ CH_2$ rule in terms of the hydrophobicity is also valid for partly fluorinated surfactants in addition to the fully fluorinated surfactants if they are compared with their exact hydrogenated counterparts. According to the results, this rule is independent on the surfactant head group type, i.e. carboxylate, sulfate or ester.

In the second part of the study, we prepared some lyotropic cholesteric phases of L-amino acid based surfactants for partly fluorinated and fully hydrogenated surfactants. The results indicated that fluorinated surfactants have higher helical twisting powers with respect to their hydrogenated counterparts. The higher helical twisting powers of the former ones may be attributed to the twist structures of the fluorocarbon chains located in the micelles. From this respect, this study supports the intramicellar chirality model which explains the chiral induction mechanism for lyotropic cholesteric phases.

Furthermore, from the experimental point of view, when the researchers compare two different surfactant systems in terms of being counterparts one another, they have to choose exact counterparts and to design experiments correctly. For instance, as we showed in this study and studies given in the literature that the researchers cannot investigate the lyotropic cholesteric phase properties of one system with including strong electrolyte but other not.

6. REFERENCES

Achilefu S, Mansuy L, Selve C, Thiebaut S (1995) "Synthesis of 2H,2H-perfluoroalkyl and 2H-perfluoroalkenyl carboxylic acids and amides, Journal of Fluorine Chemistry, 70, 19-26.

Acimis M, Reeves LW (1980) "A Type II Aqueous Cholesteric Lyomesophase", Can J Chem, 58, 1533-1541.

Acimis M, Akpinar E (2003) "Mass density measurements as a tool to distinguish between micelle size and shape in nematic and chiral nematic phases", Phys. Chem. Chem. Phys., 5, 4197-4203.

Acimis M and Karaman EB (2006) "Comparison of helical twisting powers of novel fluorinated amphiphilic enantiomers with their hydrogenated counterparts", Journal of Colloid and Interface Science, 300, 1-6.

Akpinar E, Acimis M, Ocak Ç (2001) "Strange mass density behaviour of a micellar chiral nematic phase composed of an amphiphilic racemic mixture and its L-enantiomer", Physical Chemistry Chemical Physics, 3:645-646.

Akpinar E (2010) "Determination of the structure of some lyotropic chiral nematic and racemic nematic phases by small-angle x-ray scattering", PhD Thesis, Abant Izzet Baysal University, The Graduate School of Natural and Applied Sciences, Bolu, Turkey.

Akpinar E[a], Reis D, Neto AMF (2012) "Effect of alkyl chain length of alcohols on nematic uniaxial-to-biaxial phase transitions in a potassium laurate/alcohol/K2SO4/water lyotropic mixture", Liqiud Crystals, 39:881-888.

Akpinar E[b], Reis D, Neto AMF (2012) "Lyotropic mixture made of potassium laurate/1-undecanol/K2SO4/water presenting high birefringences and large biaxial nematic phase domain: a laser conoscopy study", Eur. Phys. J. E, 35(50):1-9.

Akpinar E, Giesselmann F, Acimis M (2013) "Effect of micelle size and intermicellar distance on the chirality transfer in the intrinsic lyotropic cholesteric phases", Liquid Crystals, 40 (9), 1183-1194

Akpinar E[a], Reis D, Neto AMF (2014) "Anomalous behavior in the crossover between the negative and positive biaxial nematic mesophases in a lyotropic liquid crystal", ChemPhysChem, 19;15(7):1463-1469.

Akpinar E[b], Giesselmann F, Acimis M (2014) "Contributions of intermicellar distance, micelle volume and screw angle to the temperature dependence of helical pitch in the intrinsic lyotropic cholesteric phases", Journal of Molecular Liquids, 191, 20-28.

Akpinar E, Reis D, Neto AMF (2015) “Effect of Hofmeister anions on the existence of the biaxial nematic phase in lyotropic mixtures of dodecyltrimethylammonium bromide/sodiumsalt/1-dodecanol/water”, Liquid Crystals, 42(7):973-981.

Akpinar E[a], Otluoglu K, Turkmen M, Canioz C, Reis D, Neto AMF (2016) “Effect of the presence of strong and weak electrolytes on the existence of uniaxial and biaxial nematic phases in lyotropic mixtures”, Liquid Crystals, 43(16): 1693-1708.

Akpinar E[b], Turkmen M, Canioz C, Neto AMF (2016) “Role of kosmotrope-chaotrope interactions at micelle surfaces on the stabilization of lyotropic nematic phases”, European Physical Journal E, 39(11), 107(1-16).

Akpinar E, Canioz C, Turkmen M, Reis D, Neto AMF (2017) “Effect of the surfactant alkyl chain length on the stabilization of lyotropic nematic phases”, Liquid Crystals, published online, DOI:10.1080/02678292.2017.1309698.

Alben R (1973) “Phase Transitions in a Fluid of Biaxial Particles”, Physical review letters, 30(17):778-781.

Alcantara MR, de Melo MVMC, Paoli VR, Vanin JA (1984) “New intrinsic cholesteric lyomesophases from potassium-L-N-lauroylserinate. I. Type I systems: Textural and magnetic characterization”, Molecular Crystals Liquid Crystals, 107, 303-310.

Asakawa T, Okada, T, Hayasaka T, Kuwamoto K, Ohta A, Miyagishi S (2006) “Thu unusual micelle micropolarity of partially fluorinated Gemini surfactants sensed by pyrene fluorescence”, Langmuir, 22, 6053-6055.

Aswal VK and Goyal P (2000) “Counterions in the growth of ionic micelles in aqueous electrolyte solutions: A small-angle neutron scattering study”, Physical review E, 61(3):2947-2953.

Bartolino R, Chiaranza T, Meuti M, Compagnoni R (1982) “Uniaxial and biaxial lyotropic nematic liquid crystals”, Phys. Rev. A, 26(2):1116-1119.

Berardi R, Kuball HG, Memmer R, Zannoni C (1998) “Chiral induction in nematics: A computer simulation study”, Journal of Chemical Society Faraday Transactions, 94, 1229-1234.

Berejnov VV, Cabuil V, Perzynski R, Raikher Y, Lysenko S, Sdobnov V (2000) “Lyotropic Nematogenic System Potassium Laurate–1-Decanol–Water: Method of Synthesis and Study of Phase Diagrams”, Crystallography Reports, 45(3), 493-500.

Blanco E, Gonzalez-Perez A, Ruso JM, Pedrido R, Prieto G, Sarmiento F (2005) “A comparative study of the physicochemical properties of perfluorinated and hydrogenated amphiphiles”, Journal of Colloid and Interface Science, 288, 247-260.

Boden N, Jackson PH, McMullen K, Holmes MC (1979) “Are ‘nematic’ amphiphilic liquid crystalline mesophases thermodynamically stable?”, Chemical Physics Letters, 65, 476-479.

Boden N, Radley K, Holmes MC (1981) “On the relationship between the micellar structure and the diamagnetic anisotropy of amphiphilic nematic mesophases”, Molecular Physics, 42, 493-496.

Boden N, Holmes MC (1984) “Lamellar nematic tricritical behavior in lyotropic liquid crystals”, Chem. Rev. Lett., 109, 76-80.

Boden N, Clements J, Parker D, Smith MH (1990) “Nematic-lamellar tricritical behavior and structure of the lamellar phase in the ammonium pentadecafluorooctanoate/water system”, Journal of Chemical Physics, 93, 9096-9105.

Bouchal R, Hamel A, Hesemann P, In M, Prelot B, Zajac J (2016) “Micellization Behavior of Long-Chain Substituted Alkylguanidinium Surfactants”, International Journal of Molecular Sciences, 17, 223(1-16).

Bunn CW, Howells ER (1954) “Structures of molecules and crystals of fluoro-carbons”, Nature, 174, 549-551.

Carmelita M, Kasuya Z, Nakano S, Katayama R, Hatanaka K (2011) “Evaluation of the hydrophobicity of perfluoroalkyl chains in amphiphilic compounds that are incorporated into cell membrane”, Journal of Fluorine Chemistry, 132, 202-206.

Chattopadhyay A and Erwin L (1984) “Fluorimetric determination of critical micelle concentration avoiding interference from detergent charge”, Analytical Biochemistry, 139(2):408-412.

Chen DM, Fujiwara FY, Reeves LW (1977) “Studies of the behavior in magnetic fields of some lyomesophase systems with respect to electrolyte additions”, Canadian Journal of Chemistry, 55, 2396-2402.

Chen LJ, Lin SY,Huang CC (1998) “Effect of Hydrophobic Chain Length of Surfactants on Enthalpy-Entropy Compensation of Micellization”, Journal Physical Chemistry B, 102, 4350-4356.

Coates D (2015) “Development and applications of cholesteric liquid crystals”, Liquid Crystals, 42(5-6), 653-665.

Collins KD (1996) “Charge Density-Dependent Strength of Hydration and Biological Structure”, Biophysical Journal, 72:65-76.

Collins KD (2004) “Ions from the Hofmeister series and osmolytes: effects on proteins in solution and in the crystallization process”, Methods, 34:300-311.

Collins KD, Neilson G, Enderby J (2007) “Ions in water: Characterizing the forces that control chemical processes and biological structure”, Biophysical Chemistry, 128:95-104.

Covello PS, Forrest BJ, Helene MEM, Reeves LW, Vist M (1983) “Type II DM lyotropic nematics and their derived cholesteric forms”, Journal of Physical Chemistry, 87, 176-181.

Cox JSG, Woodard GD, McCrone WC (1971) “Solid state chemistry of cromolyn sodium (disodium cromoglycate)”, Journal of Pharmaceutical Sciences, 60, 1453-65.

Cull B, Heino M, Lee SH, Kumar S, Keast SS, Neubert ME (1994) “Effect of salt on the phase diagrams of two binary lyotropic liquid crystalline solutions”, Liquid Crystals, 17, 507-512.

Dan B, Behabtu N, Martinez A, Evans JS, Kosynkin DV, Tour JM, Pasquali M, Smalyukh II (2011) “Liquid crystals of aqueous, giant graphene oxide flakes”, Soft Matter, 7, 11154-11159.

Das D, Ismail K (2008) “Aggregation and adsorption properties of sodium dodecyl sulfate in water-acetamine mixtures”, Journal of Colloid and Interface Science, 327, 198-203.

Dawin UC, Lagerwall J, Giesselmann F (2009) “Electrolyte Effects on the Stability of Nematic and Lamellar Lyotropic Liquid Crystal Phases: Colligative and Ion-Specific Aspects”, J. Phys. Chem. B, 113:11414–11420.

Dawin UC, Osipov MA, Giesselmann F (2010) “Electrolyte Effects on the chiral induction and on its temperature dependence in a chiral nematic lyotropic liquid crystal”, J. Phys. Chem. B, 114:10327–10336.

de Sant’Ana ZA, Neto AMF (1992) “Uniaxial-to-biaxial cholesteric and nematic phase transitions on a lyotropic alcohol-free mixture’, Phys. Rev. A 1992, 46, 7630−7635.

Dominguez A, Fernandez A, Gonzalez N, Iglesias E, Montenegro L (1997) “Determination of Critical Micelle Concentration of Some Surfactants by Three Techniques”, Journal of Chemical Education, 74(10):1227-1231.

Dörfler, HD (2002) “Chirality, twist and structures of micellar lyotropic cholesteric liquid crystals in comparison to the properties of chiralic thermotropic phases”, Adv. Colloid Interface Sci., 98, 285-340.

Dreger EE, Keim GI, Miles GD, Shedlovsky L, Ross J, (1944) “Sodium alcohol sulfates. Properties involving surface activity’’, Ind Eng Chem, 36(7):610-617.

Ebnesajjad S (2015) “Fluoroplastics, Volume 2: Melt Processible Fluoropolymers - The Definitive User's Guide and Data Book”, 2nd Edition, Elsevier, Massachusetts, USA.

Ferrarini A, Nordio PL (1992) “Diffusion models for the dynamics of flexible molecules”, Journal of Chemical Society Faraday Transactions, 88, 1733-1746.

Ferrarini A, Moro GJ, Nordio PL, Luckhurst GR (1992) “A shape model for molecular ordering in nematics”, Molecular Physics, 77, 1-15.

Ferrarini A, Luckhurst GJ, Nordio PL, Roskilly SJ (1994) "Prediction of the translational properties of liquid crystal dimers. A molecular field calculation based on the surface tensor parametrization", Journal of Chemical Physics, 100, 1460-1469.

Ferrarini A, Moro GJ, Nordio PL (1995) "A shape model for the twisting power of chiral solutes in nematics", Liquid Crystals, 19, 397-399.

Ferrarini A[a], Moro GJ, Nordio PL (1996) "Shape model for ordering properties of molecular dopants inducing chiral mesophases", Molecular Physics, 87, 485-499.

Ferrarini A[b], Moro GJ, Nordio PL (1996) "Simple molecular model for induced cholesteric phases", Physical Review E., 53, 681-688.

Ferrarini A, Nordio P (1998) "On the assessment of molecular chirality", Journal of Chemical Society Perkin Transactions 2, 455-460.

Ferrarini, A, Gottarelli, E., Nordio, P.L. and Spada, G.P., 1999, Determination of absolute configuration of helicenes and related biaryls from calculation of helical twisting powers by the surface chirality model, *J. Chem. Soc. Perkin Trans*. 2, 3, 411-417.

Filho AA, Laverd Jr A, Fujiwara F (2003) "Observation of Two Biaxial Nematic Mesophases in the Tetradecyltrimethylammonium Bromide/Decanol/Water System", Langmuir, 19:1127-1132.

Fisch MR, Kumar S, Litster JD (1986) "Pressure dependence of the nematic-to-isotropic transition in the lyotropic liquid crystal cesium perfluoro-octanoate", Phys. Rev. Lett., 57, 2830-2833.

Forrest BJ and Reeves LW (1980) "Micelle motion in lyotropic nematic phases", Mol. Cryst. Liq. Cryst., 58, 233-243.

Forrest BJ and Reeves LW (1981) "New lyotropic liquid crystals composed of finite nonspherical micelles", Chem. Rev., 81, 1-14.

Forrest BJ, Reeves LW, Vist MR, Rodger C, Helene MEM (1981) "A Type I aqueous cholesteric lyomesophase", Journal of American Chemical Society, 103, 690-691.

Freiser MJ (1970) "Ordered States of a Nematic Liquid Crystals", Physical review letters, 24:1041-1043.

Furukawa GT, McCoskey RE, King GJ (1952) "Calorimetric properties of polytetrafluoroethylene", J Res Natl Bureau Stand, 49, 273.

Galerne Y and Marcerou J (1983) "Temperature Behavior of the Order-Parameter Invariants in the Uniaxial and Biaxial Nematic Phases of a Lyotropic Liquid Crystal", Physical review letters, 51(23):2109-2111.

Galerne Y and Marcerou J (1985) “Temperature-concentration behaviour of the order parameter in the nematic phases of a lyotropic liquid crystal”, J. Phys. France, 46:589-594.

Galerne Y, Neto AMF, Liebert L (1987) “Microscopical structure of the uniaxial and biaxial lyotropic nematics”, The Journal of chemical physics, 87(3):1851-1856.

Garcia-Mateos I, Velazquez M., Rodriguez L (1990) “Critical micelle concentration determination in binary mixtures of ionic surfactants by deconvolution of conductivity/concentration curves”, Langmuir, 6(6):1078-1083.

Gonzalez-Perez A, Sanchez-Dominguez M (2013) “Changes in self-assemblies induced by temperature, concentration and light”, Frontier in Bioscience, 5, 611-630.

Goossens WJA (1970) “A molecular theory of the cholesteric phase”, Phys. Lett., 31A, 413-414.

Gottarelli G[a], Mariani P, Spada GP, Samori B, Forni A, Solladie G, Hibert M (1983) “Induction of cholesteric mesophases in nematic liquid crystals, and correlation of absolute configurations of some chiral oxiranes and thiiranes”, Tetrahedron, 39, 1337-1344.

Gottarelli G[b], Hibert M, Samori B, Solladie G, Spada GP, Zimmermann R (1983) “Induction of the cholesteric mesophase in nematic liquid crystals: mechanism and application to the determination of bridged biaryl configurations”, Journal of American Chemical Society, 105, 7318-7321.

Gottarelli G, Spada GP (1985) “Induced cholesteric mesophases-origin and application”, Molecular Crystals Liquid Crystals, 123, 377-388.

Hartshorne NH, Woodard GD (1973) “Mesomorphism in the system disodium chromoglycate-water”, Molecular Crystals Liquid Crystals, 23, 343–368.

Hendrikx Y, Charvolin J, Rawiso M, Liebert L, Holmes, MC (1983) “Anisotropic aggregates of amphiphilic molecules in lyotropic nematic phases”, J. Phys. Chem., 87, 3991-3999.

Ho C, Hoetz R, El-Aasser M (1991) “A biaxial lyotropic nematic phase in dilute solutions of sodium lauryl sulfate-1-hexadecanol-water”, Langmuir, 7(4):630-635.

Holmberg K (2002), Handbook of Applied Surface and Colloid Chemistry, Vol. 1. John Wiley & Sons Ltd, New Jersey.

Hooshyar H, Sadeghi R (2015) “Influence of sodium salts on the micellization and interfacial behavior of cationic surfactant dodecyltrimethylammonium bromide in aqueous solution”, Journal of Chemical and Engineering Data, 60, 983-992.

Israelachvili J (1991), “Intermolecular and surface forces”, 1st edition, Academic Press, New york

Jiang N, Li P, Wang Y, Wang J, Yan H, Thomas R (2005) “Aggregation behavior of hexadecyltrimethylammonium surfactants with various counterions in aqueous solution”, Journal of Colloid and Interface Science, 286:755–760.

Kang KH Hong-Un K, Kyung-Hee L (2001) “Effect of temperature on critical micelle concentration and thermodynamic potentials of micellization of anionic ammonium dodecyl sulfate and cationic octadecyl trimethyl ammonium chloride”, Colloids and Surfaces A: Physicochemical and Engineering Aspects, 189(1-3):13-121.

Kim YK, Senyuk B, Shin ST, Kohlmeier A, Mehl GH, Lavrentovich OD (2014) “Surface alignment, anchoring transitions, optical properties, and topological defects in the thermotropic nematic phase of organo-siloxane tetrapodes”, Soft Matter, 10, 500-509.

Kissa E (1994) “Fluorinated Surfactants, Synthesis, Properties, Applications”, Dekker, New York, 1994.

Kleman M and Lavrentovich (2006) “Topological point defects in nematic liquid crystals”, Philosophical Magazine, 86, 4117-4137.

Krafft MP (2001) “Fluorocarbons and fluorinated amphiphiles in drug delivery and biomedical research”, Advanced Drug Delivery Reviews, 47, 209-228.

Kresheck GC (1975) “Water - A comprehensive Treatise”, vol. 4, Franks F, Ed., Plenum Press, New York and London.

Kuball, H.-G. and Türk, O., 1999, Helical twisting power and circular dichroism as chirality observations - Development of a sector rule for the intermolecular chirality transfer in a liquid crystal phase, Polish. J. Chem., 73, 209-228.

Kumar S, Sharma D, Din K (2000) “Cloud Point Phenomenon in Anionic Surfactant + Quaternary Bromide Systems and Its Variation with Additives”, Langmuir, 16(17):6821–6824.

Lasic DD, Helene MEM, Reeves LW (1983) “Cholesteric type-II micellar mesophases prepared from 2 different single center chiral amphiphiles”, Can. J. Chem., 61, 1921-1923.

Lee H, Labes MM (1982) “Lyotropic cholesteric and nematic phases of disodium cromoglycate in magnetic fields”, Molecular Crystals Liquid Crystals, 84, 137-157.

Lee H and Labes M (1984) “Helical Twisting Power of Amino Acids in a Nematic Lyophase”, Molecular Liquid Crystals, 108(1-2):125-132.

Lee JA (2000) “Observation of individual fluorine atoms from highly oriented polytetrafluoroethylene films by atomic force microscopy”, NASA Report, NASA/TM 2000-209962.

Lin IJ, Moudgil BM, Somasundaran P (1974) “Estimation the effective number of –CH_2– groups in long-chain surface active agents”, Colloid and Polymer Science, 252, 407-414.

Lin Z, Cai JJ, Scriven LE, Davis HT (1994) “Spherical-to-wormlike micelle transition in CTAB solutions”, J. Phys. Chem., 98, 5984−5993.

Lin SY, Lin YY, Chen, EM, Hsu CT, Kwan CC (1999) “A Study of the Equilibrium Surface Tension and the Critical Micelle Concentration of Mixed Surfactant Solutions”, Langmuir, 15(13):4370-4376.

Liu F, Grainger DW (2017) “Comprehensive Biomaterials II” Volume 1, Elsevier, Oxford, UK.

Long P, Yan H, Guo X, Hao J (2012) “Lyotropic liquid crystal phases of lithium perfluorinated fatty acid salts in aqueous solutions and molecular dynamics study of the lamellar phase”, Journal of Fluorine Chemistry, 135, 315-322.

Maibaum L, Dinner AR, Chandler D (2004) “Micelle Formation and the Hydrophobic Effect”, Journal of Physical Chemistry B, 108, 6778-6781.

Malik MA, Wani MY, Hashim MA (2012) “Microemulsion method: A novel route to synthesize organic and inorganic nanomaterials: 1st Nano Update”, Arabian Journal of Chemistry, 5(4), 397-417

Marcus Y (2009) “Effect of Ions on the Structure of Water: Structure Making and Breaking”, Chem. Rev, 109:1346–1370.

Mavrikis P (2003) “How It Works: Science and technology Volume 13”, 3rd edition, Marshall Cavendish Corporation, New York, USA.

Mistri EA, Ghosh, A, Banerjee S (2015) “Handbook of specialty fluorinated polymers: Preparation, properties and applications”, Elsevier, Massachusetts, USA.

Mizuno Y, Miyagawa Y, Lida M, Tada Y, Yokoyama H (1998) “Effects of tripositive cobalt(III)-complex ions on the structure of a cholesteric mesophase composed of potassium N-dodecanoyl-L-alaninate”, Langmuir, 14, 7058-7064.

Mohajeri E and Noudeh GD (2012) “Effect of temperature on the critical micelle concentration and micellization thermodynamic of nonionic surfactants: Polyoxyethylene sorbitan Fatty acid esters”, E-Journal of Chemistry, 9, 2268-2274.

Müller N (1993) “Temperature dependence of critical micelle concentrations and heat capacities of micellization for ionic surfactants”, Langmuir, 9, 96-100.

Myers D (2006), Surfactant Science and Technology, 3rd Ed.,John Wiley & Sons Inc., Hoboken, New Jersey.

Noudeh GD, Housaindokht M, Bazzaz BSF (2007) “The Effect of Temperature on Thermodynamic Parameters of Micellization of Some Surfactants”, Journal of Applied Sciences, 7, 47-52.

Neto AMF[a], Galerne Y, Levelut A, Liebert L (1985) “Pseudo-lamellar ordering in uniaxial and biaxial lyotropic nematics: a synchrotron X-ray diffraction experiment”, Journal de Physique Lettres, 46(11):409-506.

Neto AMF[b], Liebert L, Galerne Y (1985) “Temperature and concentration range ot the biaxial nematic lyomesophase in the mixture potassium laurate/1-decanol/D_2O”, Journal of Physical Chemistry, 89(17):3737-3739.

Neto AMF and Salinas S (2005), The Physics of Lyotropic Liquid Crsytals, Oxford University Press, London

Olutas EB, Acimis M (2012) “Thermodynamic parameters of some partially fluorinated and hydrogenated amphiphilic enantiomers and their racemates in aqueous solution”, J. Chem. Thermodynamics, 47, 144 153.

Pape M and Hiltrop K (1997) “Influence of lyotropic nematic host phases on the twisting power of chiral dopants”, Mol. Cryst. Liq. Cryst., 307, 155-173.

Partyka J and Hiltrop K (1996) “On chirality induction in lyotropic nematic liquid crystals”, Liq. Cryst. 20, 611-618.

Pieraccini S, Ferrarini A, Spada GP (2008) “Review article: Chiral doping of nematic phases and its application to the determination of absolute configuration”, Chirality, 20, 749-759.

Polidori A, Raynal S, Barret LA, Dahani M, Barrot-Ivolot C, Jungas C, Frotscher E, Keller S, Ebel, C, Breyton C, Bonnete F (2016) “Sparingly fluorinated maltoside-based surfactants for membrane-protein stabilization”, New J Chem, 40, 5364-5378.

Photinos PJ, Saupe A (1986) “Measurements of the conductivity and relaxation times for the micellar nematic phase of the system ammonium perfluorononanoate/H_2O”, Journal of Chemical Physics, 85, 7467-7471.

Radley K and Saupe A (1978) “Cholesteric states of micellar solutions”, Mol. Phys., 35, 1405-1412.

Radley K, Tracey AS (1985) “A laser diffraction and nuclear magnetic-resonance investigation of the cholesteric potassium N-dodecanoylalaninate mesophase system”, Can. J. Chem., 63, 95-99.

Radley K and Cattey H (1992) “Amphiphilic cholesteric liquid crystals prepared from the quaternary ammonium surfactant S-(−)-1-hexadecyl-1-methyl-2-pyrrolidinemethanol bromide”, Liquid Crystals, 12(5):875-878.

Radley K, Lilly GJ (1993) “Potassium salts of acylated amino acids as chiral dopants and hosts in the formation of amphiphilic cholesteric liquid crystals”, Mol. Cryst. Liq. Cryst., 231, 183-190.

Radley K, McLay N, Lilly GJ (1996) “Trans-cis diastereorotamerization in amphiphilic cholesteric liquid crystals*”, J. Phys. Chem*., 100, 12414-12417.

Ravey JC, Gherbi A, Stebe MJ (1988) “Comparative study of fluorinated and hydrogenated nonionic surfactants. I. Surface active properties and critical concentrations”, Prog Colloid Polymer Sci, 76, 234-241.

Reis D, Akpinar E, Neto AMF (2013) “Effect of Alkyl Chain Length of Alcohols on Cholesteric Uniaxial to Cholesteric Biaxial Phase Transitions in a Potassium Laurate/Alcohol/Potassium Sulfate/Water/Brucine Lyotropic Mixture: Evidence of a First-Order Phase Transition”, The Journal of Physical Chemistry B, 117:942-948.

Rigby HA, Bunn CW (1949) “A room-temperature transition in polytetrafluoroethylene”, Nature, 164, 583-585.

Roesler J, Harder H, Baeker M (2007) “Mechanical Behaviour Engineering Materials”, Springer-Verlag, Berlin, Germany.

Rosen MJ, Li F, Morrall SW, Versteeg DJ (2001) “The Relationship between the Interfacial Properties of Surfactants and Their Toxicity to Aquatic Organisms”, Environmental Science and Technology, 35, 954-959.

Rosen MJ (2004) “Surfactants and Interfacial Phenomena”, 3rd Ed., Wiley-Interscience.

Rosoff M (2001) “Nano-Surface chemistry”, Marcel-Dekker Inc., New York.

Sadtler VM, Giulieri F, Krafft MP, Riess, JG (1998) “Micellization and adsorption of fluorinated amphiphiles: Questioning the 1 $CF_2 \approx 1.5$ CH_2 rule”, Chem Eur J, 10, 1952-1956.

Sakai K, Umemoto N, Aburai, K, takamatsu Y, Endo T, Kitiyanan B, Matsumoto M, Sakai H, Abe M (2014) “Physicochemical properties of oleic acid-based partially fluorinated geminisurfactants”, J Ole Sci., 63, 257-267.

Salem JK, El-Nahhal I, Najri B, Hammad T, Kodeh F (2016) “Effect of anionic surfactants on the surface plasmon resonance band of silver nanoparticles: Determination of critical micelle concentration”, Journal of Molecular Liquids, 223:771-774.

Sanchez-Dominguez M, Benoit N, Krafft MP (2008) “Synthesis of triphilic, Y-shaped molecular surfactants”, Tetrahedron, 64, 522-528.

Sarac B, Bester-Rogac M (2009), “Temperature and salt-induced micellization of dodecyltrimethylammonium chloride in aqueous solution: A thermodynamic study”, Journal of Colloid and Interface Science, 338, 216-221.

Saupe A (1977) “Textures, deformations, and structural order of liquid crystals”, Journal of Colloid and Interface Science, 58, 549-558.

Sein A, Engberts J (1995) “Micelle to Lamellar Aggregate Transition of an Anionic Surfactant in Dilute Aqueous Solution Induced by Alkali Metal Chloride and Tetraalkylammonium Chloride Salts”, Langmuir, 11:455-465.

Senyuk B, Kim YK, Tortora L, Shin ST, Shiyanovskii SV, Lavrentovich OD (2011) "Surface Alignment, Anchoring Transitions, Optical Properties and Topological Defects in Nematic Bent-Core Materials C7 and C12", Molecular Crystals Liquid Crystals, 540, 20-41.

Serra F (2016) "Curvature and defects in nematic liquid crystals", Liquid Crystals, 43, 1920-1936.

Sharma NK, Singh M, Bhattarai A (2016) "Hydrophobic study of increasing alkyl chain length of platinum surfactant complexes: synthesis, characterization, micellization, thermodynamics, thermogravimetrics and surface morphology", RSC Advances, 6, 90607-90623.

Shinoda K, Nakagawa T, Tamamushi BL, Tamamushi BI (1963), Colloidal Surfactants, Academic Press, London

Shinoda K, Hato M, Hayashi T (1972) "The physicochemical properties of aqueous solutions of fluorinated surfactants", J Phys Chem, 76, 909-914.

Shinoda K and Nomura T (1980) "Miscibility of fluorocarbon and hydrocarbon surfactants in micelles and liquid mixtures. Basic studies of oil repellent and fire extinguishing agents", J Phys Chem, 84, 365-369.

Sinnko J (2006) "Physical Pharmacy and Pharmaceutical Sciences," 5th Ed., Lippincott Williams & Wilkins, Baltimore.

Sivaramakrishna D, Swamy MJ (2015) "Self-assembly, supramolecular organization and phase behavior of L-alanine alkyl esters (n=9-18) and characterization of equimolar L-alanine lauryl ester/lauroyl sulfate cationic complex", Langmuir, 31, 9546-9556.

Spada GP, Gottarelli G, Samori B, Bustamante CJ, Wells, KS (1988) "A study of some lyotropic cholesteric mesophases by circular and linear dichroism and by circular intensity differential scattering", Liquid Crystals, 3, 101-113.

Stead JA, Taylor HJ (1969) "Some solution properties of certain surface-active N-alkylpyridinium halides. I. Effect of temperature on the critical micelle concentrations", Journal of Colloid and Interface Science, 30, 482-488.

Stephenson GA, Diseroad BA (2000) "Structural relationship and desolvation behavior of cromolyn, cefazolin and fenoprofen sodium hydrates", International Journal of Pharmaceutics, 198, 167–77.

Stroobants A and Lekkerkerker H (1984) "Liquid crystal phase transitions in a solution of rodlike and disklike particles", The Journal of Physical Chemistry, 88:3669-3674.

Tadros TF (2014), An introduction to surfactants, 1st edition, Walter de Gruyder GmbH, Berlin, Germany

Tanford C (1980) "The Hydrophobic Effect", 2nd ed.; John-Wiley: New York.

Tarus J, Shamsi S, Morris K, Agbaria R, Warner I (2003) “Counterions in Polymeric Amino Acid Based Surfactants:Effect on Physical Properties and Enantioselectivity”, Langmuir, 19:7173-7181.

Tohyama K (1974) “The pitch-independent critical field in cholesteric liquid crystalline poly-γ-ethyl-L-glutamate”, J. Phys. C: Solid State Phys., 7, 270-273.

Tracey AS, Radley K (1985) “Cholesteric behaviour in lyotropic liquid crystals”, Mol. Cryst. Liq. Cryst., 122, 77-87.

Umlong IM, Ismail K (2006) “Micellization behavior of sodium dodecylsulfate and dioctyl sulfosuccinate in the presence of sodium salicylate”, J. Surface Sci. Technol., 22, 101−117.

Vlachy N, Drechsler M, Verbavatz JM, Touraud D, Kunz W (2008) “Role of the surfactant headgroup on the counterion specificity in the micelle-to-vesicle transition through salt addition”, Journal of Colloid and Interface Science, 319: 542-548.

Vlachy N, Jagoda-Cwiklik B, Vácha R, Touraud D, Jungwirth P, Kunz W (2009) “Hofmeister series and specific interactions of charged headgroups with aqueous ions”, Advances in Colloid and Interface Science, 146:42-47.

Yu L and Saupe A (1980) “Observation of a Biaxial Nematic Phase in Potassium Laurate-1-Decanol-Water Mixtures”, Physical review letters, 45:1000-1003.

7. CURRICULUM VITAE

Name SURNAME	**:** Sinan YURDAKUL
Place and Date of Birth	**:** EYÜP-14.12.1990
Universities	
Bachelor's Degree	**:** Abant Izzet Baysal University
e-mail	**:** sinanyurdakultr@gmail.com
Address	**:** Abant Izzet Baysal University, Science & Art Faculty, Gölköy Campus, BOLU

Publication

Erol Akpinar, **Sinan Yurdakul**, Antonio Martins Figueiredo Neto, "Comparison between lyotropic cholesteric phase behavior with partly fluorinated surfactants and their exact hydrogenated counterparts", submitted to a journal, 28th December 2017.